EPRI
Electric Power
Research Institute

Topics:
Reactor safety
Reactor licensing
Reactor transients
LWR

EPRI NP-6614
Project 2941-7
Final Report
December 1989

ARROTTA–HERMITE Code Comparison

Prepared by
Combustion Engineering, Inc.
Windsor, Connecticut

REPORT SUMMARY

SUBJECT	Nuclear reload management
TOPICS	Reactor safety Reactor licensing Reactor transients LWR
AUDIENCE	Safety analysis engineers / Core design engineers

ARROTTA–HERMITE Code Comparison

This report documents the verification of the ARROTTA space-time kinetics computer program against a similar industry code for a PWR rod ejection accident. The ARROTTA code can be run much faster and at a small fraction of the cost than any other known code of its class.

BACKGROUND

The ARROTTA computer program is a multidimensional space-time kinetics program developed by EPRI for solving LWR transient problems in which spatial effects in the core are significant. Because reactor core power distributions and other quantities of interest are not amenable to measurement in power reactors under transient conditions, verification of computer code predictions of such events generally rely on numerical comparisons of computer codes.

OBJECTIVE

To verify the ARROTTA computer program for transient applications.

APPROACH

The computer program HERMITE, one of several codes in the industry available for this type of comparison, was chosen to verify the ARROTTA code for transient applications. An NRC-approved topical report for the HERMITE code exists, and the code has been used repeatedly in licensing applications. The investigators found the common input options between the HERMITE and ARROTTA codes. They ran both codes and compared the results.

RESULTS

The EPRI ARROTTA verification program is comprehensive. This study provides further reassurance of the program's capabilities for addressing space-time effects. The good agreement of the ARROTTA and HERMITE results for the analyzed 3-D rod ejection event verifies the transient neutronics, transient fuel temperature, transient control rod motion, and transient cross-section treatments in the ARROTTA code. The ARROTTA code can, therefore, be reliably used for any rod ejection type transient, including transients up to hot, full-power conditions.

EPRI PERSPECTIVE

This report not only verifies that the ARROTTA computer program can be used to analyze off-normal conditions or accident situations but it also establishes an industry benchmark. The details of the analysis and input decks used by both the ARROTTA and HERMITE codes are given. Thus,

others can repeat this analysis knowing that they are representing the problem in the same manner as was done in this study. The ARROTTA code has state-of-the-art algorithms that give accurate results with a minimum of detail. Thus the code produces excellent results with reduced running time and a factor of 10 lower cost than other codes of the same type.

PROJECT RP2941-7
EPRI Project Manager: Lance J. Agee
Nuclear Power Division
Contractor: Combustion Engineering, Inc.

For further information on EPRI research programs, call EPRI Technical Information Specialists (415) 855-2411.

ARROTTA-HERMITE Code Comparison

NP-6614
Research Project 2941-7

Final Report, December 1989

Prepared by

COMBUSTION ENGINEERING, INC.
C-E Power Systems
1000 Prospect Hill Road
Windsor, Connecticut 06095

Principal Investigators
P. E. Rohan
S. G. Wagner

C-E Project Manager
J. M. Betancourt

Prepared for

Electric Power Research Institute
3412 Hillview Avenue
Palo Alto, California 94304

EPRI Project Manager
L. J. Agee

Nuclear Reload Management Program
Nuclear Power Division

ORDERING INFORMATION

Requests for copies of this report should be directed to Research Reports Center (RRC), Box 50490, Palo Alto, CA 94303, (415) 965-4081. There is no charge for reports requested by EPRI member utilities and affiliates, U.S. utility associations, U.S. government agencies (federal, state, and local), media, and foreign organizations with which EPRI has an information exchange agreement. On request, RRC will send a catalog of EPRI reports.

NOTICE

This report was prepared by the organization(s) named below as an account of work sponsored by the Electric Power Research Institute, Inc. (EPRI). Neither EPRI, members of EPRI, the organization(s) named below, nor any person acting on behalf of any of them: (a) makes any warranty, express or implied, with respect to the use of any information, apparatus, method, or process disclosed in this report or that such use may not infringe privately owned rights; or (b) assumes any liabilities with respect to the use of, or for damages resulting from the use of, any information, apparatus, method, or process disclosed in this report.

Prepared by
Combustion Engineering, Inc.
Windsor, Connecticut

ABSTRACT

This report documents the verification of EPRI's ARROTTA space-time kinetics computer program against a similar industry code. A three-dimensional space-time kinetics calculation of a PWR rod ejection transient was run using the ARROTTA code. The results were compared against those of Combustion Engineering's HERMITE code. The transient used an initial zero power condition and ejected a rod worth of $1.16. Additionally, steady state cases were compared in support of the transient analysis problem definition. Excellent agreement was obtained in all phases of the comparison including steady state and transient total core power, peak assembly power, core average fuel temperature, and maximum fuel temperature. A complete problem description, including all of the input, is contained in an appendix.

ACKNOWLEDGMENTS

The following individuals and organizations are recognized for their contributions to this work. Mr. Kenneth Doran, S. Levy, Inc., who was responsible for running ARROTTA and providing the results to the authors, and for his consultation on all aspects of the work. Dr. Laurance Eisenhart, S. Levy, Inc., for supplying needed information on the ARROTTA program of which he is the principal author. Dr. R. R. Lee, Leaders in Management, Inc., who provided general guidance and consultation throughout the effort. Mr. R. P. Harris, Combustion Engineering, Inc., for several helpful suggestions and discussions with the authors on the use of HERMITE.

CONTENTS

ILLUSTRATIONS

TABLES

EXECUTIVE SUMMARY

The ARROTTA computer code is a multi-dimensional space-time kinetics program developed for the Electric Power Research Institute (EPRI) by S. Levy, Inc. The code objective is to solve boiling water reactor (BWR) and pressurized water reactor (PWR) transient problems where spatial effects in the core are significant. The EPRI ARROTTA verification program is a comprehensive one, of which this study provides further reassurance of the code's capabilities for addressing space-time effects.

The objective of this study is to verify the ARROTTA computer program for transient applications. This has been accomplished by comparing results from ARROTTA to results from Combustion Engineering's HERMITE code for the same problem. Since reactor core power distributions and other quantities of interest are not amenable to measurement in power reactors under such conditions, verification of computer code predictions of such events must rely on numerical intercomparisons between computer codes. Fortunately, there are several computer codes such as HERMITE which can be used for this comparison. HERMITE was chosen because of its licensing status with the Nuclear Regulatory Commission. An approved topical report for HERMITE exists and the code has been used extensively in licensing applications.

A three-dimensional (3-D) space-time kinetics calculation of a PWR rod ejection transient was run using both ARROTTA and HERMITE. The results of the two transient calculations were then compared. The transient used an initial zero power condition and ejected a rod worth of $1.16. This is a rather severe test of the space-time capabilities of ARROTTA since ejected rod worths this large are unusual and the transient is very rapid, resulting in a power increase of a factor of one million within one third of a second. Additionally, steady state cases were compared in support of the transient analysis problem definition. Excellent agreement was obtained in all phases of the comparison including steady state and transient total core power, peak assembly power, core average fuel temperature and maximum fuel temperature.

The principal conclusion from this study is the following:

The good agreement of the ARROTTA and HERMITE results for the 3-D rod ejection event analyzed serves to verify the transient neutronics, transient fuel temperature, transient control rod motion and transient cross section treatments in ARROTTA. The ARROTTA code can, therefore, be reliably used for any rod ejection type transient, including transients up to hot full power conditions.

Section 1

GENERAL

1.1 OBJECTIVE AND BACKGROUND

The objective of this study is to verify the ARROTTA computer program for transient applications. This has been accomplished by comparing results from ARROTTA to results from Combustion Engineering's (C-E's) HERMITE code for the same problem. Space-time kinetics calculations are typically used to analyze off-nominal conditions or accident situations. Since reactor core power distributions and other parameters of interest are not amenable to measurement in power reactors under such conditions, verification of computer code predictions of such events must rely on numerical intercomparisons between computer codes. Fortunately, there are available a number of codes including Combustion Engineering's HERMITE code which are capable of this type of calculation.

The ARROTTA code was developed for the Electric Power Research Institute (EPRI) by S. Levy, Inc. under Research Project (RP) 1936-6. ARROTTA, which stands for Advanced Rapid Reactor Operational Transient Analyzer, was developed to solve transient problems where spatial effects in the core are of significance. Among this class of transients is the control rod ejection accident in pressurized water reactors (PWRs). ARROTTA is built on the Analytic Nodalization Method as developed for QUANDRY (Reference 1.1) in EPRI RP 1936-1. The thermal hydraulics model in ARROTTA is taken directly from the BEACH program (Reference 1.2) as developed under EPRI RP 1761-18. ARROTTA itself was originally initiated as ANITA under Research Project 1936-4 at Brookhaven National Laboratory.

The HERMITE code was developed at Combustion Engineering for the analysis of transients in large PWRs where space-time effects are important. This was accomplished by means of a numerical solution to the multi-dimensional, few-group, time dependent neutron diffusion equation including feedback effects from fuel temperature, moderator temperature, moderator density and control rod motion. A topical report (Reference 1.3) describing the code, its input, and its verification was submitted to the Nuclear Regulatory Commission (NRC) in March, 1976.

A submittal was made at the same time as a separate C-E topical report (Reference 1.4) on the rod ejection accident. The NRC approval for both topical reports was obtained in July, 1976. In their evaluation of the HERMITE Topical Report, the NRC staff concluded that "The subject report describes an acceptable neutron kinetics computer code for solving the few-group transient diffusion equations in one, two and three dimensions." In addition, they stated: "It has been used to support the C-E Control Element Assembly Ejection Analysis Topical Report (CENPD-190, January 1976) and may be referenced in future license applications and topical reports."

Since the HERMITE Topical Report was approved, the code has undergone a number of incremental improvements and has been applied to a variety of analyses. Key improvements include the addition of the Nodal Expansion Method (NEM) neutronics (References 1.5 and 1.6) and the inclusion of the TORC thermal-hydraulics calculation (References 1.7 and 1.8). Results of the comparisons of the Nodal Expansion Method with C-E's ROCS coarse mesh program employing the Higher Order Difference (HOD) method and PDQ were described in 1983 in the ROCS/DIT Topical Report (Reference 1.9). In its acceptance, the NRC observed that based on the good agreement for two- and three- dimensional power distributions between the NEM and HOD methods and between NEM and HOD and fine mesh PDQ-7 calculations, they find either method (NEM or HOD) acceptable for coarse-mesh power distribution calculations. Further, the NRC recommended that C-E perform further verification when NEM is incorporated into the ROCS code in order to be assured that equivalent calculational biases and uncertainties are obtained with ROCS-NEM as compared to ROCS-HOD. Subsequently, NEM has been incorporated into ROCS (including assembly discontinuity factors) and the additional recommended determination of biases and uncertainties is in progress. C-E's experience with NEM has shown it to be superior to the finite element method used originally on both theoretical and empirical grounds.

HERMITE has been applied over the years in a variety of licensing analyses on specific dockets. The major applications have included one-dimensional space-time calculations for the loss of flow accident, time dependent reactivity insertion due to control rod motion, three-dimensional calculations for the steam line break accident and two-dimensional (2-D) analysis of asymmetric steam generator events.

1.2 SCOPE

This report describes a comparison between ARROTTA and HERMITE for a control rod ejection transient initiated from hot zero power conditions. In addition to comparing transient power levels and power distributions, several static comparisons of power, eigenvalue and rod worth are also presented.

1.3 FORMAT

Section 2 of this report outlines the principal features of ARROTTA and HERMITE and discusses differences which can impact the calculational results of the codes. Section 3 describes the transient of interest - a control rod ejection from hot zero power conditions. Section 4 presents the results for the steady state and transient cases which comprise the study. Conclusions are given in Section 5. Appendix A presents HERMITE sensitivity studies, while Appendix B provides a complete input description.

1.4 SUMMARY

The first task was to take the ARROTTA input deck and convert it to a HERMITE input deck. The major effort in this area was in the cross section treatment. While the ARROTTA and HERMITE cross section representations are quite different, the flexibility of the HERMITE representation permitted the two codes to produce essentially identical macroscopic cross sections for the same values of moderator density and fuel temperature. Therefore, any differences in results are not due to differences in cross section representation.

The thermal-hydraulic models and input for the two codes also differ. After some manipulation and sensitivity studies, the HERMITE input was generated, which showed acceptable steady state agreement with ARROTTA.

A series of steady state cases and one-dimensional transients were run to make some basic assessments of the accuracy and consistency of the HERMITE and ARROTTA models. These studies also provided guidance in the selection of options to be used in HERMITE for the three-dimensional (3-D) transient. Overall, the steady-state ARROTTA-HERMITE comparison showed very good agreement.

The final task was execution of the 3-D rod ejection transient in half core geometry. The agreements on core power, peak power, time of peak power and radial power distribution are all excellent. The core total power peaks, for example, differ by only 31 MW out of some 4300 MW (0.7%). The time of peak power differs by only 5 ms. Agreement in peak core power is comparable to the total core power agreement.

The good agreement obtained for the comparisons performed provides verification of ARROTTA for analyzing problems where there are significant transient neutronic and fuel temperature feedback effects.

1.5 REFERENCES

1.1 K. S. Smith, "An Analytic Nodal Method for Solving the 2-Group, Multi-dimensional, Static and Transient Neutron Diffusion Equations," Nuc. Eng. Thesis, Dept. of Nuc. Eng., MIT, Cambridge, MA., February, 1979.

1.2 D. J. Diamond, H. S. Cheng, and L. D. Eisenhart, "BEAGL-01, A Computer Code for Calculating Rapid Core Transients, Volume I-Modeling," EPRI NP-3243-CCM Vol. I, Electric Power Research Institute (1983).

1.3 P. E. Rohan, S. G. Wagner, S. E. Ritterbusch, "HERMITE: A Multi-dimensional Space-Time Kinetics Code for PWR Transients," Combustion Engineering, Inc., CENPD-188-A, July, 1976.

1.4 "CEA Ejection Analysis," Combustion Engineering, Inc., CENPD-190-NP-A, July, 1976.

1.5 H. Finnemann, H. Raum, "Nodal Expansion Method for the Analysis of Space-Time Effects in LWRs," Proceedings of NEACRP Specialists Meeting, Paris, November, 1979.

1.6 H. Finnemann, F. Bennewitz, M. R. Wagner, "Interface Current Techniques for Multidimensional Reactor Calculations," Atomkernenergie, 30, 123 (1977).

1.7 "TORC Code: A Computer Code for Determining the Thermal Margin of a Reactor Core," Combustion Engineering, Inc., CENPD-161-NP-A, July, 1975.

1.8 "TORC Code: Verification and Simplified Modelling Methods," Combustion Engineering, Inc., CENPD-206-NP-A, January, 1977.

1.9 "The ROCS and DIT Computer Codes for Nuclear Design," Combustion Engineering, Inc., CENPD-266-NP-A, April, 1983.

Section 2

CALCULATIONAL MODELS

2.1 INTRODUCTION

This section summarizes principal features of the ARROTTA and HERMITE computer programs. This is followed by a discussion of the major differences between the codes which have a bearing on the comparisons and their results.

2.2 ARROTTA KEY FEATURES

The ARROTTA code (Reference 2.1) is designed to solve the three-dimensional, time-dependent diffusion theory equations in rectangular geometry including thermal feedback effects. ARROTTA's geometric description of the core consists first of specifying the location of each assembly type in the XY plane and the associated mesh in all three dimensions. The neutronic mesh is specified next. Each assembly mesh interval must contain one or more neutronic mesh intervals subject to a maximum of 40 neutronic mesh intervals in each direction. The thermal-hydraulic mesh is specified next. The thermal-hydraulic mesh must be commensurate with the assembly mesh but not necessarily with the neutronic mesh. Again the maximum number of thermal-hydraulic mesh intervals in each dimension is 40. There are a number of features which can minimize and simplify the geometric description of the core. The code can handle both PWRs and BWRs with RCC or cruciform type control rods. Features also enable the code to expand input geometry from one size to another such as quarter core to full core.

The neutronic model uses the Analytic Nodalization Method (ANM) as developed for QUANDRY. This is a coarse-mesh method which breaks the problem down into a one-dimensional representation in each coordinate direction within each coarse-mesh node. With the assumption of constant cross sections within each node, the one-dimensional problems are solved analytically. The three one-dimensional equation sets are linked through transverse leakage. The ARROTTA implementation of ANM also incorporates assembly discontinuity factors to better represent the true heterogeneous reactor. Boundary conditions that can be used include zero flux and zero current conditions on external boundaries. The initial condition for transients is that the problem is in the steady state.

The thermal-hydraulic model in ARROTTA is taken directly from the BEAGL code. The fluid dynamics model considers inhomogeneous, non-equilibrium two-phase flow. The flow equations are one-dimensional in the axial direction and, therefore, do not consider cross flow between neighboring channels. The boundary conditions employed are specified inlet temperature and flow for each of the thermal-hydraulic channels. Pressure, inlet temperature, and flow can be varied as functions of time during a transient. In all, five flow regimes are considered. ARROTTA essentially solves a four equation system: one mass balance equation for the liquid-vapor mixture, two energy balance equations for liquid and vapor phases and an algebraic slip relationship. The momentum balance is not considered because it is decoupled from the energy equations and because the inlet mass flux is specified for the core as a boundary condition.

The fuel temperature model solves the radial heat conduction equation for each thermal-hydraulic unit cell. The unit thermal-hydraulic cell consists of a fuel pellet, gap, clad and surrounding moderator. Axial heat conduction is ignored. The heat source in the fuel pellet is represented as a parabolic function of pellet radius with a free parameter that can be varied on input to govern the curvature of the parabola. With this distribution and the assumption of uniform thermal conductivity and specific heat in the pellet, the heat conduction equation is solved analytically. The pellet-clad gap is modeled with a gap conductivity. The heat conduction equation is again solved in the clad. A fraction of the heat can be deposited directly in the clad and coolant.

The cross section treatment begins with the concept of "assembly types" which consist of one or more axial material compositions such as the bottom reflector, fuel and top reflector. The assembly type concept is general enough to include baffles and radial reflectors as well. Cross sections are specified by composition. In each composition the macroscopic cross sections are quadratic functions of void fraction for boiling water reactors (BWRs) and the relative change in moderator density with respect to a reference value for PWRs. Separate sets of quadratic coefficients are input for rodded and unrodded conditions. The moderator temperature dependence of each cross section type in each group is treated as a linear function moderator temperature. Fuel temperature dependence is treated as a linear function of the square root of the absolute fuel temperature. The fuel temperature dependence is only allowed in group 1. The moderator and fuel temperature dependence is the same for both rodded and unrodded macroscopic cross sections.

To account for rod cusping, cross sections for partially rodded nodes are obtained by blending the unrodded and rodded cross sections using a factor which can be up to a third order polynomial in the fraction of the node which is rodded. However, in both the ARROTTA and HERMITE analyses a simple volume weighting was used. Kinetics parameters can vary by composition. Assembly discontinuity factors can be composition, group and node-face dependent. Different sets of discontinuity factors can be used for rodded and unrodded conditions.

2.3 HERMITE KEY FEATURES

Like ARROTTA, the HERMITE code is designed to solve the time-dependent diffusion theory equations in rectangular geometry including thermal feedback effects. HERMITE can solve one-, two- or three-dimensional problems. The neutronics mesh is specified separately for each of the three spatial dimensions with a non-uniform mesh permitted. Thermal-hydraulic channels are assigned to various regions of the neutronics mesh. Typically, though not necessarily, one thermal-hydraulic channel is assigned per fuel assembly. The axial thermal-hydraulic mesh may be coarser than the neutronic mesh but they must share common mesh points. There are no fixed limits on the number of neutronic or thermal-hydraulic mesh points. The code treats PWR type control rods.

HERMITE originally used a linear finite element method to solve the space-time diffusion equation. As noted previously, the Nodal Expansion Method has been added and is the current standard method. The Nodal Expansion Method and the Analytical Nodalization Method are similar in that both reduce the three dimensional spatial problem to one-dimensional (1-D) representations in each of the three spatial directions in each node. In the Nodal Expansion Method, these one-dimensional problems are solved by using a fourth-order polynomial flux representation. The three one-dimensional equation sets are linked through transverse leakage. The time-dependence is handled by use of a frequency transformation. Boundary conditions that can be used include vacuum and zero current on external boundaries. The initial condition for transients is that the problem is in the steady state. For one-dimensional axial problems, there is also a finite difference method in the code. Its results are equivalent to those from the Nodal Expansion Method but it is much faster than the Nodal Expansion Method for the fine axial mesh typically used in reload analyses.

HERMITE has two thermal-hydraulic models. The original model is a closed channel model where the mass balance, energy balance and equation of state are solved simultaneously. The boundary conditions employed are specified inlet temperature, and flow for each of the thermal-hydraulic channels. Inlet temperature, flow and decay heat can be varied as functions of time during a transient. The second flow model in HERMITE is taken from C-E's TORC code. This is an open channel flow model which is based on that of COBRA IIIC (Reference 2.2). The open channel flow model can handle more complex conditions and includes such features as flow balancing. The original closed channel model is used for this study.

The fuel temperature model solves the radial heat conduction equation for each thermal-hydraulic unit cell which consists of a fuel pellet, gap, clad and surrounding moderator. Axial heat conduction is ignored. The heat source in the fuel pellet is spatially constant across the pellet. The heat conduction equation is solved by a finite difference technique which permits the thermal conductivity and specific heat to vary across the pellet. The pellet-clad gap is modelled with a gap conductivity. For steady-state problems there is an alternative fuel temperature model which correlates fuel temperature with linear heat rate and burnup. A fraction of the heat can be deposited directly in the coolant.

The cross section treatment in HERMITE is based upon the HARMONY system used in PDQ (Reference 2.3). This system permits microscopic and macroscopic cross sections to be functions of up to three independent variables. These variables can be number densities or other quantities such as moderator density or fuel temperature. In addition there is another set of factors which multiply cross sections and which can also be functions of up to three variables. This treatment permits a very general representation of cross section changes due to changes in moderator temperature, moderator density, fuel temperature or control rod position. The code accepts one set of kinetics parameters.

HERMITE also includes a depletion capability similar to that in the GAUGE code (Reference 2.4). Depletion chains for individual nuclides are specified on input.

2.4 MAJOR DIFFERENCES BETWEEN CALCULATION MODELS

Since the problem of interest had already been set up for ARROTTA, the task at hand was to model the same problem using the same data in HERMITE. The differences between ARROTTA and HERMITE are generally small for the purposes of this comparison. Only differences between the codes which were considered or which impact results are discussed.

The current version of HERMITE does not use assembly discontinuity factors, which have become standard and widely accepted in steady-state coarse mesh codes. Under a reasonable set of assumptions (face independence of the discontinuity factors) the HERMITE cross sections could be modified to incorporate the effect of discontinuity factors, with the only approximation being in the axial reflector regions. It was decided for this comparison not to use them because they added complexity to the problem set up and were not considered significant from the point of view of comparing and verifying the transient neutronic and thermal hydraulic aspects of ARROTTA.

ARROTTA accepts composition dependent kinetics parameters whereas HERMITE can accept only one set. For this problem, ARROTTA and HERMITE both used the same, single set of kinetics parameters.

Since it is the fuel temperature which limits the power increase during the transient, the fuel temperature models in the two codes are important. There are some minor differences in the fuel temperature model. ARROTTA is able to handle a non-uniform heat source within the pellet but assumes spatially constant thermal conductivity and specific heat, while HERMITE can handle a spatially varying conductivity but assumes a spatially constant heat source.

Another area of difference in the fuel temperature calculation is the way in which the two codes derive the power in the representative fuel pin in each thermal-hydraulic unit cell. In HERMITE the code is given the number of fuel pins in the fuel assembly as part of the input. With that the power in the average pin is easily derivable. In ARROTTA, the input quantities are unit cell pitch, the thermal-hydraulic channel dimensions, and a factor which excludes the area not considered part of the fuel rod or coolant. This factor is interpreted to mean that the area of the gap around the assembly and the guide tube cell area is excluded. From the thermal-hydraulic channel mesh, the input cell pitch and

fraction of excluded area, an implied number of fuel pins in a fuel assembly in ARROTTA is derived. This number implied from the ARROTTA input and used in HERMITE is 282.36 pins.

The solution strategy for the neutronics and fuel temperature has an important bearing on the results of the transient. Both ARROTTA and HERMITE first advance the neutronics from time t_n to time t_{n+1} and then advance the thermal-hydraulics. The thermal-hydraulics and neutronics are not solved simultaneously or implicitly. Time step size studies described later in detail explored the effect of this approximation. For the purpose of highlighting the differences between ARROTTA and HERMITE, a brief discussion of the transient aspect of the fuel temperature model is provided. The general form of the transient fuel temperature equations in both codes is

$$\frac{dT}{dt} = q(t) + \text{other terms}$$

where q(t) is the heat source in the fuel. The discretized form of this equation in HERMITE is

$$\frac{T^n - T^{n-1}}{\Delta t} = 1/2\,(q^n + q^{n-1}) + \text{other terms}$$

This approximation is equivalent to assuming that the heat source varies linearly in time from t_{n-1} to t_n. A more general form of this equation is

$$\frac{T^n - T^{n-1}}{\Delta t} = \theta\, q^n + (1-\theta)\, q^{n-1} + \text{other terms}$$

The default theta (θ) value used in HERMITE is 0.5. Another common approximation is θ=1. This second approximation is the one used in ARROTTA, based on the ARROTTA documentation. The sensitivity of the HERMITE results to θ is discussed in Appendix A. A value of θ=1 was used in the 3-D HERMITE calculation for compatibility with the ARROTTA calculation.

In addition to the heat deposited in the fuel, ARROTTA permits heat to be deposited directly in both the clad and coolant. HERMITE permits direct deposition only in the fuel and coolant. For purposes of consistency and since the effect is not significant for this study, all heat was deposited in the fuel pellet in both codes.

Another area of minor difference is in the neutronic boundary condition where ARROTTA has a zero flux condition and HERMITE has a vacuum boundary condition. This difference is insignificant.

The water properties and fuel properties in the two codes come from different sources. A limited comparison has been made between them and the differences are small.

The HERMITE cross section treatment is very flexible. For these comparisons this flexibility enables HERMITE to exactly duplicate the ARROTTA cross section treatment after some preliminary manipulations. Conceptual differences in the cross section treatment include polynomial fits in HERMITE compared to tabular data in ARROTTA.

2.5 REFERENCES

2.1 Laurance D. Eisenhart, "ARROTTA: Advanced Rapid Reactor Operational Transient Analysis Computer Code Documentation Package," Volume 1: Theory and Numerical Analysis, and Volume 2: User's Manual, Electric Power Research Institute, February, 1989.

2.2 D. S. Rowe, "COBRA-IIIC: A Digital Computer Program for Steady-State and Transient Thermal-Hydraulic Analysis of Rod Bundle Nuclear Fuel Elements," BNWL-1695, March, 1973.

2.3 M. R. Wagner, "GAUGE: A Two-Dimensional Few Group Neutron Diffusion-Depletion Program for a Uniform Triangular Mesh," GA-8307, March, 1968.

2.4 R. J. Breen, O. J. Marlowe, C. J. Pfeifer, "HARMONY: System for Nuclear Reactor Depletion Computation," WAPD-TM-473, January, 1965.

Section 3

PROBLEM SELECTION

3.1 DEFINITION OF THE PROBLEM

The rod ejection accident in a PWR is postulated to be the result of the failure of a control rod pressure housing leading to the rapid ejection of the control rod itself. The reactivity insertion produces a transient and a relatively peaked power distribution. If the reactivity insertion is great enough, a prompt transient leads to a large power increase which may result in DNB (Departure from Nucleate Boiling) and fuel damage. The transient is limited by the Doppler reactivity and is terminated by a scram caused by flux signals.

The main reactor parameters affecting the course and magnitude of the transient are typically the ejected rod worth, the delayed neutron fraction, the precursor half-lives, the Doppler feedback, the prompt neutron lifetime and the power peaking. Additional parameters of generally less significance are the moderator reactivity feedback, rod ejection time, trip time and trip reactivity. For this comparison it was not necessary to simulate the transient out to the time of trip.

3.2 MODELING ASSUMPTIONS

The problem chosen for this comparison was the ejection of a single control rod from the reactor at hot zero power conditions. The problem is typical of a large modern PWR core. The hot zero power transient rather than the hot full power case was chosen because it represents a more severe test of the computer programs. The rod worths are generally higher, leading to a prompt critical transient in this case. The power level and fuel temperature increases are also greater. Conclusions drawn from the hot zero power transient will apply to a hot full power transient of similar duration.

A more detailed description of the problem is presented in Appendix B including both ARROTTA and HERMITE inputs. Figure 3-1 shows a core layout with the location of the various fuel types and control rods. The ejected control rod is located one assembly in from the right hand edge of the core along the major axis. As

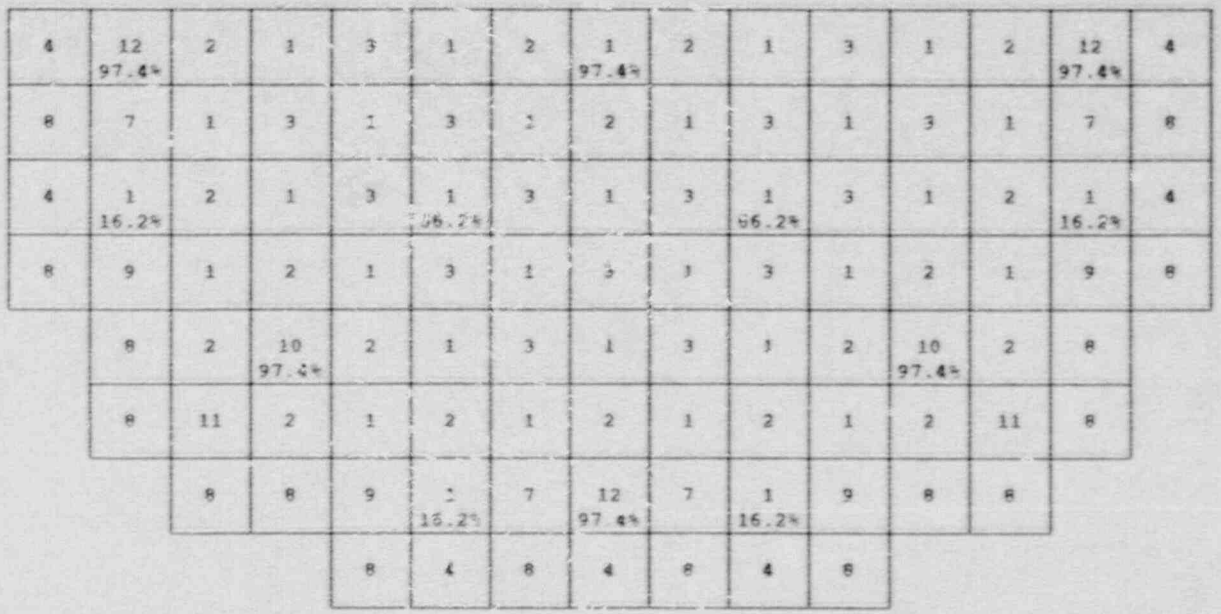

Fuel Type	k-infinity	Fuel Type	k-infinity
1	0.99579	8	1.21973
2	0.98039	9	1.06780
3	1.01849	10	1.13931
4	1.16456	11	1.08233
7	1.03258	12	0.99579

Rod insertion expressed as %-inserted from top of core.

Figure 3-1. Core Layout

such, it was modeled in half core geometry in both ARROTTA and HERMITE. The thermal absorption cross section of the rod to be ejected and its symmetric partners was appropriately increased so that the ejected rod worth was $1.16 in order to create a severe prompt critical transient.

ARROTTA was run with one neutronic mesh and one thermal-hydraulic mesh per fuel assembly. These are the typical mesh structures used in ARROTTA applications. The baffle was also one fuel assembly (21.608 cm) wide. The minimum thickness of the radial reflector was also one assembly mesh (21.608 cm). There were sixteen axial planes with twelve 30.48 cm planes in the core and two 20 cm reflector planes at both the top and bottom of the core.

HERMITE was run with a 2x2 neutronic mesh and one thermal-hydraulic mesh per fuel assembly. These are the typical mesh structures used in HERMITE applications. The baffle was one fuel assembly wide which means it had two 10.804 cm neutronic mesh intervals in it. The radial reflector had a minimum of two mesh intervals of 10.804 cm each. Thus the HERMITE neutronics radial mesh was everywhere finer than the ARROTTA mesh. The HERMITE axial mesh structure was identical to that of ARROTTA. The thermal-hydraulic mesh was also identical in the two codes.

The initial condition was steady state operation with a number of control rods inserted. The rod to be ejected was inserted approximately 97%. The rod was ejected in about 0.10 s at constant velocity. The initial power level was 0.001 MW (which is referred to as "zero power" throughout this report).

The transient was followed out to 0.50 s. ARROTTA used 1 ms timesteps throughout the transient. HERMITE used 10 ms timesteps throughout.

Both moderator density and fuel temperature feedback were used. Since the initial power level is so low and the transient so rapid (~0.40 s) there is no significant moderator heating. The fuel temperature feedback is, therefore, the important phenomenon to model.

Section 4

ANALYSIS RESULTS

4.1 INTRODUCTION

The steady state and transient comparisons between ARROTTA and HERMITE are presented and discussed in this section. Preliminary sensitivity studies using HERMITE are described in Appendix A. These sensitivity studies were used to choose modeling options, such as timestep sizes and to explore the sensitivity of the results. Similar sensitivity studies were performed for ARROTTA in a separate study. These are described in Reference 4.1.

4.2 STEADY STATE CALCULATIONS

The first comparison was at hot zero power, all rods out. The purpose of this case was to assure consistent modeling of cross sections without feedback or control rods effects. The axially integrated radial power distribution and eigenvalue comparisons are shown in Figure 4-1. Edited results demonstrate that the cross sections in both codes are the same. Agreement for this case is good.

The next task was to run an all-rods-out problem at hot full power conditions. The primary purpose of this test was to verify consistent treatment of thermal feedback and the associated cross section changes. The axially integrated radial power distribution and eigenvalue comparisons are shown in Figure 4-2. The agreement is even better than for the zero power case as one would expect because full power conditions with thermal feedback tend to smooth differences. The axial power shapes also show excellent agreement. The fuel temperature comparison is of particular importance since it will impact the power peak during the transient. Figure 4-3 shows the axial distribution of the average fuel temperature for both codes. The maximum difference is about 23°F at a fuel temperature of 1460°F. From an engineering viewpoint this is good agreement.

A steady state comparison for the zero power condition with control rods inserted at their initial conditions for the transient is shown in Figure 4-4. The agreement is again good.

0.5331	0.6255	0.6329	0.8130	0.7624	0.9394	0.[illegible]856	1.1831
0.5439	0.6390	0.6436	0.8254	0.7688	0.9434	[illegible]	1.1751
-2.0%	-2.1%	-1.7%	-1.5%	-0.8%	-0.4%	[illegible]%	0.7%
0.6247	0.5918	0.7571	0.7212	0.9017	0.8574	1.2236	1.2218
0.6390	0.6025	0.7712	0.7299	0.9106	0.8584	1.2195	1.2112
-2.2%	-1.8%	-1.8%	-1.2%	-1.0%	-0.1%	0.3%	0.9%
0.6329	0.7563	0.7068	0.8855	0.8240	1.0018	1.0011	1.1194
0.6436	0.7712	0.7161	0.8963	0.8270	1.0046	0.9934	1.1071
-1.7%	-1.9%	-1.3%	-1.2%	-0.4%	-0.3%	0.8%	1.1%
0.8112	0.7201	0.8846	0.8481	1.0551	1.0245	1.2999	0.9553
0.8254	0.7299	0.8963	0.8518	1.0584	1.0187	1.2868	0.9401
-1.7%	-1.3%	-1.3%	-0.4%	-0.3%	0.5%	1.0%	1.6%
0.7606	0.8989	0.8218	1.0537	1.4200	1.2795	1.4269	
0.7738	0.9106	0.8270	1.0586	1.4133	1.2687	1.4038	
-1.7%	-1.3%	-0.6%	-0.4%	0.5%	0.8%	1.6%	
0.9041	0.8537	0.9579	1.0214	1.2774	1.4139	1.0830	
0.9434	0.8584	1.0046	1.0187	1.2687	1.3917	1.0749	
-1.0%	-0.5%	-0.7%	0.3%	0.7%	1.6%	0.8%	
0.9803	1.2160	0.9947	1.2932	1.4218	1.0821		
0.9925	1.2195	0.9934	1.2868	1.4038	1.0749		
-0.2%	-0.3%	0.1%	0.5%	1.3%	0.7%		
1.1734	1.2137	1.1120	0.9487				
1.1751	1.2112	1.1071	0.9401				
-0.1%	0.2%	0.4%	0.9%				

Legend ARROTTA
KERMITE
%--difference

		Maximum Difference		Standard Deviation
k-effective ARROTTA	1.008527	Positive	1.65%	
k-effective HERMITE	1.008222	Negative	-2.24%	1.00%
Difference	0.000305			

Figure 4-1. ARROTTA-HERMITE Comparison All Rods Out, Hot Zero Power

0.6923	0.7981	0.7805	0.9515	0.8494	0.9776	0.9623	1.1100
0.6937	0.8016	0.7822	0.9554	0.8502	0.9793	0.9609	1.1081
-0.2%	-0.4%	-0.2%	-0.4%	-0.1%	-0.2%	0.2%	0.2%
0.7971	0.7467	0.9175	0.8382	0.9877	0.8876	1.1753	1.1391
0.8016	0.7478	0.9221	0.8394	0.9914	0.8865	1.1752	1.1346
-0.6%	-0.2%	-0.5%	-0.1%	-0.4%	0.1%	0.0%	0.4%
0.7812	0.9169	0.8323	0.9088	0.8779	1.0056	0.9591	1.0452
0.7822	0.9221	0.8333	0.9932	0.8773	1.0088	0.9550	1.0398
-0.1%	-0.6%	-0.1%	-0.4%	0.1%	-0.3%	0.4%	0.5%
0.9506	0.8379	0.9885	0.9022	1.0535	0.9820	1.1929	0.8893
0.9554	0.8394	0.9932	0.9020	1.0569	0.9798	1.1895	0.8811
-0.5%	-0.2%	-0.5%	0.0%	-0.3%	0.2%	0.3%	0.9%
0.8492	0.9865	0.8769	1.0530	1.3205	1.1577	1.2617	
0.8502	0.9914	0.8773	1.0569	1.3198	1.1565	1.2534	
-0.1%	-0.5%	0.0%	-0.4%	0.1%	0.1%	0.7%	
0.9749	0.8867	1.0043	0.9809	1.1568	1.2385	0.9610	
0.9793	0.8865	1.0088	0.9798	1.1565	1.2309	0.9620	
-0.4%	0.0%	-0.4%	0.1%	0.0%	0.6%	-0.1%	
0.9609	1.1724	0.9563	1.1900	1.2594	0.9608		
0.9609	1.1752	0.9550	1.1895	1.2534	0.9620		
0.0%	-0.2%	0.1%	0.0%	0.5%	-0.1%		
1.1063	1.1361	1.0425	0.8863				
1.1081	1.1346	1.0398	0.8811				
-0.2%	0.1%	0.3%	0.6%				

Legend ARROTTA
HERMITE
%--difference

		Maximum Difference		Standard Deviation
k-effective ARROTTA	0.994287	Positive	0.93%	
k-effective HERMITE	0.994345	Negative	-0.56%	0.36%
Difference	-0.00005			

Figure 4-2. ARROTTA-HERMITE Comparison All Rods Out, Hot Full Power

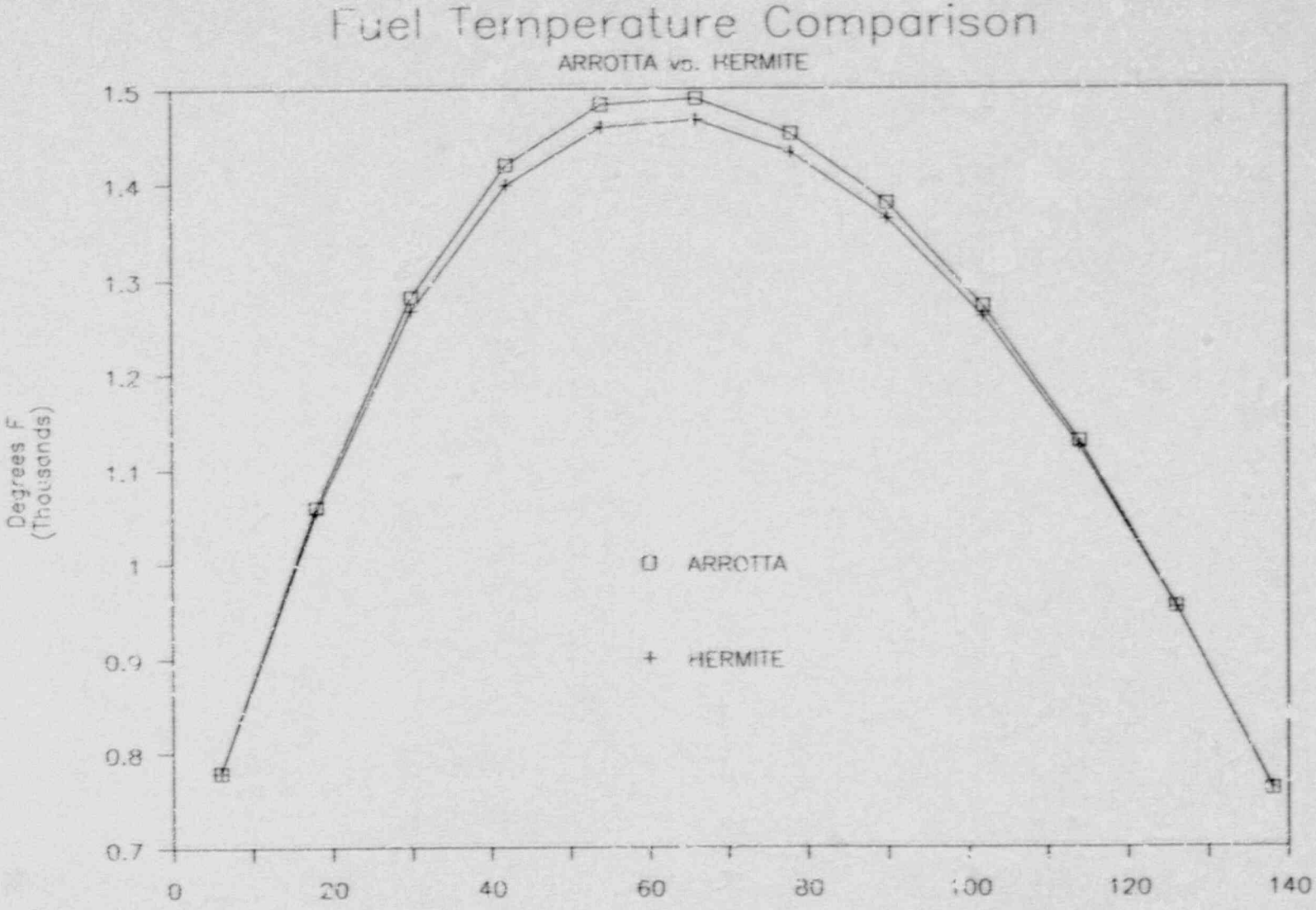

Figure 4-3. Core Average Axial Fuel Temperature Comparison at Hot Full Power

0.2466	0.5372	0.6552	0.8901	0.7886	0.6579	0.1795	0.6846
0.2551	0.5556	0.6742	0.9142	0.8073	0.6984	0.1800	0.5047
-3.3%	-3.3%	-2.8%	-2.6%	-2.3%	-1.5%	-0.2%	0.0%

0.5309	0.5638	0.7228	0.7590	0.9535	0.7629	0.9158	0.8995
0.5556	0.5816	0.7443	0.7763	0.9719	0.7905	0.9152	0.9945
-3.4%	-3.2%	-2.9%	-2.2%	-1.9%	-1.0%	0.1%	0.5%

0.6551	0.7228	0.4994	0.8479	0.8651	1.0859	1.0850	1.2515
0.6742	0.7443	0.5142	0.9644	0.8720	1.0899	1.0786	1.2311
-2.8%	-2.9%	-2.9%	-1.9%	-0.8%	-0.4%	0.7%	1.7%

0.8906	0.7592	0.8472	0.7666	0.9192	1.1162	1.6219	1.2312
0.9142	0.7763	0.8644	0.7765	0.9217	1.1088	1.5987	1.2045
-2.6%	-2.2%	-2.0%	-1.3%	-0.3%	0.7%	1.6%	2.2%

0.7925	0.9533	0.8628	0.9178	0.7205	1.3366	1.8544	
0.8073	0.8719	0.8720	0.9217	0.7187	1.3166	1.8116	
-1.8%	-1.9%	-1.1%	-0.4%	0.2%	1.7%	2.4%	

0.6882	0.7810	1.0807	1.1126	1.3338	1.7107	1.4489	
0.6984	0.7505	1.0899	1.1088	1.3166	1.6710	1.4263	
-1.5%	-1.2%	-0.8%	0.3%	1.5%	2.4%	1.6%	

0.1777	0.8117	1.0790	1.6130	1.8687	1.4479	
0.1800	0.9152	1.0786	1.5987	1.8116	1.4263	
-1.3%	-0.4%	0.0%	0.9%	2.0%	1.5%	

0.6813	0.9928	1.2410	1.2317	
0.6847	0.9945	1.2311	1.2045	
-0.5%	-0.2%	0.8%	1.4%	

Legend ARROTTA
KERMITE
%--difference

		Maximum Difference		Standard Deviation
k-effective ARROTTA	0.987026	Positive	2.37%	
k-effective KERMITE	0.986523	Negative	-3.37%	1.75%
Difference	0.000503			

Figure 4-4. ARROTTA-HERMITE Comparison Rodded, Hot Zero Power

A steady state comparison for zero power conditions with the ejected rod out of the core was also run. The power distribution for this case is shown in Figure 4-5. This case together with the previous one determine the ejected rod worth. The eigenvalue and rod worth are summarized in Table 4-1. The difference in rod worth in these calculations is approximately 0.8 of a cent. To a first order approximation, this difference could be expected to cause a 0.7% change in the heat deposited during the transient.

Overall, the steady state agreement between ARROTTA and HERMITE is very good. Such good agreement means that both codes start the transient from the same set of conditions. The static ejected worths also agree very well. The numerical methods in the two codes have comparable accuracy. This is substantiated by the fact that the transient results compare very favorably as discussed in Section 4.3.

4.3 TRANSIENT CALCULATIONS

Based on the problem definition and the results of the steady state and sensitivity studies described in Appendix A, the 3-D, half-core rod ejection transient was run with HERMITE using 10 ms timesteps. This timestep size is typical for transients of this type in HERMITE. Figures 4-6 and 4-7 display the total core power as a function of time. The plots show exactly the same data, the only difference being that Figure 4-6 uses a logarithmic scale to emphasize the early phase of the transient, while Figure 4-7 uses a linear scale to emphasize the peak power portion of the transient. ARROTTA results using 1 ms timesteps are also shown for comparison. This is a typical timestep size in ARROTTA for this type transient. Agreement is excellent.

Figures 4-8 and 4-9 display, on logarithmic and linear scales respectively, the peak power density from both codes. The location of the peak power (assembly and axial plane) is the same in both ARROTTA and HERMITE. Again, the agreement is excellent.

The core average and maximum fuel temperatures as a function of time are shown in Figures 4-10 and 4-11. The location of the maximum fuel temperature is the same in both codes. The difference in the two curves appears to be due to the 5 ms shift in the time of the power peak rather than any other differences in accuracy of the two codes.

0.0790	0.0227	0.1041	0.1419	0.2015	0.2012	0.2399	0.1906	0.6580	1.0823	1.9373	2.3493	3.4690	4.0659	5.1017
0.0775	0.0225	0.1051	0.1445	0.2064	0.2063	0.2456	0.1952	0.6742	1.0999	1.9667	2.3640	3.4920	4.0657	5.0832
1.9%	0.9%	-1.0%	-1.8%	-2.4%	-2.5%	-2.3%	-2.4%	-2.4%	-1.6%	-1.5%	-1.0%	-0.7%	0.0%	0.4%
0.1158	0.1136	0.1137	0.1677	0.1703	0.2268	0.2533	0.3930	0.6044	1.1275	1.5774	2.6375	3.0115	4.8367	5.0987
0.1131	0.1121	0.1138	0.1702	0.1736	0.2324	0.2600	0.4029	0.6172	1.1482	1.5968	2.6375	3.0231	4.8361	5.0740
2.4%	1.4%	-0.1%	-1.5%	-1.9%	-2.4%	-2.6%	-2.3%	-2.1%	-1.8%	-1.2%	-1.1%	-0.4%	0.0%	0.5%
0.1456	0.1329	0.1501	0.1466	0.1873	0.1608	0.3405	0.4356	0.6658	0.6512	1.5298	1.9722	3.0091	3.4550	4.2362
0.1408	0.1302	0.1495	0.1473	0.1902	0.1645	0.3496	0.4452	0.6815	0.6619	1.5508	1.9823	3.0250	3.4450	4.2116
3.4%	2.1%	0.4%	-0.5%	-1.5%	-2.3%	-2.6%	-2.1%	-1.7%	-1.6%	-1.4%	-0.5%	-0.5%	0.3%	0.6%
0.1448	0.1987	0.1496	0.1516	0.1697	0.2616	0.3329	0.5393	0.6168	0.9221	1.2125	1.6972	2.3683	3.7955	3.1816
0.1392	0.1932	0.1474	0.1517	0.1721	0.2671	0.3396	0.5508	0.6268	0.9333	1.1226	1.7062	2.3637	3.7707	3.1530
4.0%	2.8%	1.5%	-0.1%	-1.4%	-2.0%	-2.0%	-2.1%	-1.6%	-1.2%	-0.9%	-0.5%	0.2%	0.7%	0.9%
	0.2323	0.1789	0.1164	0.1960	0.2455	0.3775	0.4465	0.7148	0.8116	1.0542	1.0288	2.2321	3.3731	
	0.2242	0.1744	0.1159	0.1979	0.2490	0.3854	0.4514	0.7251	0.8167	1.0556	1.0295	2.2138	3.3319	
	3.6%	2.6%	0.4%	-1.0%	-1.4%	-2.0%	-1.5%	-1.4%	-0.6%	-0.1%	-0.1%	0.8%	1.2%	
	0.1881	0.2381	0.2138	0.2183	0.2720	0.2689	0.3637	0.5632	0.9249	1.1031	1.9446	2.3172	2.1872	
	0.1833	0.2314	0.2107	0.2182	0.2754	0.2733	0.3685	0.5668	0.9304	1.0948	1.5265	2.2812	2.1803	
	2.6%	2.9%	1.5%	0.1%	-1.3%	-1.6%	-1.3%	-0.6%	-0.6%	0.3%	1.2%	1.6%	0.3%	
		0.2105	0.3006	0.3079	0.2491	0.2690	0.0879	0.6416	0.0682	1.4764	1.9482	1.7273		
		0.2069	0.2949	0.3061	0.2505	0.2702	0.0888	0.6429	0.8650	1.4636	1.9129	1.7088		
		1.7%	1.9%	0.6%	-0.6%	-0.5%	-1.0%	-0.2%	0.4%	0.9%	1.9%	1.1%		
				0.2395	0.2838	0.2897	0.3226	0.6660	0.9557	1.0460				
				0.2372	0.2828	0.2925	0.3237	0.6641	0.9659	1.0288				
				1.0%	0.3%	-1.0%	-0.3%	0.3%	1.0%	1.7%				

Legend ARROTTA
HERMITE
%--difference

	Maximum Difference			Standard Deviation
k-effective ARROTTA	0.99547	Positive	3.99%	
k-effective HERMITE	0.99503	Negative	-2.60%	1.25%
Difference	0.00044			

Figure 4-5. ARROTTA-HERMITE Comparison Static Ejected Worth

Table 4-1

EIGENVALUE AND EJECTED ROD WORTH COMPARISONS

k - effective

Code	Rods In	Ejected Rod Out	Change in k-effective	$
ARROTTA	0.987027	0.995479	0.008452	1.158
HERMITE	0.986523	0.995033	0.008510	1.166
Beta Effective		0.00729634		

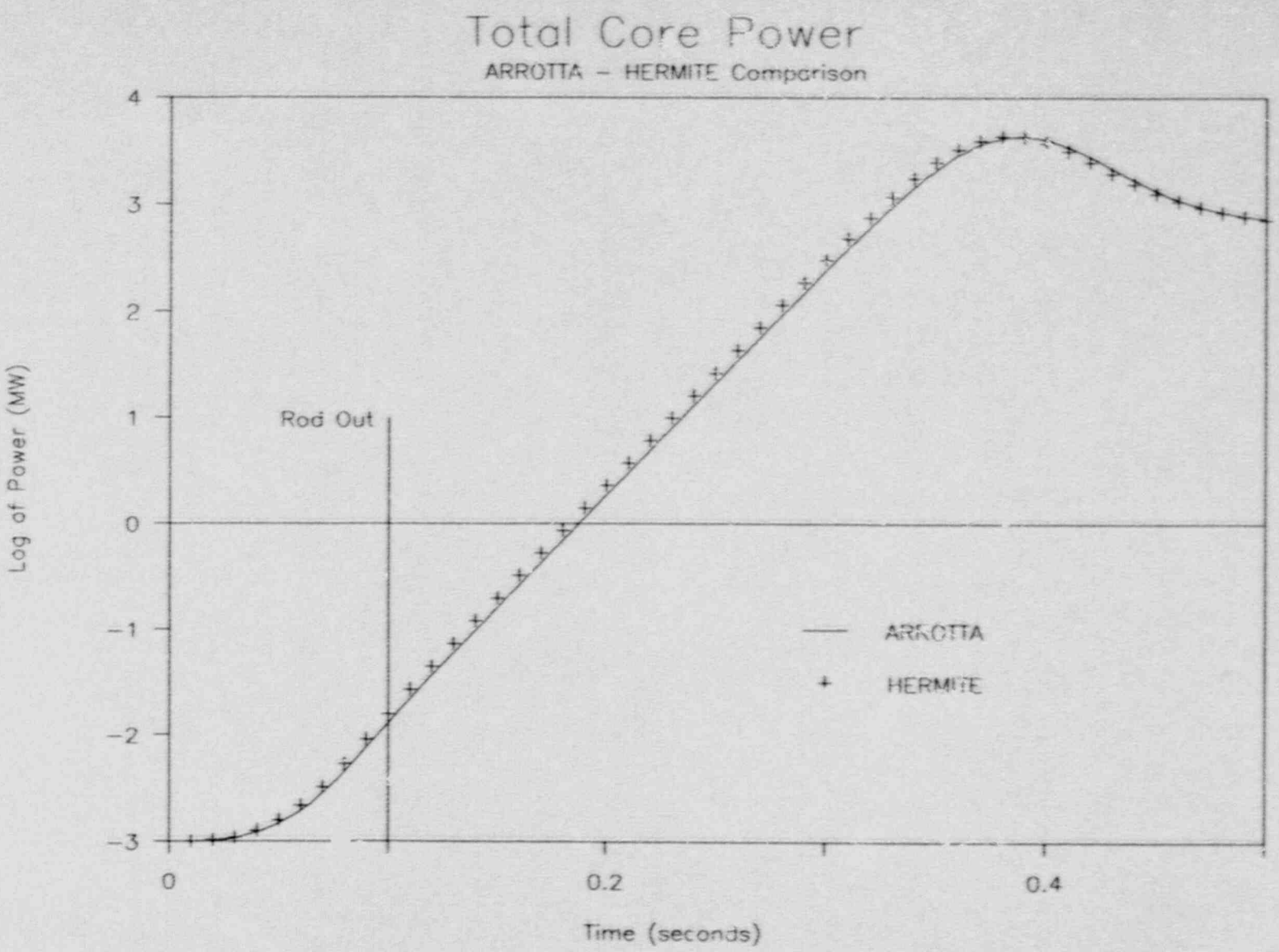

Figure 4-6. ARROTTA-HERMITE Comparison of Total Core Power

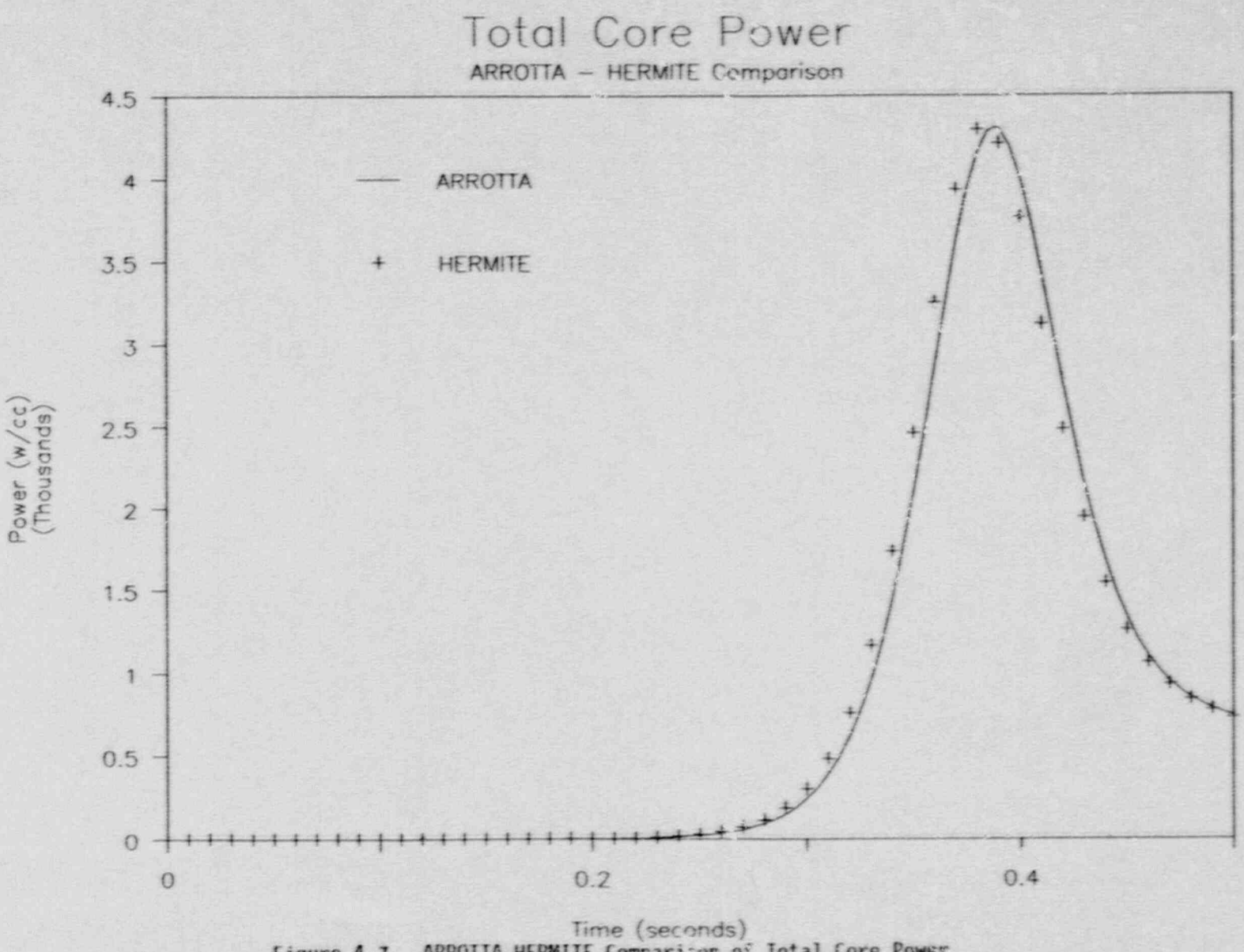

Figure 4-7. ARROTTA-HERMITE Comparison of Total Core Power

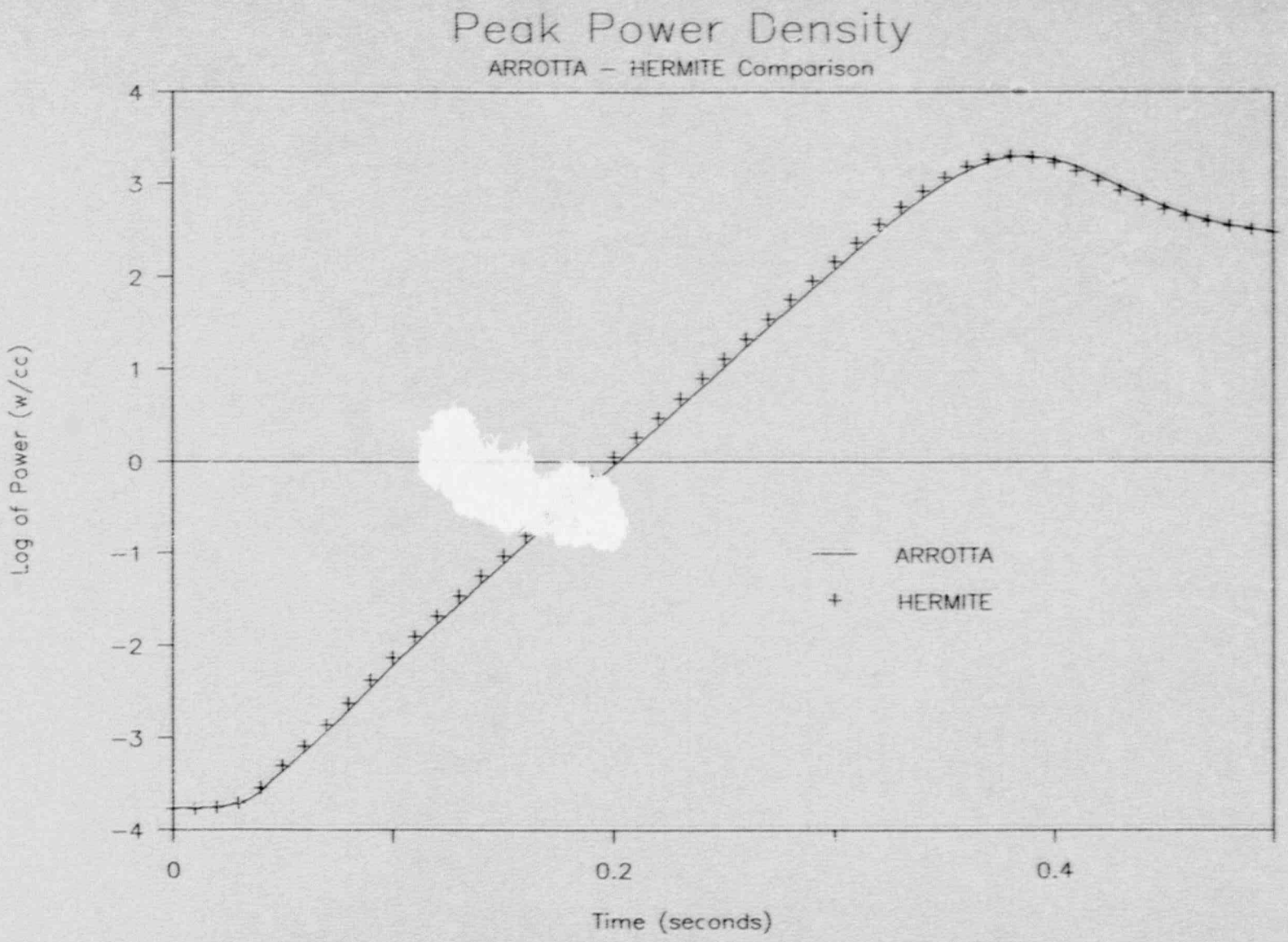

Figure 4-8. ARROTTA-HERMITE Comparison of Peak Power Density

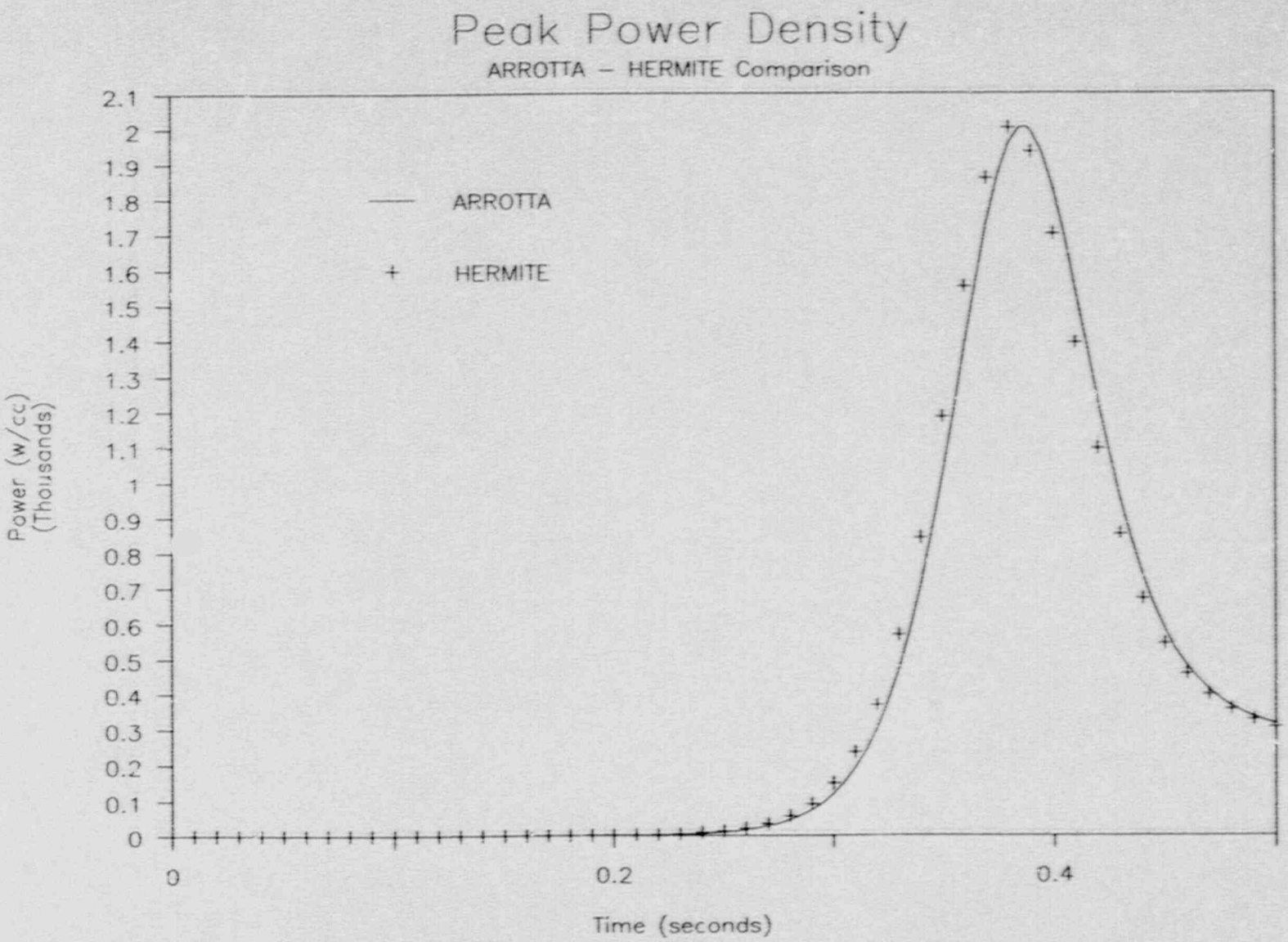

Figure 4-9. ARROTTA-HERMITE Comparison of Peak Power Density

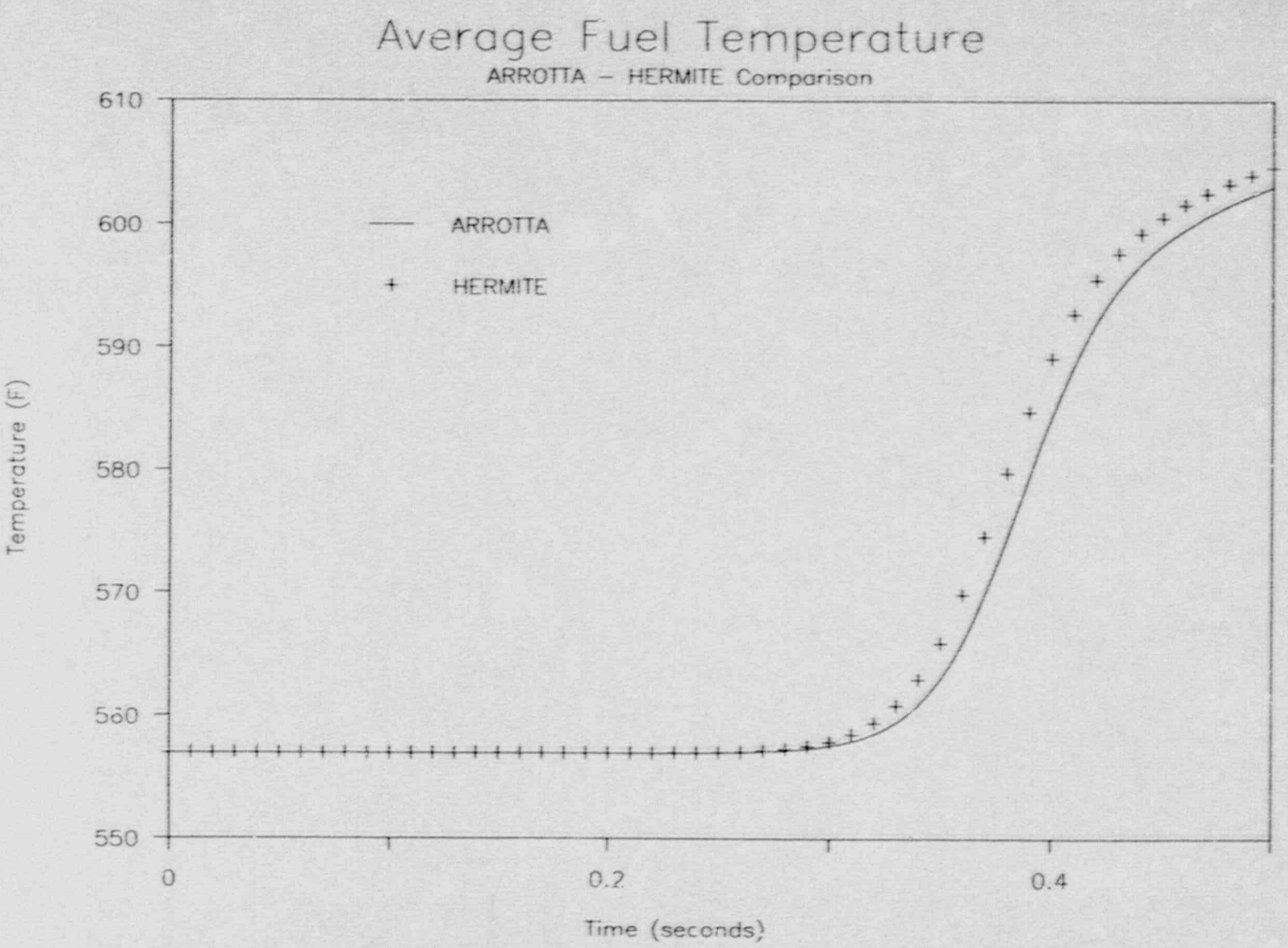

Figure 4-10. ARROTTA-HERMITE Comparison of Core Average Fuel Temperature

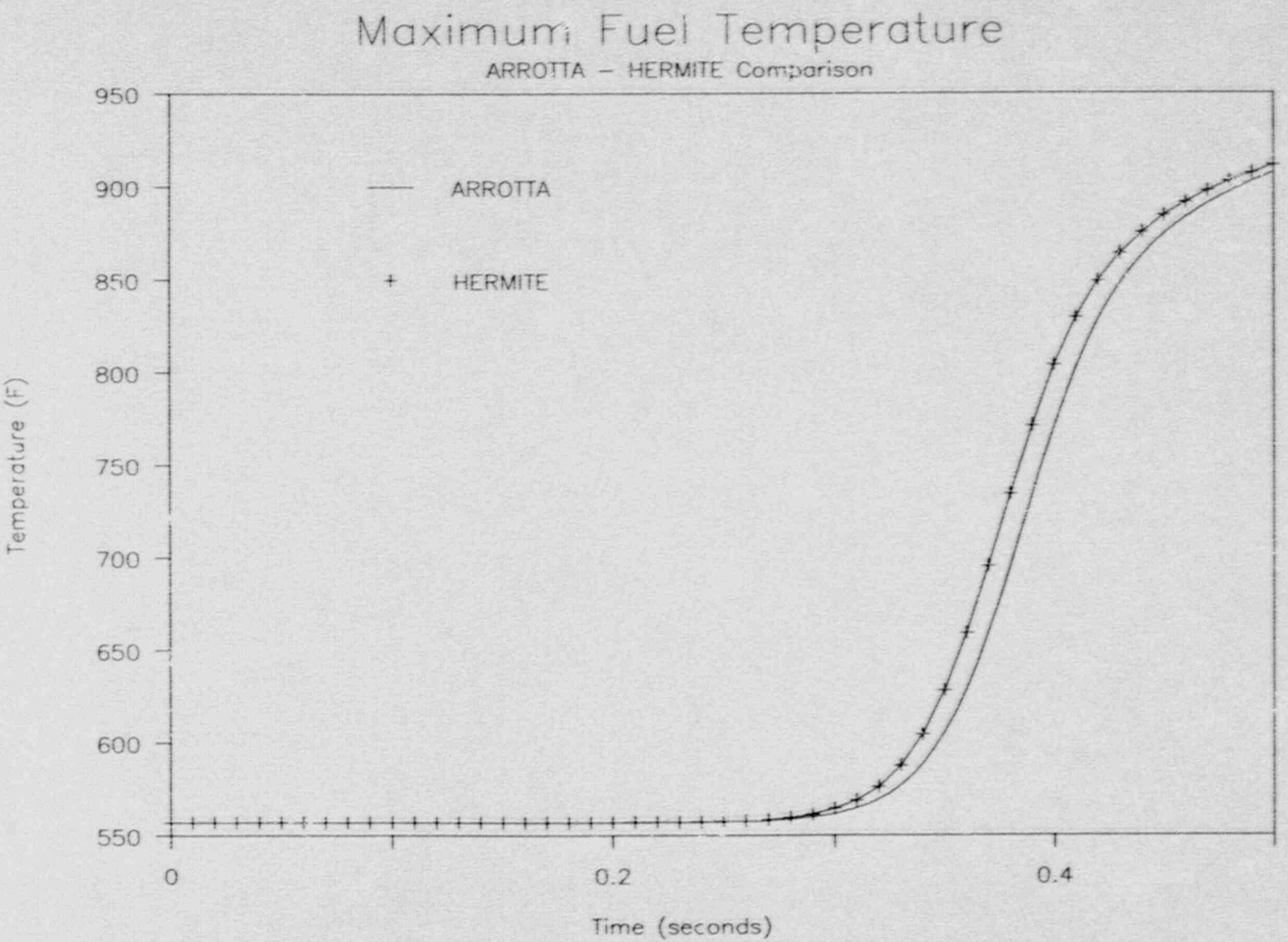

Figure 4-11. ARROTTA-HERMITE Comparison of Maximum Fuel Temperature

Selected transient results are summarized in tabular form in Table 4-2.

Comparisons of normalized radial power distributions at several points during the transient have been made. The first comparison, Figure 4-12, was made at 0.20 s, a point before significant heat is added to the core. In both ARROTTA and HERMITE the peak fuel temperature has risen less than 0.1 °F. The assembly powers differ by almost a factor of 70 across the core. (Because of the large variation in power, numerical differences rather than %-differences are shown on the transient radial power distribution comparisons.) The agreement between ARROTTA and HERMITE is excellent. The second comparison is made at 0.23 s, the point where the relative power distribution is most peaked. The agreement shown in Figure 4-13 is again excellent. The third comparison, Figure 4-14, is at the 0.39 s, a point near the peak in total core power and peak assembly power. The fourth comparison, Figure 4-15, is at 0.50 s, the last analyzed time in the transient. Again, the agreement is excellent.

Table 4-2

SELECTED TRANSIENT RESULTS

Quantity	ARROTTA	HERMITE
Maximum total core power (MW)	4308	4339
Time of maximum total core power (s)	0.388	0.383
Maximum assembly power density (w/cc)	2005	2014
Time of maximum assembly power density (s)	0.387	0.382
Average fuel temperature (°F)		
.2 s	557	557
.3 s	558	558
.4 s	584	589
.5 s	603	605
Maximum fuel temperature (°F)		
.2 s	557	557
.3 s	562	565
.4 s	770	804
.5 s	907	911

0.0751	0.0218	0.1002	0.1372	0.1962	0.1973	0.2369	0.1894	0.6556	1.0795	1.9355	2.3412	3.4762	4.0788	5.1233
0.0775	0.0225	0.1046	0.1434	0.2049	0.2048	0.2440	0.1942	0.6709	1.0948	1.9601	2.3580	3.4893	4.0665	5.0892
-0.0024	-0.0007	-0.0044	-0.0062	-0.0087	-0.0075	-0.0071	-0.0048	-0.0153	-0.0153	-0.0246	-0.0168	-0.0131	0.0124	0.0341
0.1100	0.1085	0.1091	0.1621	0.1657	0.2226	0.2502	0.3903	0.6018	1.1250	1.5758	2.6091	3.0174	4.8857	5.1215
0.1131	0.1119	0.1133	0.1691	0.1723	0.2308	0.2582	0.4007	0.6139	1.1434	1.5912	2.6320	3.0201	4.8403	5.0807
-0.0031	-0.0034	-0.0042	-0.0070	-0.0066	-0.0082	-0.0080	-0.0104	-0.0121	-0.0184	-0.0154	-0.0229	-0.0027	0.0454	0.0408
0.1385	0.1268	0.1440	0.1416	0.1824	0.1579	0.3367	0.4323	0.6668	0.6496	1.5294	1.9739	3.0171	3.4672	4.2554
0.1407	0.1299	0.1490	0.1465	0.1891	0.1635	0.3475	0.4426	0.6783	0.6594	1.5467	1.9785	3.0242	3.4468	4.2175
-0.0022	-0.0031	-0.0050	-0.0049	-0.0067	-0.0056	-0.0108	-0.0103	-0.0115	-0.0098	-0.0173	-0.0046	-0.0071	0.0204	0.0379
0.1379	0.1898	0.1435	0.1466	0.1655	0.2572	0.3291	0.5353	0.6142	0.9208	1.1127	1.7010	2.3761	3.8133	3.1966
0.1392	0.1932	0.1471	0.1512	0.1711	0.2656	0.3376	0.5481	0.6241	0.9308	1.1203	1.7055	2.3646	3.7771	3.1580
-0.0013	-0.0034	-0.0036	-0.0046	-0.0056	-0.0084	-0.0085	-0.0128	-0.0099	-0.0100	-0.0076	-0.0045	0.0115	0.0362	0.0386
	0.2224	0.1719	0.1128	0.1914	0.2412	0.3732	0.4415	0.7128	0.8111	1.0562	1.0332	2.2436	3.3913	
	0.2243	0.1745	0.1158	0.1972	0.2478	0.3837	0.4495	0.7231	0.8152	1.0556	1.0314	2.2190	3.3399	
	-0.0019	-0.0026	-0.0030	-0.0058	-0.0066	-0.0105	-0.0080	-0.0103	-0.0041	0.0006	0.0018	0.0246	0.0515	
	0.1805	0.2296	0.2073	0.2129	0.2670	0.2656	0.3619	0.5625	0.9263	1.1066	1.5530	2.3318	2.2001	
	0.1835	0.2317	0.2108	0.2178	0.2747	0.2724	0.3677	0.5661	0.9306	1.1012	1.5312	2.2894	2.1868	
	-0.0030	-0.0021	-0.0035	-0.0049	-0.0077	-0.0068	-0.0058	-0.0036	-0.0043	0.0054	0.0218	0.0424	0.0133	
		0.2032	0.2917	0.3005	0.2444	0.2658	0.0877	0.6427	0.8705	1.4832	1.9400	1.7378		
		0.2072	0.2951	0.3061	0.2502	0.2702	0.0890	0.6438	0.8663	1.4678	1.9193	1.7148		
		-0.0040	-0.0034	-0.0056	-0.0058	-0.0044	-0.0013	-0.0011	0.0042	0.0154	0.0408	0.0230		
				0.2340	0.2787	0.2865	0.3220	0.6676	0.9591	1.0506				
				0.2373	0.2829	0.2928	0.3244	0.6656	0.9483	1.0312				
				-0.0033	-0.0042	-0.0063	-0.0024	0.0020	0.0108	0.0194				

Maximum Difference		Standard Deviation
Positive	0.0515	
Negative	-0.0246	0.0155

Legend: ARROTTA / HERMITE / Difference

Figure 4-12. ARROTTA-HERMITE Comparison of Radial Power Distributions at 0.20s

0.0749	0.0217	0.1000	0.1370	0.1960	0.1972	0.2368	0.1894	0.6556	1.0796	1.9359	2.3417	3.4769	4.0797	5.1245
0.0773	0.0224	0.1044	0.1433	0.2047	0.2047	0.2439	0.1942	0.6710	1.0950	1.9604	2.3584	3.4899	4.0671	5.0901
-0.0024	-0.0007	-0.0044	-0.0063	-0.0087	-0.0075	-0.0071	-0.0048	-0.0154	-0.0154	-0.0245	-0.0167	-0.0130	0.0126	0.0345
0.1097	0.1082	0.1089	0.1618	0.1655	0.2224	0.2501	0.3902	0.6018	1.1125	1.5761	2.6096	3.0180	4.8567	5.1227
0.1128	0.1116	0.1131	0.1689	0.1722	0.2307	0.2581	0.4007	0.6140	1.1436	1.5915	2.6325	3.0206	4.8411	5.0815
-0.0031	-0.0034	-0.0042	-0.0071	-0.0067	-0.0083	-0.0080	-0.0105	-0.0122	-0.0311	-0.0154	-0.0229	-0.0026	0.0156	0.0412
0.1381	0.1265	0.1437	0.1414	0.1822	0.1578	0.3366	0.4322	0.6668	0.6497	1.5296	1.9743	3.0177	3.4679	4.2563
0.1404	0.1297	0.1487	0.1463	0.1889	0.1634	0.3474	0.4426	0.6783	0.6595	1.5469	1.9789	3.0247	3.4473	4.2182
-0.0023	-0.0032	-0.0050	-0.0049	-0.0067	-0.0056	-0.0108	-0.0104	-0.0115	-0.0098	-0.0173	-0.0046	-0.0070	0.0206	0.0381
0.1375	0.1893	0.1432	0.1463	0.1653	0.2570	0.3289	0.5352	0.6142	0.9209	1.1129	1.7013	2.3765	3.8140	3.1973
0.1389	0.1928	0.1468	0.1509	0.1710	0.2655	0.3375	0.5480	0.6241	0.9308	1.1205	1.7057	2.3650	3.7776	3.1585
-0.0014	-0.0035	-0.0036	-0.0046	-0.0057	-0.0085	-0.0086	-0.0128	-0.0099	-0.0099	-0.0076	-0.0044	0.0115	0.0364	0.0388
	0.2218	0.1715	0.1126	0.1911	0.2410	0.3730	0.4414	0.7127	0.8111	1.0563	1.0334	2.2440	3.3919	
	0.2239	0.1742	0.1157	0.1970	0.2477	0.3835	0.4494	0.7231	0.8152	1.0557	1.0315	2.2193	3.3403	
	-0.0021	-0.0027	-0.0031	-0.0059	-0.0067	-0.0105	-0.0080	-0.0104	-0.0041	0.0006	0.0019	0.0248	0.0516	
	0.1800	0.2290	0.2069	0.2126	0.2667	0.2654	0.3618	0.5625	0.9263	1.1067	1.5532	2.3322	2.2005	
	0.1831	0.2313	0.2105	0.2175	0.2745	0.2723	0.3676	0.5661	0.9306	1.1013	1.5313	2.2897	2.1870	
	-0.0031	-0.0023	-0.0036	-0.0049	-0.0078	-0.0069	-0.0058	-0.0036	-0.0043	0.0054	0.0219	0.0425	0.0135	
		0.2027	0.2911	0.3001	0.2441	0.2656	0.0877	0.6427	0.8705	1.4833	1.9602	1.7381		
		0.2068	0.2946	0.3058	0.2500	0.2700	0.0889	0.6438	0.8663	1.4678	1.9194	1.7150		
		-0.0041	-0.0035	-0.0057	-0.0059	-0.0044	-0.0012	-0.0011	0.0042	0.0155	0.0408	0.0232		
				0.2337	0.2784	0.2862	0.3219	0.6675	0.9591	1.0507				
				0.2370	0.2827	0.2926	0.3243	0.6656	0.9483	1.0312				
				-0.0033	-0.0043	-0.0064	-0.0024	0.0019	0.0108	0.0195				

Maximum Difference		Standard Deviation
Positive	0.0516	
Negative	-0.0311	0.0151

Legend: ARROTTA / HERMITE / Difference

Figure 4-13. ARROTTA-HERMITE Comparison of Radial Power Distributions at 0.23s

0.0928	0.0265	0.1197	0.1608	0.2244	0.2193	0.2554	0.1969	0.6655	1.0799	1.9099	2.2831	3.3505	3.9010	4.8849
0.0965	0.0276	0.1258	0.1693	0.2357	0.2288	0.2641	0.2022	0.6816	1.0953	1.9328	2.2965	3.3567	3.8979	4.8357
-0.0037	-0.0011	-0.0061	-0.0085	-0.0113	-0.0095	-0.0087	-0.0054	-0.0161	-0.0154	-0.0229	-0.0134	-0.0062	0.0031	0.0492
0.1359	0.1327	0.1310	0.1904	0.1897	0.2469	0.2692	0.4073	0.6140	1.1273	1.5570	2.5457	2.9125	4.6441	4.8886
0.1407	0.1379	0.1370	0.1999	0.1985	0.2574	0.2788	0.4192	0.6270	1.1458	1.5713	2.5648	2.9098	4.6183	4.8323
-0.0048	-0.0052	-0.0060	-0.0095	-0.0088	-0.0105	-0.0096	-0.0119	-0.0130	-0.0185	-0.0143	-0.0191	0.0027	0.0258	0.0563
0.1709	0.1555	0.1738	0.1669	0.2090	0.1750	0.3622	0.4544	0.6867	0.6559	1.5164	1.9329	2.9208	3.3312	4.0774
0.1750	0.1605	0.1811	0.1738	0.2179	0.1820	0.3750	0.4665	0.6995	0.6659	1.5326	1.9352	2.9227	3.3040	4.0287
-0.0041	-0.0050	-0.0073	-0.0069	-0.0089	-0.0070	-0.0128	-0.0121	-0.0128	-0.0100	-0.0162	-0.0023	-0.0019	0.0272	0.0487
0.1699	0.2324	0.1737	0.1730	0.1895	0.2857	0.3558	0.5659	0.6371	0.9368	1.1123	1.6736	2.3143	3.6865	3.0817
0.1728	0.2383	0.1794	0.1796	0.1971	0.2964	0.3665	0.5811	0.6486	0.9478	1.1197	1.6763	2.2994	3.6434	3.0358
-0.0029	-0.0059	-0.0057	-0.0066	-0.0076	-0.0107	-0.0107	-0.0152	-0.0115	-0.0110	-0.0074	-0.0027	0.0149	0.0431	0.0459
	0.2714	0.2079	0.1333	0.2197	0.2696	0.4061	0.4688	0.7423	0.8316	1.0664	1.0254	2.2011	3.3105	
	0.2758	0.2125	0.1378	0.2276	0.2785	0.4191	0.4788	0.7545	0.8368	1.0661	1.0229	2.1736	3.2520	
	-0.0044	-0.0046	-0.0045	-0.0079	-0.0089	-0.0130	-0.0100	-0.0122	-0.0052	0.0003	0.0025	0.0275	0.0585	
	0.2191	0.2761	0.2452	0.2465	0.3015	0.2918	0.3850	0.5868	0.9535	1.1254	1.5573	2.3110	2.1681	
	0.2245	0.2806	0.2509	0.2536	0.3118	0.3006	0.3924	0.5918	0.9591	1.1203	1.5349	2.2659	2.1502	
	-0.0054	-0.0045	-0.0057	-0.0071	-0.0103	-0.0088	-0.0074	-0.0050	-0.0056	0.0051	0.0224	0.0451	0.0179	
		0.2432	0.3445	0.3487	0.2782	0.2952	0.0934	0.6702	0.8989	1.5141	1.9778	1.7383		
		0.2496	0.3507	0.3573	0.2863	0.3015	0.0950	0.6725	0.8958	1.4991	1.9360	1.7133		
		-0.0064	-0.0062	-0.0086	-0.0081	-0.0063	-0.0016	-0.0023	0.0031	0.0150	0.0418	0.0250		
				0.2710	0.3173	0.3182	0.3440	0.6982	0.9933	1.0793				
				0.2762	0.3238	0.3266	0.3476	0.6975	0.9834	1.0599				
				-0.0052	-0.0065	-0.0084	-0.0036	0.0007	0.0099	0.0194				

Maximum Difference		Standard Deviation
Positive	0.0585	
Negative	-0.0229	0.0173

Legend: ARROTTA / HERMITE / Difference

Figure 4-14. ARROTTA-HERMITE Comparison of Radial Power Distributions at 0.39s

0.1201	0.0338	0.1486	0.1949	0.2640	0.2491	0.2793	0.2059	0.6755	1.0761	1.8724	2.2065	3.1931	3.6777	4.5773
0.1247	0.0352	0.1561	0.2053	0.2775	0.2602	0.2894	0.2117	0.6919	1.0914	1.8936	2.2173	3.1941	3.6500	4.5226
-0.0046	-0.0014	-0.0075	-0.0104	-0.0135	-0.0111	-0.0101	-0.0058	-0.0164	-0.0153	-0.0212	-0.0106	-0.0010	0.0277	0.0547
0.1757	0.1693	0.1636	0.2314	0.2235	0.2798	0.2934	0.4278	0.6267	1.1261	1.5287	2.4621	2.7798	4.3792	4.8844
0.1818	0.1762	0.1711	0.2431	0.2340	0.2920	0.3043	0.4407	0.6404	1.1446	1.5420	2.4781	2.7731	4.3454	4.5236
-0.0061	-0.0065	-0.0075	-0.0117	-0.0105	-0.0122	-0.0109	-0.0129	-0.0137	-0.0185	-0.0133	-0.0160	0.0067	0.0338	0.0608
0.2208	0.1993	0.2185	0.2038	0.2465	0.1979	0.3945	0.4809	0.7087	0.6615	1.4954	1.8773	2.7979	3.1576	3.8458
0.2259	0.2056	0.2276	0.2122	0.2573	0.2061	0.4089	0.4941	0.7227	0.6720	1.5107	1.8780	2.7959	3.1262	3.7930
-0.0051	-0.0063	-0.0091	-0.0084	-0.0108	-0.0082	-0.0144	-0.0132	-0.0140	-0.0105	-0.0153	-0.0007	0.0020	0.0314	0.0528
0.2191	0.2976	0.2194	0.2119	0.2233	0.3240	0.3899	0.6029	0.6630	0.9528	1.1074	1.6355	2.2316	3.5195	2.9293
0.2227	0.3049	0.2263	0.2199	0.2323	0.3365	0.4019	0.6196	0.6753	0.9643	1.1145	1.6368	2.2144	3.4723	2.8810
-0.0036	-0.0073	-0.0069	-0.0080	-0.0090	-0.0125	-0.0120	-0.0167	-0.0123	-0.0115	-0.0071	-0.0013	0.0172	0.0472	0.0483
	0.3462	0.2625	0.1636	0.2599	0.3084	0.4487	0.5020	0.7758	0.8528	1.0743	1.0132	2.1408	3.1924	
	0.3515	0.2681	0.1690	0.2692	0.3186	0.4634	0.5131	0.7890	0.8582	1.0740	1.0099	2.1111	3.1319	
	-0.0053	-0.0056	-0.0054	-0.0093	-0.0102	-0.0147	-0.0111	-0.0132	-0.0054	0.0003	0.0034	0.0297	0.0606	
	0.2780	0.3465	0.3014	0.2947	0.3494	0.3265	0.4136	0.6143	0.9823	1.1421	1.5549	2.2733	2.1157	
	0.2845	0.3517	0.3081	0.3031	0.3614	0.3365	0.4219	0.6198	0.9881	1.1365	1.5314	2.2263	2.0955	
	-0.0065	-0.0052	-0.0067	-0.0084	-0.0120	-0.0100	-0.0083	-0.0056	-0.0058	0.0056	0.0235	0.0470	0.0202	
		0.3033	0.4226	0.4185	0.3258	0.3354	0.1007	0.7016	0.9290	1.5432	1.9862	1.7269		
		0.3108	0.4297	0.4284	0.3351	0.3429	0.1025	0.7042	0.9258	1.5274	1.9435	1.7012		
		-0.0075	-0.0071	-0.0099	-0.0093	-0.0075	-0.0018	-0.0026	0.0032	0.0158	0.0427	0.0257		
				0.3241	0.3720	0.3619	0.3720	0.7333	1.0301	1.1070				
				0.3301	0.3794	0.3713	0.3761	0.7328	1.0199	1.0876				
				-0.0060	-0.0074	-0.0094	-0.0041	0.0005	0.0102	0.0194				

Maximum Difference		Standard Deviation
Positive	0.0608	
Negative	-0.0212	0.0187

Legend: ARROTTA
HERMITE
Difference

Figure 4-15. ARROTTA-HERMITE Comparison of Radial Power Distributions at 0.50s

4.4 SUMMARY

Excellent agreement has been obtained in all phases of these comparisons. This includes steady-state radial power distributions at hot zero power conditions, with rods out, rods inserted and the ejected rod out. The steady-state eigenvalues and the ejected rod worth also show comparable agreement. The hot full power case demonstrates acceptable agreement in fuel temperature.

The 3-D rod ejection transient at hot zero power conditions showed excellent agreement between ARROTTA and HERMITE in the important parameters: total core power, peak assembly power, core average fuel temperature and maximum fuel temperature.

4.5 REFERENCES

4.1 K. Doran, B. Zolotar, "PWR Rod Ejection Accident ARROTTA Sensitivity Studies," Electric Power Research Institute (to be issued).

Section 5

CONCLUSIONS

The following conclusions can be drawn from this study:

1. The ARROTTA code, using a 1x1 mesh, showed acceptable agreement with itself using a 2x2 mesh and with HERMITE using a 2x2 mesh. A 1x1 mesh is, therefore, adequate for ARROTTA applications such as the rod ejection accident and for both rodded and unrodded static calculations.

2. Twelve axial planes to model the active core is adequate based on the sensitivity studies using HERMITE and the ARROTTA-HERMITE comparisons.

3. The good agreement of key parameters for the 3-D rod ejection transient initiated at hot zero power conditions served to verify the transient neutronics, transient fuel temperature, transient control rod motion and transient cross section treatments in ARROTTA. The ARROTTA code can, therefore, be reliably used for any rod ejection type transient, including transients up to hot full power conditions.

4. The analysis and sensitivity studies performed for the rod ejection transient showed that the peak power, for both ARROTTA and HERMITE, decreases as timesteps are made smaller. This means that results can be biased in the conservative direction (higher peak power) by using larger timesteps.

5. The ARROTTA and HERMITE static fuel temperature calculations showed reasonable agreement.

Appendix A

HERMITE SENSITIVITY STUDIES

The objective of this study was to model as closely as possible in HERMITE the same problem that had been run in ARROTTA. Further, it was necessary to assure that the HERMITE case was converged and as accurate as possible. To do this a number of sensitivity studies were run to select options for the 3-D rod ejection analysis. These sensitivity studies are described in this appendix.

The first set of sensitivity studies examines the sensitivity to the radial mesh. ARROTTA is typically run with one mesh interval in a fuel assembly (referred to as a 1x1 mesh). HERMITE typically uses a 2x2 mesh in each fuel assembly. HERMITE cases were run with both a 1x1 and 2x2 mesh structure and the results are shown in Figure A-1. The assembly powers change by up to about 4% with a general shift in power towards the core periphery as the mesh becomes finer. ARROTTA results for 1x1 and 2x2 meshes were run as part of a separate study (Reference 4.1) and the results are reproduced here as Figure A-2. In ARROTTA, the assembly powers change by less than 1% with a general shift in power towards the core center as the mesh becomes finer. An examination of the pattern of the differences suggests that the two methods are converging to the same powers but from opposite directions--HERMITE powers are higher in the center of the core but decrease with the finer mesh, while the ARROTTA power is lower in the center of the core but increases with the finer mesh. Additional cases with a finer mesh would be required to estimate the order of the two methods and to extrapolate the results to zero mesh spacing. This is beyond the scope of this study. For purposes of this study, it was decided to use the 1x1 mesh in ARROTTA and the 2x2 mesh in HERMITE.

Sensitivity of results to the axial mesh structure was also addressed in this study with HERMITE. The HERMITE study employed a 3-D model as well as a 1-D axial model of the core with cross sections taken from a steady-state, hot zero power, all rods out volume-weighted edit. The purpose of this analysis was to look at axial mesh spacing effects and no serious attempt was made to produce an axial

0.5610	0.6579	0.6613	0.8431	0.7815	0.9512	0.9839	1.1612
0.5439	0.6390	0.6436	0.8254	0.7688	0.9434	0.9825	1.1751
3.1%	3.0%	2.7%	2.1%	1.6%	0.8%	0.1%	-1.2%
0.6579	0.6201	0.7903	0.7457	0.9238	0.8659	1.2167	1.1948
0.6390	0.6025	0.7712	0.7299	0.9106	0.8584	1.2195	1.2112
3.0%	2.9%	2.5%	2.2%	1.4%	0.9%	-0.2%	-1.4%
0.6613	0.7903	0.7331	0.9116	0.8377	1.0079	0.9939	1.0922
0.6436	0.7712	0.7161	0.8963	0.8270	1.0046	0.9934	1.1071
2.7%	2.5%	2.4%	1.7%	1.3%	0.3%	0.1%	-1.3%
0.8431	0.7457	0.9116	0.8634	1.0653	1.0211	1.2772	0.9150
0.8254	0.7299	0.8963	0.8518	1.0584	1.0187	1.2868	0.9401
2.1%	2.2%	1.7%	1.4%	0.7%	0.2%	-0.7%	-2.7%
0.7815	0.9238	0.8377	1.0653	1.4128	1.2643	1.3746	
0.7688	0.9106	0.8270	1.0584	1.4133	1.2687	1.4038	
1.6%	1.4%	1.3%	0.7%	0.0%	-0.3%	-2.1%	
0.9512	0.8659	1.0079	1.0211	1.2643	1.3731	1.0357	
0.9434	0.8584	1.0046	1.0187	1.2687	1.3917	1.0749	
0.8%	0.9%	0.3%	0.2%	-0.3%	-1.3%	-3.6%	
0.9839	1.2167	0.9939	1.2772	1.3746	1.0357		
0.9825	1.2195	0.9934	1.2868	1.4038	1.0749		
0.1%	-0.2%	0.1%	-0.7%	-2.1%	-3.6%		
1.1612	1.1948	1.0922	0.9150				
1.1751	1.2112	1.1071	0.9401				
-1.2%	-1.4%	-1.3%	-2.7%				

Legend HERMITE 1x1
HERMITE 2x2
%--difference

				Maximum Difference		Standard Deviation
k-effective 1x1		1.007677	Positive	3.14%		
k-effective 2x2		1.008222	Negative	-3.65%		1.62%
Difference		-0.00054				

Figure A-1. HERMITE Comparison of 2x2 and 1x1 Mesh Structures

0.5327	0.6260	0.6335	0.8132	0.7624	0.9391	0.9851	1.1823
0.5362	0.6302	0.6359	0.8172	0.7635	0.9402	0.9833	1.1801
-0.7%	-0.7%	-0.4%	-0.5%	-0.1%	-0.1%	0.2%	0.2%
0.6257	0.5921	0.7576	0.7213	0.9016	0.8571	1.2229	1.2209
0.6302	0.5947	0.7622	0.7231	0.9047	0.8561	1.2215	1.2175
-0.7%	-0.4%	-0.6%	-0.2%	-0.3%	0.1%	0.1%	0.3%
0.6334	0.7570	0.7070	0.8856	0.8238	1.0013	1.0004	1.1187
0.6359	0.7623	0.7090	0.8894	0.8231	1.0030	0.9954	1.1129
-0.4%	-0.7%	-0.3%	-0.4%	0.1%	-0.2%	0.5%	0.5%
0.8124	0.7206	0.8848	0.8480	1.0547	1.0237	1.2991	0.9546
0.8173	0.7232	0.8894	0.8476	1.0562	1.0198	1.2926	0.9467
-0.6%	-0.4%	-0.5%	0.0%	-0.1%	0.4%	0.5%	0.8%
0.7614	0.9000	0.8222	1.0535	1.4193	1.2787	1.4259	
0.7637	0.9048	0.8232	1.0562	1.4159	1.2733	1.4141	
-0.3%	-0.5%	-0.1%	-0.3%	0.2%	0.4%	0.8%	
0.9367	0.8549	0.9983	1.0208	1.2764	1.4128	1.0821	
0.9404	0.8563	1.0032	1.0200	1.2735	1.4017	1.0841	
-0.4%	-0.2%	-0.5%	0.1%	0.2%	0.8%	-0.2%	
0.9855	1.2195	0.9935	1.2915	1.4204	1.0812		
0.9836	1.2219	0.9957	1.2930	1.4142	1.0841		
0.2%	-0.2%	-0.2%	-0.1%	0.4%	-0.3%		
1.1855	1.2181	1.1068	0.9469				
1.1806	1.2181	1.1135	0.9475				
0.4%	0.0%	-0.6%	-0.1%				

Legend ARROTTA 1x1
ARROTTA 2x2
%--difference

Maximum Difference		Standard Deviation
Positive	0.83%	
Negative	-0.71%	0.40%

Figure A-2. ARROTTA Comparison of 2x2 and 1x1 Mesh Structures

model which was fully consistent with the more detailed three-dimensional model. The results are summarized in Figure A-3. In all six cases were run: 12 and 24 planes in the core using the 3-D model, 12 and 24 planes in the core using the 1-D model, and 100 planes in the core using the 1-D Nodal Expansion Method and the finite difference method (all other cases used the Nodal Expansion Method). All cases give essentially the same result. The two 100-plane 1-D cases are essentially coincidental with each other. From this it is concluded that 12 axial mesh intervals in the core for the three-dimensional calculation is adequate. Axial mesh spacing was also studied separately for ARROTTA. The results are presented in Reference 4.1.

A sensitivity study on timestep size for the transient was performed. Again the one-dimensional HERMITE model was used. The absorption cross section in HERMITE was arbitrarily adjusted to give a rod worth of about \$1.16. Two effects contribute to the sensitivity of the results to timestep size--the neutronics equation solution algorithm and the fuel temperature calculation. The first half of the transient from t=0 to about t=.25 s gives a good indication of the sensitivity of the neutronics algorithm because there is no heating of the fuel. Figure A-4 is a plot of total core power as a function of time on a logarithmic scale for timesteps of 10 ms, 5 ms, and 1 ms. The early portion of the transient demonstrates that HERMITE neutronics are quite insensitive to the timestep size. This, therefore, suggests that the peak power level is most sensitive to the timestep size in the fuel temperature calculation. Recall that in Section 2.4 two different approximations for the time dependence of the heat source in the pellet were presented. They were characterized by the parameter θ. Figure A-5 shows the power for HERMITE cases using 10 ms and 1 ms timestep and θ=.5--the default HERMITE option. As expected, the peak decreases with smaller timesteps. The cases were repeated with a value of θ=1. These results, together with those for θ=.5 are shown on Figure A-6. Several conclusions can be drawn from this figure. First, for small timesteps (1 ms) the results are not too sensitive to the value of θ. Secondly, the results for 10 ms timesteps and θ=1 agree well with the small timestep case. The 3-D transient was run using both θ=.5 and θ=1 to further explore the sensitivity of the peak power to the fuel temperature calculation. These results are shown in Figure A-7. Based on these results, it was decided to use 10 ms timesteps and θ=1 for the ARROTTA-HERMITE comparisons described in Section 4.3. Figures A-8 and A-9 show the core average and peak fuel temperature sensitivity to θ for the 3-D transient.

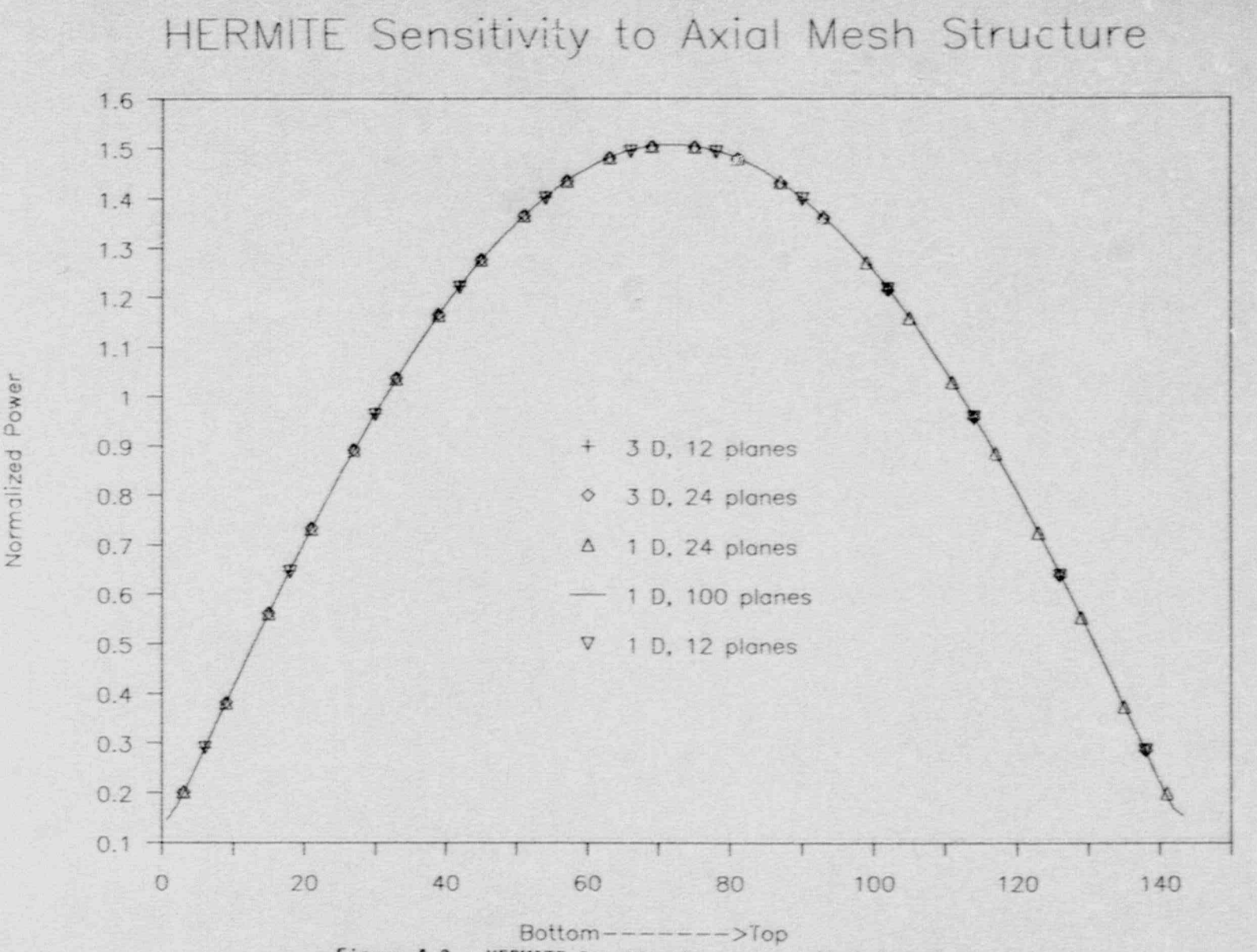

Figure A-3. HERMITE Sensitivity to Axial Mesh Structure

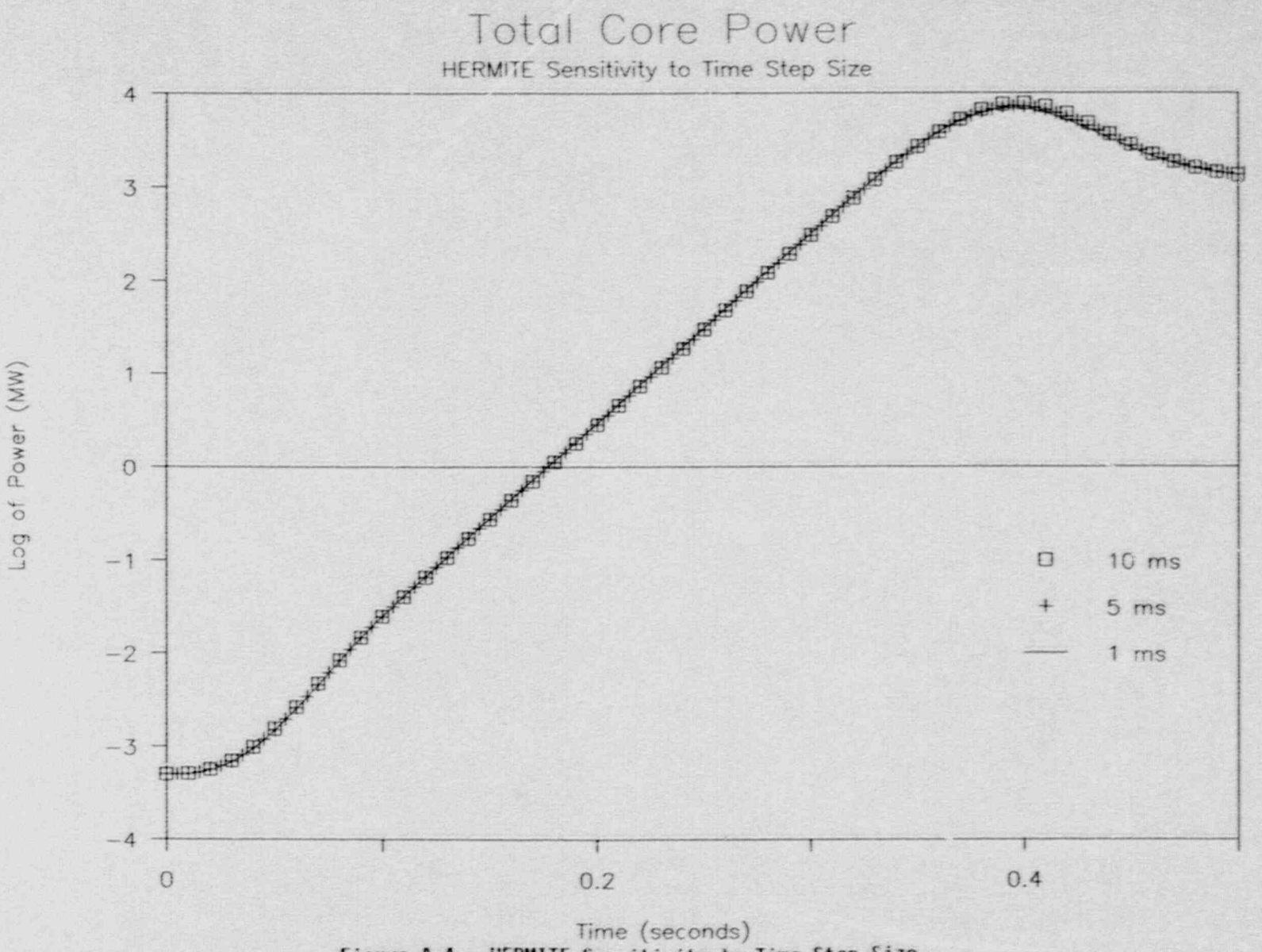

Figure A-4. HERMITE Sensitivity to Time Step Size

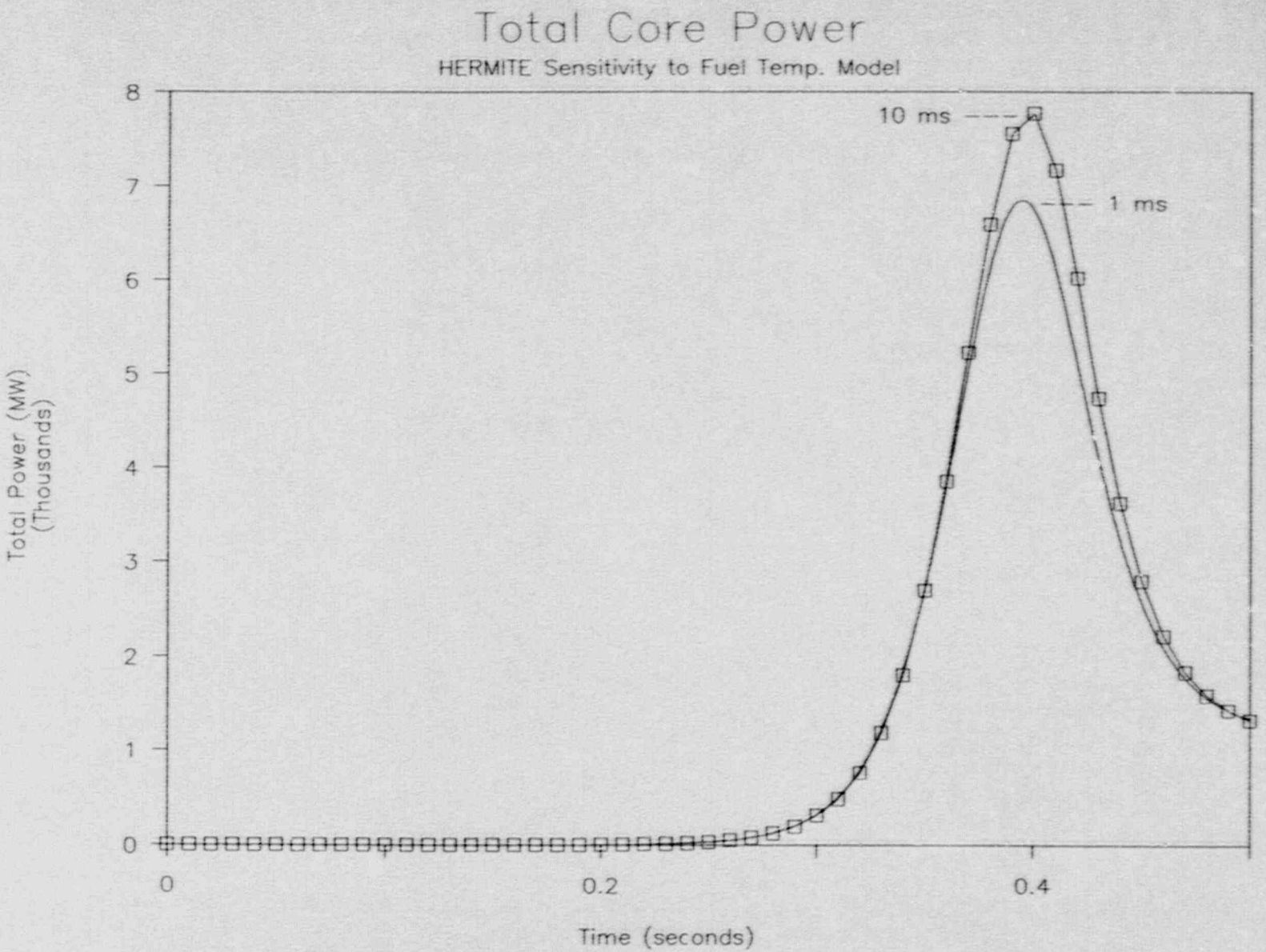

Figure A-5. HERMITE Sensitivity to Fuel Temperature Model

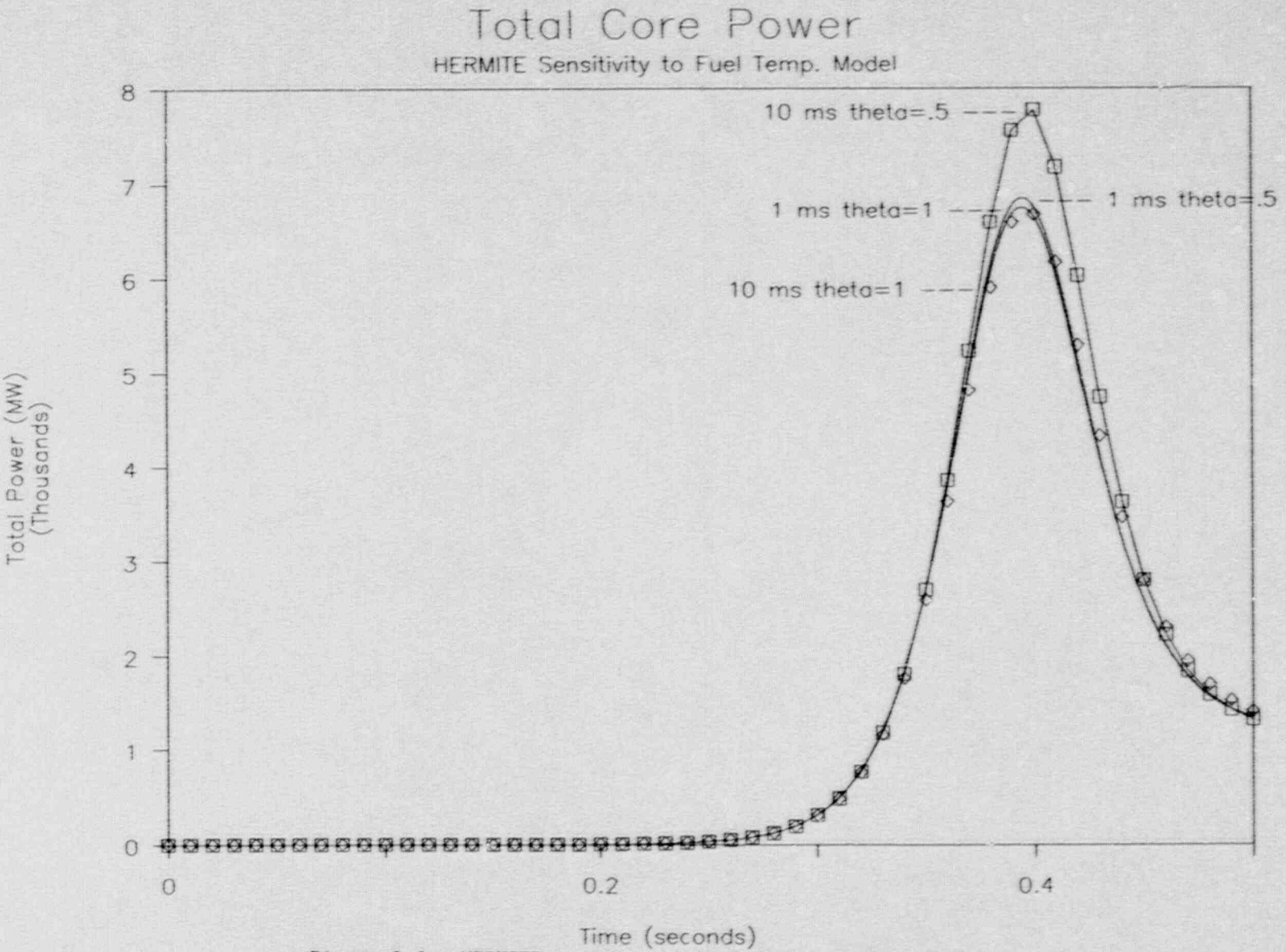

Figure A-6. HERMITE Sensitivity to Fuel Temperature Model

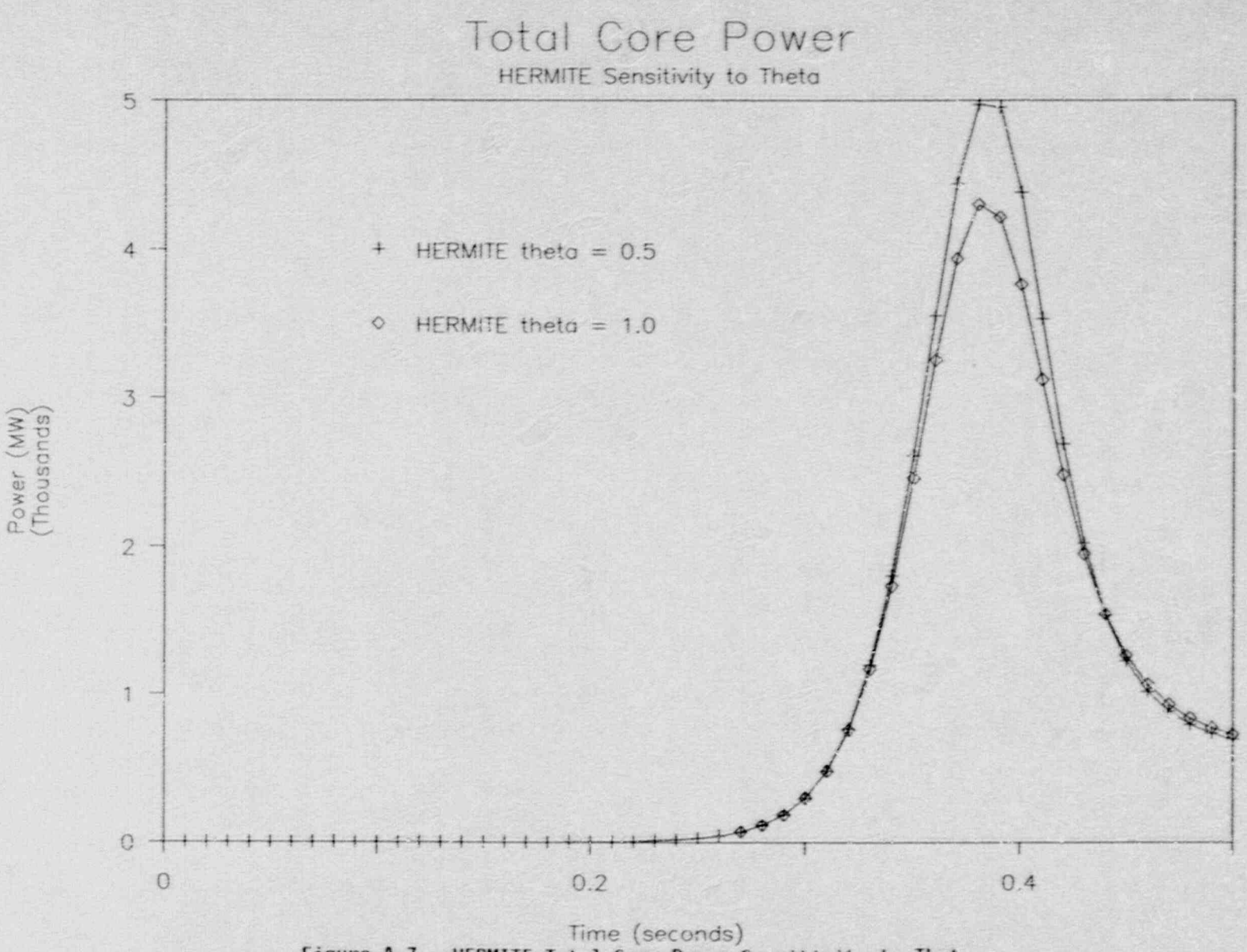

Figure A-7. HERMITE Total Core Power Sensitivity to Theta

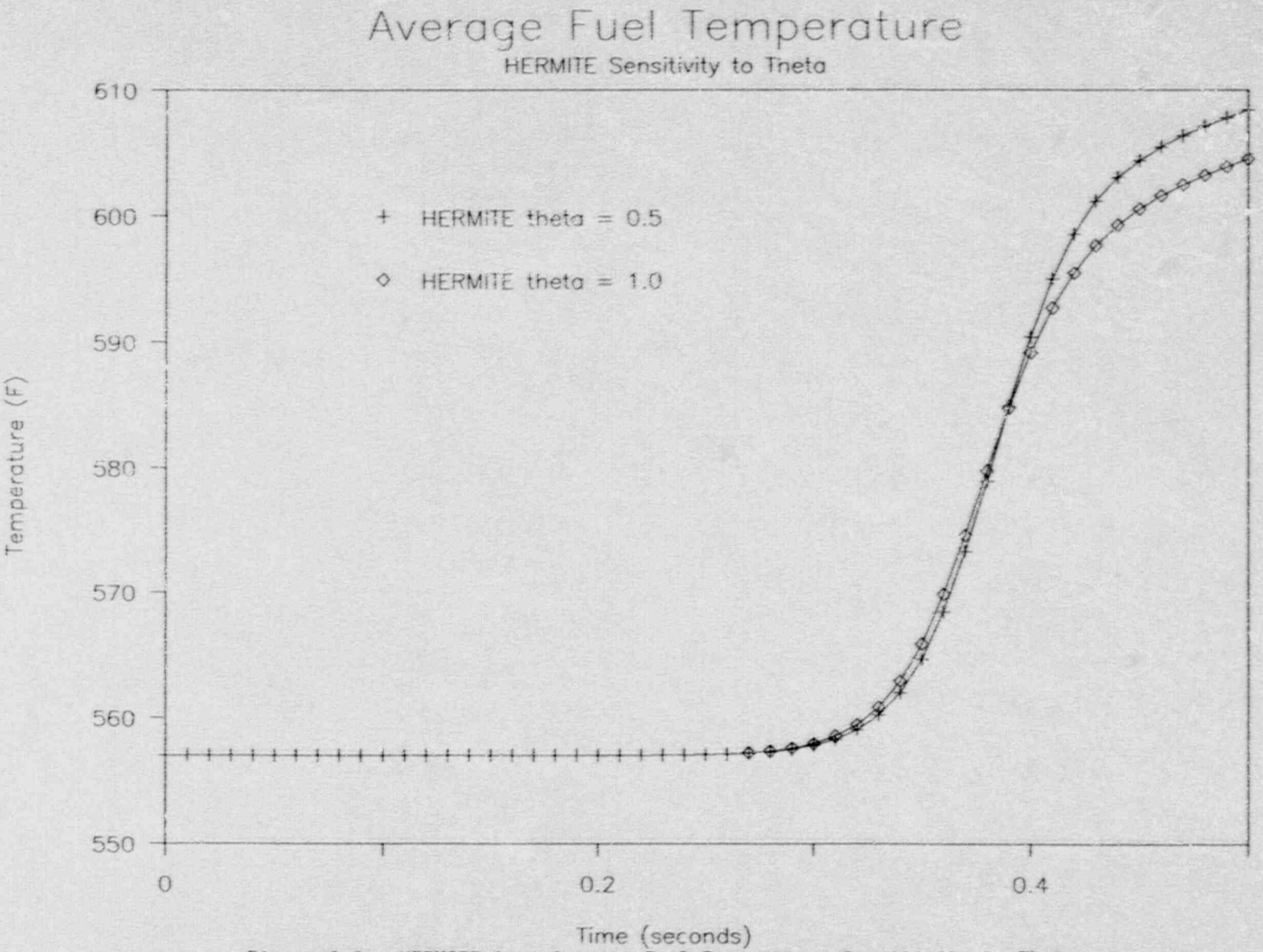

Figure A-8. HERMITE Core Average Fuel Temperature Sensitivity to Theta

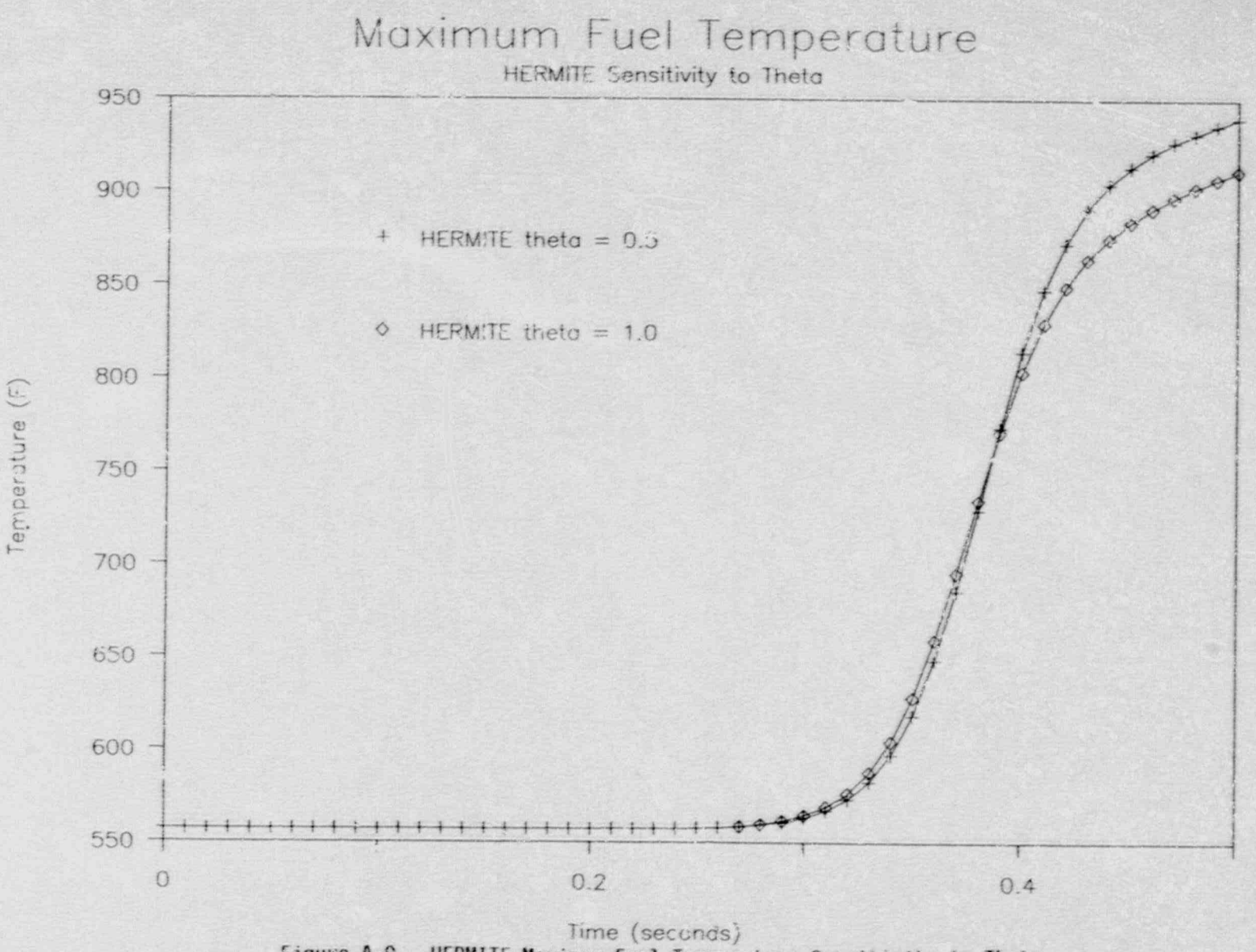

Figure A-9. HERMITE Maximum Fuel Temperature Sensitivity to Theta

The reason for this behavior appears to be as follows: When the neutronics is advanced from t_n to t_{n+1}, one would like to use some average fuel temperature in the interval (t_n, t_{n+1}) to compute cross sections and fuel temperature feedback. Since the fuel temperature is not advanced simultaneously with the neutronics, the best that can be done is to use the fuel temperature at t_n. In this transient we know that the fuel temperature is increasing, thus any fuel temperature at t_n underestimates the actual fuel temperature and tends to result in a higher peak power. This effect is minimized for this particular transient by picking θ=1 which uses the (higher) heat generation rate at t_n, rather than θ=.5 which assumes a linear variation in heat generation rate between t_{n-1} and t_n and takes an average of these two values for the interval (t_n, t_{n+1}).

A time step study has been made independently for ARROTTA (Reference 4.1). In ARROTTA the sensitivity of the peak to the time step size is greater than it is in HERMITE. The time of peak power also changes more. Since there is evidence of a timestep effect during the early part of the transient before there is any significant heat addition, it suggests the ARROTTA sensitivity to timestep size is due in part to the neutronics. Based on the ARROTTA documentation (Reference 2.1), its heat source treatment corresponds to θ=1 in HERMITE. Therefore, this also suggests that the sensitivity of the peak power in ARROTTA to timestep size has a significant neutronics component.

As mentioned previously, the thermal properties of UO_2 and the clad come from different sources in ARROTTA and HERMITE. These properties have a direct impact on the temperature of the fuel during the transient and thus the power level and stored energy. The thermal conductivity of UO_2 is the same in both codes. However, the specific heat is somewhat different. Figure A-10 shows the specific heat as a function of fuel temperature in both codes. While they appear to be quite different, it is the integral between the initial fuel temperature and the instantaneous fuel temperature that determines the associated energy deposition. This integral, which is the change in fuel enthalpy, is shown in Figure A-11. On the figure the integral is relative to 400°F. The difference in temperature for a given energy deposition for a transient starting at 557°F is never more than $\pm$ 9°F in the range 557°F to 1500°F.

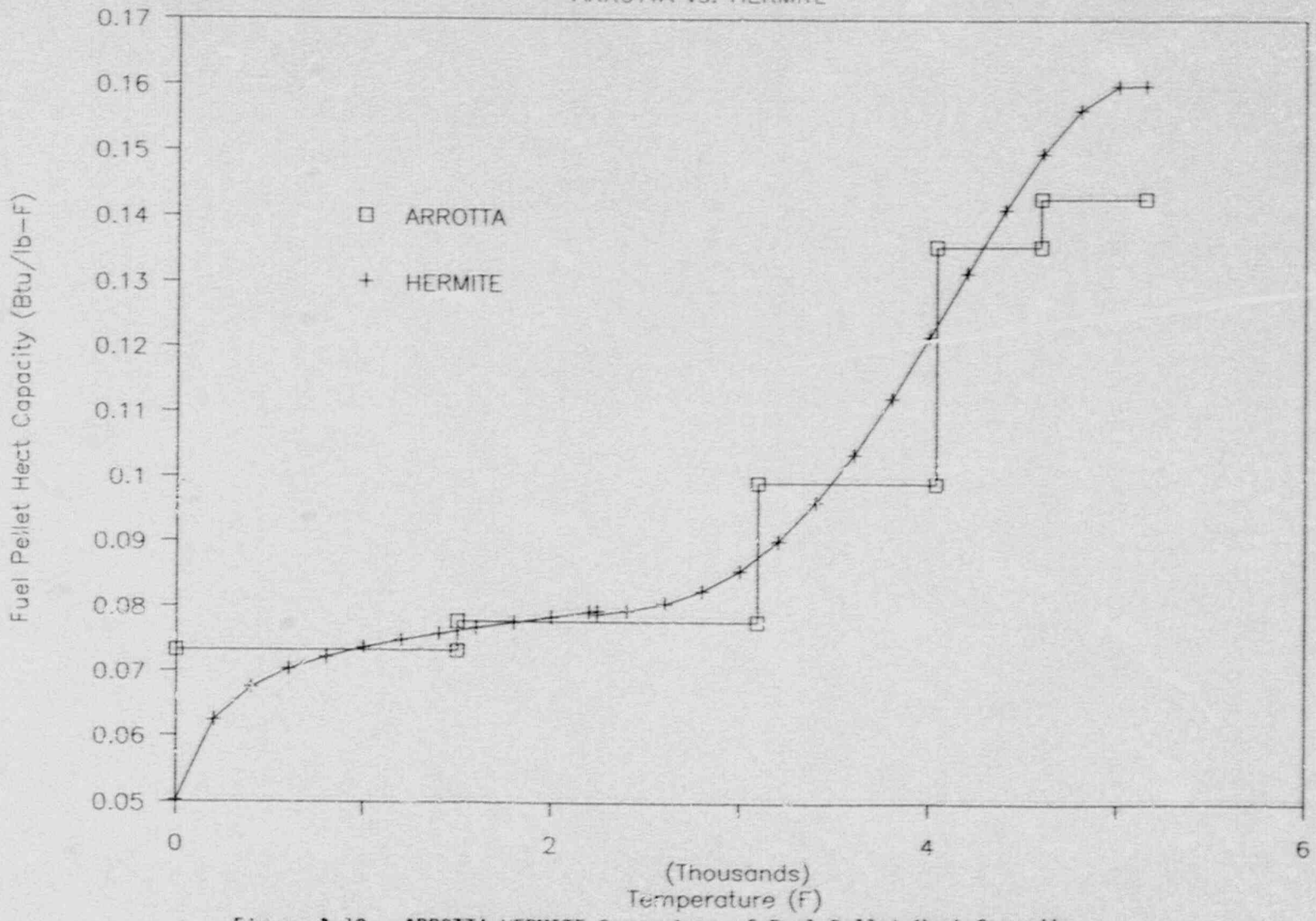

Figure A-10. ARROTTA-HERMITE Comparison of Fuel Pellet Heat Capacity

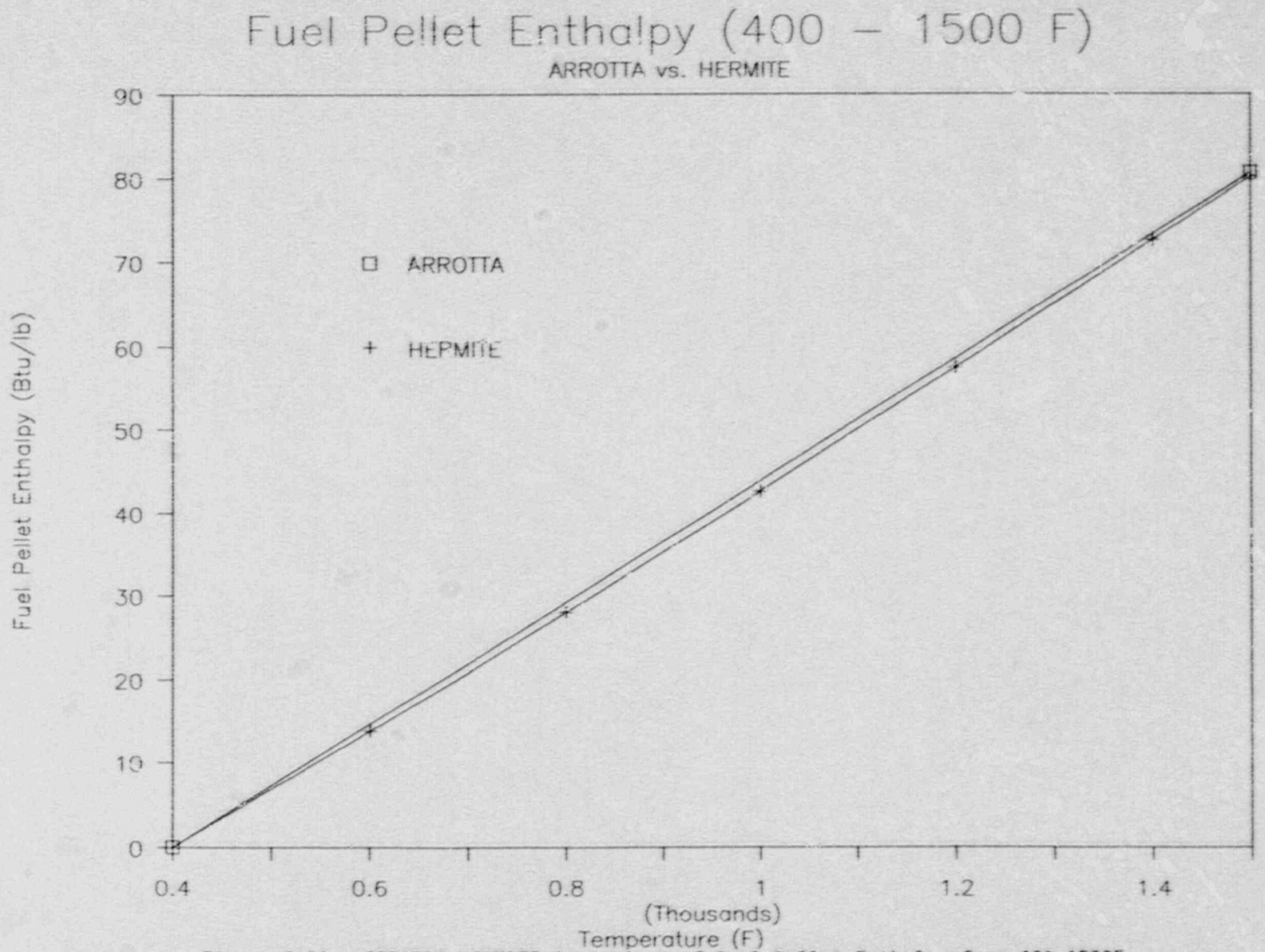

Figure A-11. ARROTTA-HERMITE Comparison of Fuel Pellet Enthalpy from 400-1500F

As mentioned previously, HERMITE originally used a finite element neutronics algorithm. HERMITE was run in the steady-state using the finite element method on the hot zero power case with rods inserted. The comparison with the Nodal Expansion Method is shown in Figure A-12. The agreement shown is typical of that exhibited with the finite element method. (See Figure 4-6 of Reference 1.1.) The 1-D HERMITE model was also run for a rod ejection transient using the finite element method. The results are shown in Figure A-13. These figures demonstrate, quantitatively, the improvement realized by using the Nodal Expansion Method.

It should be noted that the clad properties are different between HERMITE and ARROTTA but clad heating is not a significant effect in the case studied.

0.2419	0.5153	0.6011	0.8712	0.7304	0.6458	0.1840	0.6186
0.2551	0.5556	0.6742	0.9142	0.8073	0.6984	0.1800	0.6847
-5.2%	-7.3%	-10.8%	-4.7%	-9.5%	-7.5%	2.2%	-9.6%
0.5153	0.4906	0.6964	0.7009	0.9372	0.7128	0.8779	0.9388
0.5556	0.5616	0.7443	0.7763	0.9719	0.7905	0.9152	0.9945
-7.3%	-12.6%	-6.4%	-9.7%	-3.6%	-9.8%	-4.1%	-5.6%
0.6011	0.6964	0.4780	0.8309	0.8140	1.1054	1.0353	1.2792
0.6742	0.7443	0.5142	0.8644	0.8720	1.0899	1.0786	1.2311
-10.8%	-6.4%	-7.0%	-3.9%	-6.7%	1.4%	-4.0%	3.9%
0.8712	0.7009	0.8309	0.7168	0.9266	1.0815	1.7082	1.3115
0.9142	0.7763	0.8644	0.7765	0.9217	1.1088	1.5987	1.2045
-4.7%	-9.7%	-3.9%	-7.7%	0.5%	-2.5%	6.8%	8.9%
0.7304	0.9372	0.8140	0.9266	0.7780	1.3844	1.9463	
0.8073	0.9719	0.8720	0.9217	0.7187	1.3146	1.8116	
-9.5%	-3.6%	-6.7%	0.5%	8.2%	5.3%	7.4%	
0.6458	0.7128	1.1054	1.0815	1.3844	1.8109	1.5869	
0.6984	0.7905	1.0899	1.1088	1.3146	1.6710	1.4263	
-7.5%	-9.8%	1.4%	-2.5%	5.3%	8.4%	11.3%	
0.1840	0.8779	1.0353	1.7082	1.9463	1.5869		
0.1800	0.9152	1.0786	1.5987	1.8116	1.4263		
2.2%	-4.1%	-4.0%	6.8%	7.4%	11.3%		
0.6186	0.9388	1.2792	1.3115			Legend	Finite El
0.6847	0.9945	1.2311	1.2045				Nodal Exp
-9.6%	-5.6%	3.9%	8.9%				%--differ

		Maximum Difference		Standard Deviation
k-effective HERMITE-FEM	0.987373	Positive	11.27%	
k-effective HERMITE-NEM	0.986523	Negative	-12.63%	7.17%
Difference	0.000850			

Figure A-12. HERMITE Finite Element and Nodal Expansion Radial Power Distribution Comparison

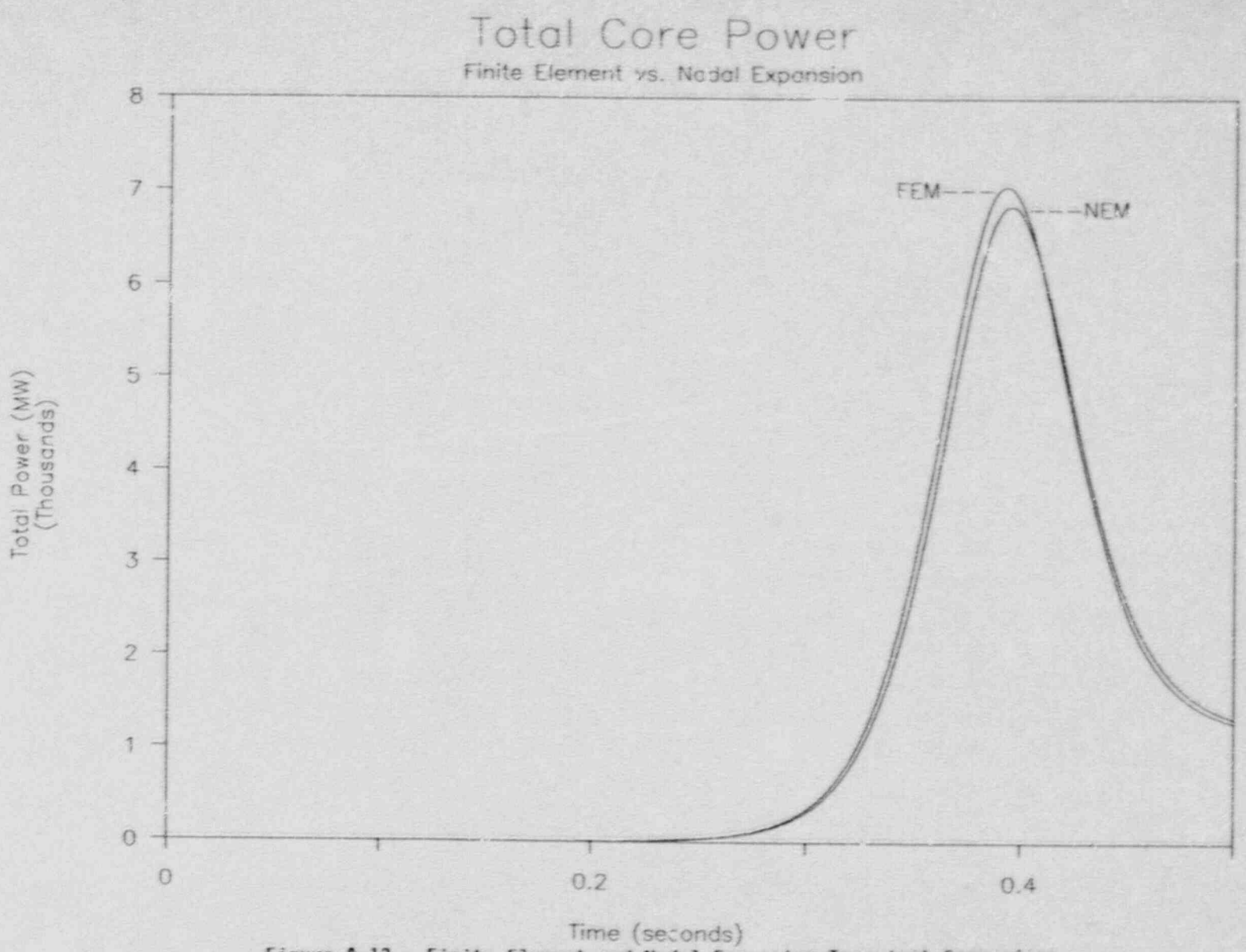

Figure A-13. Finite Element and Nodal Expansion Transient Comparison

Appendix B

PROBLEM DESCRIPTION

The purpose of this appendix is to provide the description of the problem used in the rod ejection transient analysis. This is done through a series of tables and figures as well as complete input listings for ARROTTA and HERMITE.

Core Layout

The layout of the core showing the location of the various fuel assembly types and control rod groups is given in Figure B-1. Note that the upper and lower reflectors extend across all fuel assemblies and the baffle, but not across the radial reflectors. The radial reflectors extend the entire height of the core (445.76 cm).

Problem Parameters

Many of the various input quantities, except cross sections, are listed in Table B-1.

Cross Sections

The cross section representation, in terms of the ARROTTA nomenclature is:

$$\Sigma = R \left[A + B \frac{(X-X')}{X'} + C \left[\frac{X-X'}{X'}\right]^2 \right]$$

$$+ (1-R) \left[A' + B' \frac{(X-X')}{X'} + C' \left[\frac{X-X'}{X'}\right]^2 \right]$$

$$+ \frac{d\Sigma}{d\sqrt{T_F}} \left(\sqrt{T_F} - \sqrt{T_F'}\right) + N_B \sigma_B$$

where

Σ macroscopic cross section (transport, absorption, removal, nu-fission and kappa-fission)

R linear function of rod insertion where R=0.0 for the unrodded node and R=1.0 for a rod fully inserted in a node

A, B, C, A′, B′, C′ input quantities

X moderator density (lb/ft^3)

X′ input reference moderator density (lb/ft^3)

$\frac{d\Sigma}{d\sqrt{T_F}}$ cross section change due to fuel temperature change

T_F fuel temperature (absolute, °F)

T_F' input reference fuel temperature (absolute, °F)

N_B soluble boron number density

σ_B boron microscopic cross section

The various input quantities for each of the compositions are given in Tables B-2 through B-15 for the fourteen compositions.

Input Listings

Figures B-2 and B-3 are the ARROTTA and HERMITE input listings.

Table B-1

PROBLEM PARAMETERS

Total problem power	0.001 MW
Soluble boron level	975 PPM
Fuel assembly dimensions	21.608 cm x 21.608 cm
Active fuel height	365.76 cm
Lower reflector	40 cm
Upper reflector height	40 cm
Radial reflector thickness	21.608 cm
Control rod group 5 withdrawal rate	3,546.52 cm/s
System pressure	2250 psia
Coolant flow rate	839.81 lb/s ft^2
Coolant inlet temperature	557 °F
Fuel rod cell pitch	0.041333 ft
Fraction of fuel assembly area not considered part of fuel rod or coolant	0.04015
Fuel pellet radius	0.012867 ft
Fuel-clad gap width	2.87-3 ft
Clad thickness	1.875-3 ft
Fuel pellet density	641.75 lb/ft^3
Constant gap thermal conductivity	1000 Btu/hr-ft^2-°F
Number of delayed neutron groups	6
Delayed neutron data	

Group	λ	β
1	1.27535-2	2.46358-4
2	3.17843-2	1.45914-3
3	1.19458-1	1.33969-3
4	3.18858-1	2.94599-3
5	1.40265+0	1.05456-3
6	3.92952+0	2.50605-4

Inverse neutron group velocities	$1/v_1$	5.86-8 s/cm
	$1/v_2$	2.42-6 s/cm

Initial control rod positions (cm above bottom of problem)

Rod Group	Position
1	49.47 cm
2	49.47 cm
3	163.77 cm
4	346.33 cm
5	49.47 cm

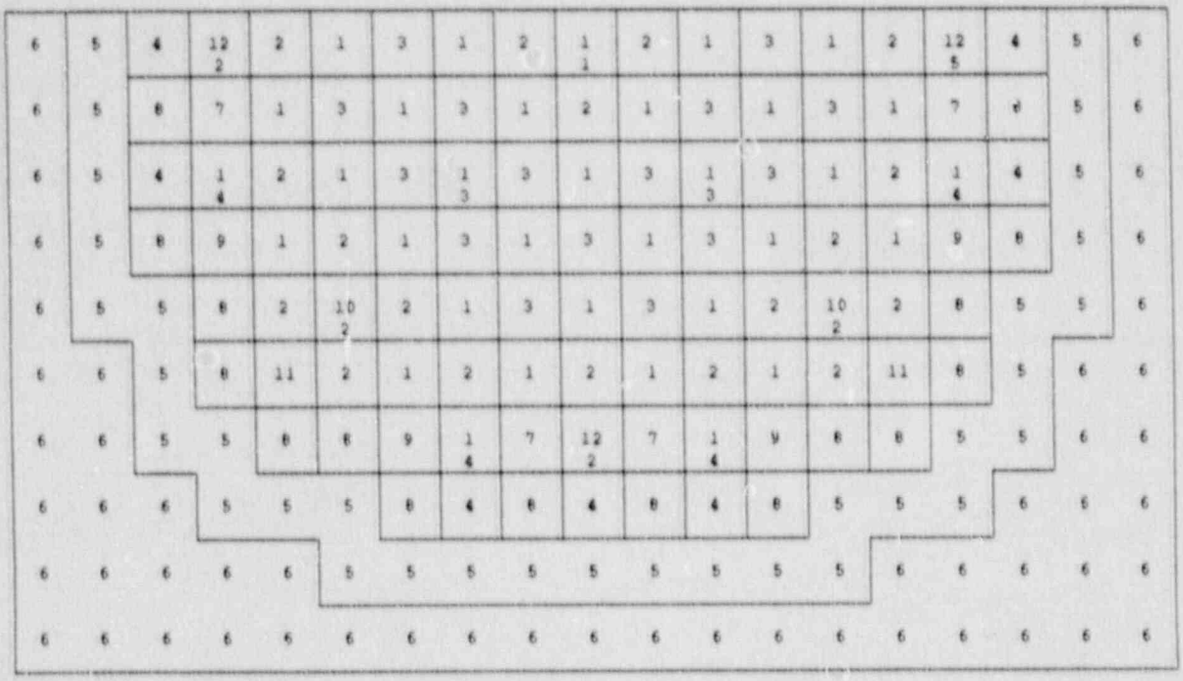

ARROTTA Fuel Assembly Type	Description	ARROTTA/HERMITE Composition Numbers
1	Fuel type 1	1
2	Fuel type 2	2
3	Fuel type 3	3
4	Fuel type 4	4
7	Fuel type 7	5
8	Fuel type 8	6
9	Fuel type 9	7
10	Fuel type 10	8
11	Fuel type 11	9
--	Lower Reflector	10
5	Baffle	11
6	Radial Reflector	12
--	Upper Reflector	13
12	Fuel type 12	14

Figure B-1. ARROTTA Fuel Assembly Type and Control Rod Group Layout

Table B-2

COMPOSITION 1 -- FUEL TYPE 1 CROSS SECTIONS

		Ref. Fuel Temp. (F)	Ref Mod Dens (lb/ft**3)	Moderator Volume Fraction
		1249.95	43.8646	0.619503
Group	Type	A'	B' (unrodded)	C'
1	TR	2.30928E-01	1.12514E-01	3.52986E-03
	A	7.68564E-03	1.24034E-03	-4.75972E-04
	R	1.79005E-02	1.96439E-02	6.39194E-04
	NSF	4.37267E-03	5.99922E-04	-2.68501E-04
	KSF	5.78566E-14	8.32702E-15	-3.79664E-15
2	TR	8.73971E-01	8.53641E-01	3.46966E-01
	A	4.87367E-02	1.85151E-02	2.11087E-02
	NSF	6.86748E-02	1.83138E-02	2.76542E-02
	KSF	9.08664E-13	2.48450E-13	3.62756E-13
Group	Type	A	B (rodded)	C
1	TR	2.36824E-01	1.12514E-01	3.52986E-03
	A	1.30354E-02	1.24034E-03	-4.75972E-04
	R	1.51801E-02	1.96439E-02	6.39194E-04
	NSF	4.30622E-03	5.99922E-04	-2.68501E-04
	KSF	5.66186E-14	8.32702E-15	-3.79664E-15
2	TR	8.68288E-01	8.53641E-01	3.46966E-01
	A	7.53092E-02	1.85151E-02	2.11087E-02
	NSF	6.99272E-02	1.83138E-02	2.76542E-02
	KSF	9.19408E-13	2.48450E-13	3.62756E-13
Group	Type	Fuel Temperature Feedback	Boron Micros	
1	TR	-5.65285E-05	0	
	A	2.38661E-05	7.68707E+01	
	R	-1.40929E-05	8.15305E+01	
	NSF	-1.99619E-06	0	
	KSF	-2.67962E-17	0	
2	A	0	1.95628E+03	

Table B-3

COMPOSITION 2 -- FUEL TYPE 2 CROSS SECTIONS

Ref. Fuel Temp. (F)	Ref Mod Dens (lb/ft**3)	Moderator Volume Fraction
1249.95	43.8646	0.594052

Group	Type	A'	B' (unrodded)	C'
1	TR	2.31132E-01	1.06894E-01	3.58709E-03
	A	8.86226E-03	1.30244E-03	-6.48451E-04
	R	1.65086E-02	1.85643E-02	4.03922E-04
	NSF	5.38884E-03	6.69172E-04	-3.57250E-04
	KSF	7.12520E-14	9.40733E-15	-5.04631E-15
2	TR	8.56898E-01	8.02693E-01	2.95213E-01
	A	7.50066E-02	2.23210E-02	2.18614E-02
	NSF	9.81175E-02	2.74854E-02	3.15468E-02
	KSF	1.29732E-12	3.73593E-13	4.12842E-13

Group	Type	A	B (rodded)	C
1	TR	2.31132E-01	1.06894E-01	3.58709E-03
	A	8.86226E-03	1.30244E-03	-6.48451E-04
	R	1.65083E-02	1.85643E-02	4.03922E-04
	NSF	5.38884E-03	6.69172E-04	-3.57250E-04
	KSF	7.12520E-14	9.40733E-15	-5.04631E-15
2	TR	8.56898E-01	8.02693E-01	2.95213E-01
	A	7.50066E-02	2.23210E-02	2.18614E-02
	NSF	9.81175E-02	2.74854E-02	3.15468E-02
	KSF	1.29732E-12	3.73593E-13	4.12842E-13

Group	Type	Fuel Temperature Feedback	Boron Micros
1	TR	-5.63395E-05	0
	A	2.33022E-05	6.92607E+01
	R	-1.35019E-05	3.89555E+01
	NSF	-2.36366E-06	0
	KSF	-3.18172E-17	0
2	A	0	1.86644E+03

Table B-4

COMPOSITION 3 -- FUEL TYPE 3 CROSS SECTIONS

Ref. Fuel Temp. (F)	Ref Mod Den. (lb/ft**3)	Moderator Volume Fraction
1249.95	43.8646	0.600415

Group	Type	A'	B' (unrodded)	C'
1	TR	2.30728E-01	1.08263E-01	3.92980E-03
	A	8.68072E-03	1.29031E-03	-6.28189E-04
	R	1.66596E-02	1.86970E-02	4.58229E-04
	NSF	5.38836E-03	6.61442E-04	-3.50382E-04
	KSF	7.12747E-14	9.28904E-15	-4.95145E-15
2	TR	8.61057E-01	8.13425E-01	3.03342E-01
	A	7.16198E-02	2.20689E-02	2.12240E-02
	NSF	9.80550E-02	2.70222E-02	3.16330E-02
	KSF	1.29703E-12	3.67276E-13	4.13950E-13

Group	Type	A	B (rodded)	C
1	TR	2.30728E-01	1.08263E-01	3.92980E-03
	A	8.68072E-03	1.29031E-03	-6.28189E-04
	R	1.66596E-02	1.86970E-02	4.58229E-04
	NSF	5.38836E-03	6.61442E-04	-3.50382E-04
	KSF	7.12747E-14	9.28904E-15	-4.95145E-15
2	TR	8.61057E-01	8.13425E-01	3.03342E-01
	A	7.16198E-02	2.20689E-02	2.12240E-02
	NSF	9.80550E-02	2.70222E-02	3.16330E-02
	KSF	1.29703E-12	3.67276E-13	4.13950E-13

Group	Type	Fuel Temperature Feedback	Boron Micros
1	TR	-5.61257E-05	0
	A	2.32928E-05	6.99841E+01
	R	-1.34387E-05	4.39008E+01
	NSF	-2.35533E-06	0
	KSF	-3.16922E-17	0
2	A	0	1.87695E+03

Table B-5

COMPOSITION 4 -- FUEL TYPE 4 CROSS SECTIONS

Ref. Fuel Temp. (F)	Ref Mod Dens (lb/ft**3)	Moderator Volume Fraction
1249.95	43.8646	0.609959

Group	Type	A'	B (unrodded)	C'
1	TR	2.29205E-01	1.10299E-01	3.87365E-03
	A	8.80488E-03	1.32189E-03	-5.70446E-04
	R	1.63110E-02	1.86197E-02	5.90810E-04
	NSF	6.24526E-03	7.13495E-04	-3.87558E-04
	KSF	8.26946E-14	1.00394E-14	-5.56182E-15
2	TR	8.67789E-01	8.21630E-01	3.00537E-01
	A	7.77139E-02	2.44548E-02	1.98783E-02
	NSF	1.21515E-01	3.20648E-02	3.25952E-02
	KSF	1.60900E-12	4.36066E-13	4.24570E-13

Group	Type	A	B (rodded)	C
1	TR	2.29205E-01	1.10299E-01	3.87365E-03
	A	8.80488E-03	1.32189E-03	-5.70446E-04
	R	1.63110E-02	1.86197E-02	5.90810E-04
	NSF	6.24526E-03	7.13495E-04	-3.87558E-04
	KSF	8.26946E-14	1.00394E-14	-5.56182E-15
2	TR	8.67789E-01	8.21630E-01	3.00537E-01
	A	7.77139E-02	2.44548E-02	1.98783E-02
	NSF	1.21515E-01	3.20648E-02	3.25952E-02
	KSF	1.60900E-12	4.36066E-13	4.24570E-13

Group	Type	Fuel Temperature Feedback	Boron Micros
1	TR	-5.49694E-05	0
	A	2.28228E-05	6.79433E+01
	R	-1.29062E-05	4.01900E+01
	NSF	-2.59853E-06	0
	KSF	-3.48548E-17	0
2	A	0	1.85250E+03

Table B-6

COMPOSITION 5 -- FUEL TYPE 7 CROSS SECTIONS

Ref. Fuel Temp. (F)	Ref Mod Dens (lb/ft**3)	Moderator Volume Fraction
1249.95	43.8646	0.58769

Group	Type	A'	B' (unrodded)	C'
1	TR	2.30486E-01	1.05630E-01	4.02163E-03
	A	9.42218E-03	1.39062E-03	-7.10698E-04
	R	1.57303E-02	1.81029E-02	4.43800E-04
	NSF	6.25176E-03	7.41566E-04	-4.28445E-04
	KSF	8.26790E-14	1.04644E-14	-6.06422E-15
2	TR	8.53257E-01	7.82959E-01	2.73246E-01
	A	8.98709E-02	2.57032E-02	1.97482E-02
	NSF	1.22047E-01	3.42033E-02	3.21008E-02
	KSF	1.61406E-12	4.65220E-13	4.18523E-13

Group	Type	A	B (rodded)	C
1	TR	2.30486E-01	1.05630E-01	4.02163E-03
	A	9.42218E-03	1.39062E-03	-7.10698E-04
	R	1.57303E-02	1.81029E-02	4.43800E-04
	NSF	6.25176E-03	7.41566E-04	-4.28445E-04
	KSF	8.26790E-14	1.04644E-14	-6.06422E-15
2	TR	8.53257E-01	7.82959E-01	2.73246E-01
	A	8.98709E-02	2.57032E-02	1.97482E-02
	R	1.22047E-01	3.42033E-02	3.21008E-02
	NSF	1.61406E-12	4.65220E-13	4.18523E-13

Group	Type	Fuel Temperature Feedback	Boron Micros
1	TR	-5.58216E-05	0
	A	2.28303E-05	6.52955E+01
	R	-1.30755E-05	2.63488E+01
	NSF	-2.64127E-06	0
	KSF	-3.55219E-17	0
2	A	0	1.80209E+03

Table B-7

COMPOSITION 6--FUEL TYPE 8 CROSS SECTIONS

		Ref. Fuel Temp. (F)	Ref Mod Dens (lb/ft**3)	Moderator Volume Fraction
		1249.95	43.8646	0.619503
Group	Type	A'	B' (unrodded)	C'
1	TR	2.28724E-01	1.12173E-01	3.64155E-03
	A	8.56543E-03	1.31259E-03	-5.76616E-04
	R	1.65373E-02	1.88142E-02	7.16741E-04
	NSF	6.24368E-03	7.04904E-04	-3.70293E-04
	KSF	8.27091E-14	9.90261E-15	-5.30412E-15
2	TR	8.72742E-01	8.34474E-01	3.09186E-01
	A	7.36409E-02	2.43555E-02	1.91499E-02
	NSF	1.21359E-01	3.13560E-02	3.29814E-02
	KSF	1.60762E-12	4.26330E-13	4.31055E-13
Group	Type	A	B (rodded)	C
1	TR	2.34343E-01	1.12173E-01	3.64155E-03
	A	1.35402E-02	1.31259E-03	-5.76616E-04
	R	1.38410E-02	1.88142E-02	7.16741E-04
	NSF	6.11932E-03	7.04904E-04	-3.70293E-04
	KSF	8.07136E-14	9.90261E-15	-5.30412E-15
2	TR	8.70468E-01	8.34474E-01	3.09186E-01
	A	1.01492E-01	2.43555E-02	1.91499E-02
	NSF	1.24049E-01	3.13560E-02	3.29814E-02
	KSF	1.63620E-12	4.26330E-13	4.31055E-13
Group	Type	Fuel Temperature Feedback	Boron Micros	
1	TR	-5.44405E-05	0	
	A	2.28510E-05	6.81913E+01	
	R	-1.28950E-05	4.60102E+01	
	NSF	-2.58394E-06	0	
	KSF	-3.46463E-17	0	
2	A	0	1.84712E+03	

Table B-8

COMPOSITION 7--FUEL TYPE 9 CROSS SECTIONS

		Ref. Fuel Temp. (F)	Ref Mod Dens (lb/ft**3)	Moderator Volume Fraction
		1249.95	43.8646	0.594052
Group	Type	A'	B' (unrodded)	C'
1	TR	2.30120E-01	1.06945E-01	3.90052E-03
	A	9.24707E-03	1.36884E-03	-6.89465E-04
	R	1.59016E-02	1.82467E-02	5.26963E-04
	NSF	6.24984E-03	7.31615E-04	-4.18828E-04
	KSF	8.26831E-14	1.03171E-14	-5.90554E-15
2	TR	8.57615E-01	7.94650E-01	2.81980E-01
	A	8.62629E-02	2.51750E-02	1.89671E-02
	NSF	1.21828E-01	3.35504E-02	3.20988E-02
	KSF	1.61174E-12	4.56343E-13	4.18871E-13
Group	Type	A	B (rodded)	C
1	TR	2.30120E-01	1.06945E-01	3.90052E-03
	A	9.24707E-03	1.36884E-03	-6.89465E-04
	R	1.59016E-02	1.82467E-02	5.26963E-04
	NSF	6.24984E-03	7.31615E-04	-4.18828E-04
	KSF	8.26831E-14	1.03171E-14	-5.90554E-15
2	TR	8.57615E-01	7.94650E-01	2.81980E-01
	A	8.62629E-02	2.51750E-02	1.89671E-02
	NSF	1.21828E-01	3.35504E-02	3.20988E-02
	KSF	1.61174E-12	4.56343E-13	4.18871E-13
Group	Type	Fuel Temperature Feedback	Boron Micros	
1	TR	-5.57125E-05	0	
	A	2.28386E-05	6.60404E+01	
	R	-1.30331E-05	3.01824E+01	
	NSF	-2.62773E-06	0	
	KSF	-3.53448E-17	0	
2	A	0	1.81849E+03	

Table B-9

COMPOSITION 8--FUEL TYPE 10 CROSS SECTIONS

		Ref. Fuel Temp. (F)	Ref Mod Dens (lb/ft**3)	Moderator Volume Fraction
		1249.95	43.8646	0.619503
Group	Type	A'	B' (unrodded)	C'
1	TR	2.29573E-01	1.12292E-01	3.59181E-03
	A	8.14989E-03	1.26831E-03	-5.51194E-04
	R	1.70858E-02	1.91168E-02	6.85128E-04
	NSF	5.38707E-03	6.44816E-04	-3.19735E-04
	KSF	7.13370E-14	9.02413E-15	-4.56132E-15
2	TR	8.72468E-01	8.42302E-01	3.24061E-01
	A	6.25005E-02	2.18299E-02	2.11957E-02
	NSF	9.78341E-02	2.56885E-02	3.22854E-02
	KSF	1.29554E-12	3.49044E-13	4.23666E-13
Group	Type	A	B (rodded)	C
1	TR	2.35348E-01	1.12292E-01	3.59181E-03
	A	1.32802E-02	1.26831E-03	-5.51194E-04
	R	1.43857E-02	1.91168E-02	6.85128E-04
	NSF	5.28997E-03	6.44816E-04	-3.19735E-04
	KSF	6.97056E-14	9.02413E-15	-4.56132E-15
2	TR	8.68746E-01	8.42302E-01	3.24061E-01
	A	8.97602E-02	2.18299E-02	2.11957E-02
	NSF	9.98313E-02	2.56885E-02	3.22854E-02
	KSF	1.31547E-12	3.49044E-13	4.23666E-13
Group	Type	Fuel Temperature Feedback	Boron Micros	
1	TR	-5.50669E-05	0	
	A	2.32509E-05	7.16049E+01	
	R	-1.33011E-05	5.93390E+01	
	NSF	-2.33344E-06	0	
	KSF	-3.12857E-17	0	
2	A	0	1.89265E+03	

Table B-10

COMPOSITION 9--FUEL TYPE 11 CROSS SECTIONS

Ref. Fuel Temp. (F)	Ref Mod Dens (lb/ft**3)	Moderator Volume Fraction
1249.95	43.8646	0.595643

Group	Type	A'	B' (unrodded)	C'
1	TR	2.29998E-01	1.07384E-01	3.83927E-03
	A	9.18663E-03	1.34724E-03	-7.40410E-04
	R	1.59491E-02	1.83179E-02	6.09895E-04
	NSF	6.25061E-03	7.33275E-04	-4.13434E-04
	KSF	8.27045E-14	1.03320E-14	-5.89046E-15
2	TR	8.59056E-01	7.98715E-01	2.85338E-01
	A	8.48884E-02	2.49271E-02	1.83736E-02
	NSF	1.21905E-01	3.33241E-02	3.22233E-02
	KSF	1.61297E-12	4.53183E-13	4.20490E-13

Group	Type	A	B (rodded)	C
1	TR	2.29998E-01	1.07384E-01	3.83927E-03
	A	9.18663E-03	1.34724E-03	-7.40410E-04
	R	1.59491E-02	1.83179E-02	6.09895E-04
	NSF	6.25061E-03	7.33275E-04	-4.13434E-04
	KSF	8.27045E-14	1.03320E-14	-5.89046E-15
2	TR	8.59056E-01	7.98715E-01	2.85338E-01
	A	8.48884E-02	2.49271E-02	1.83736E-02
	NSF	1.21905E-01	3.33241E-02	3.22233E-02
	KSF	1.61297E-12	4.53183E-13	4.20490E-13

Group	Type	Fuel Temperature Feedback	Boron Micros
1	TR	-5.53976E-05	0
	A	2.28594E-05	6.66776E+01
	R	-1.30433E-05	3.15782E+01
	NSF	-2.62458E-06	0
	KSF	-3.52508E-17	0
2	A	0	1.83585E+03

Table B-11

COMPOSITION 10--LOWER REFLECTOR CROSS SECTIONS

Ref Mod Dens (lb/ft**3)	Moderator Volume Fraction
47.0249	1.0

Group	Type	A'	B'
1	TR	2.73940E-01	1.23669E-01
	A	2.25826E-03	-1.95228E-04
	R	3.13602E-02	3.42303E-02
2	TR	1.22432E+00	1.19548E+00
	A	4.15451E-02	1.54364E-02
	Boron Micros		
1	A	1.85923E+01	
2	A	6.86497E+02	

Table B-12

COMPOSITION 11 -- BAFFLE CROSS SECTIONS

Ref Mod Dens (lb/ft**3)	Moderator Volume Fraction
46.3836	1.0

Group	Type	A'	B'
1	TR	2.67710E 01	0.00000E+00
	A	1.93990E-03	0.00000E+00
	R	2.89336E-02	0.00000E+00
2	TR	1.27873E+00	0.00000E+00
	A	1.88902E-02	0.00000E+00
	Boron Micros		
1	A	4.64806E+01	
2	A	2.17710E-03	

Table B-13

COMPOSITION 12--RADIAL REFLECTOR CROSS SECTIONS

Ref Mod Dens (lb/ft**3)	Moderator Volume Fraction
46.383600	1.0

Group	Type	A'	B'
1	TR	2.24013E-01	0.00000E+00
	A	3.93110E-04	0.00000E+00
	R	4.45079E-02	0.00000E+00
2	TR	1.29687E+00	0.00000E+00
	A	1.01244E-02	0.00000E+00
	Boron Micros		
1	A	7.24347E+01	
2	A	2.33738E+03	

Table B-14

COMPOSITION 13 -- UPPER REFLECTOR CROSS SECTIONS

		Ref Mod Dens (lb/ft**3)	Moderator Volume Fraction
		47.0249	1.0
Group	Type	A'	B'
1	TR	1.54949E-01	1.36735E-01
	A	3.57151E-04	4.07490E-04
	R	2.99239E-02	2.85707E-02
2	TR	9.34036E-01	1.00942E+00
	A	8.36477E-03	8.36477E-03
		Boron Micros	
1	A	4.59733E+01	
2	A	1.62739E+03	

Table B-15

COMPOSITION 14 -- FUEL TYPE 12 CROSS SECTIONS

		Ref. Fuel Temp. (F)	Ref Mod Dens (lb/ft**3)	Moderator Volume Fraction
		1249.95	43.8646	0.619503
Group	Type	A'	B' (unrodded)	C'
1	TR	2.30928E-01	1.12514E-01	3.52986E-03
	A	7.68564E-03	1.24034E-03	-4.75972E-04
	R	1.79005E-02	1.96439E-02	6.39194E-04
	NSF	4.37267E-03	5.99922E-04	-2.68501E-04
	KSF	5.78566E-14	8.32702E-15	-3.79664E-15
2	TR	8.73971E-01	8.53641E-01	3.46966E-01
	A	4.87367E-02	1.85151E-02	2.11087E-02
	NSF	6.86748E-02	1.83138E-02	2.76542E-02
	KSF	9.08664E-13	2.48450E-13	3.62756E-13
Group	Type	A	B (rodded)	C
1	TR	2.35824E-01	1.12514E-01	3.52986E-03
	A	1.30354E-02	1.24034E-03	-4.75972E-04
	R	1.51801E-02	1.96439E-02	6.39194E-04
	NSF	4.30622E-03	5.99922E-04	-2.68501E-04
	KSF	5.66186E-14	8.32702E-15	-3.79664E-15
2	TR	8.68288E-01	8.53641E-01	3.46966E-01
	A	2.00000E-01	1.85151E-02	2.11087E-02
	NSF	6.99272E-02	1.83138E-02	2.76542E-02
	KSF	9.19408E-13	2.48450E-13	3.62756E-13
Group	Type	Fuel Temperature Feedback	Boron Micros	
1	TR	-5.65285E-05	0	
	A	2.38661E-05	7.68707E+01	
	R	-1.40929E-05	8.15305E+01	
	NSF	-1.99619E-06	0	
	KSF	-2.67962E-17	0	
2	A	0	1.95628E+03	

```
 19  10  14   0  12  14   1   3   6   5   0   0   1   0   0   0   0   1   0   0
          010000 HALF CORE FOR COMPARISON WITH HERMITE
          020101 0 975 3 5 5 500 100 3 5 0
          020114 1 1 1 0 0 0 0 1 1 0 0 0 0 0 0 1
          020201 1.0 0.001 0.0 0.5 0.002 0.01 0.002 0.002
          020211 1.0E-6 0.0005 0.0005
          020225 0.0
(  1- 19) 030100  6  5  4 12  2  1  3  1  2  1  2  1  3  1  2 12  4  5  6
(  1- 19) 030200  6  5  8  7  1  3  1  3  1  2  1  3  1  3  1  7  8  5  6
(  1- 19) 030300  6  5  4  1  2  1  3  1  3  1  3  1  3  1  2  1  4  5  6
(  1- 19) 030400  6  5  8  9  1  2  1  3  1  3  1  3  1  2  1  9  8  5  6
(  1- 19) 030500  6  5  5  8  2 10  2  1  3  1  3  1  2 10  2  8  5  5  6
(  1- 19) 030600  6  6  5  8 11  2  1  2  1  2  1  2  1  2 11  8  5  6  6
(  1- 19) 030700  6  6  5  5  8  8  9  1  7 12  7  1  9  8  8  5  5  6  6
(  1- 19) 030800  6  6  6  5  5  5  8  4  8  4  8  4  8  5  5  5  6  6  6
(  1- 19) 030900  6  6  6  6  6  5  5  5  5  5  5  5  5  5  6  6  6  6  6
(  1- 19) 031000  6  6  6  6  6  6  6  6  6  6  6  6  6  6  6  6  6  6  6
(  1- 14) 040100 10  1  1  1  1  1  1  1  1  1  1  1  1 13
(  1- 14) 040200 10  2  2  2  2  2  2  2  2  2  2  2  2 13
(  1- 14) 040300 10  3  3  3  3  3  3  3  3  3  3  3  3 13
(  1- 14) 040400 10  4  4  4  4  4  4  4  4  4  4  4  4 13
(  1- 14) 040500 10 11 11 11 11 11 11 11 11 11 11 11 11 13
(  1- 14) 040600 12 12 12 12 12 12 12 12 12 12 12 12 12 12
(  1- 14) 040700 10  5  5  5  5  5  5  5  5  5  5  5  5 13
(  1- 14) 040800 10  6  6  6  6  6  6  6  6  6  6  6  6 13
(  1- 14) 040900 10  7  7  7  7  7  7  7  7  7  7  7  7 13
(  1- 14) 041000 10  8  8  8  8  8  8  8  8  8  8  8  8 13
(  1- 14) 041100 10  9  9  9  9  9  9  9  9  9  9  9  9 13
(  1- 14) 041200 10 14 14 14 14 14 14 14 14 14 14 14 14 13
          050100         21.608 R18
          050200 10.804  21.608 R8
          050300 40.0       30.48 R11       40.0
          051300 20.0 20.0  30.48 R11 20.0  20.0
          052300 -1.0
(  1-  4) 060101  2.30928E-01  7.68564E-03  1.79005E-02  4.37267E-03
(  5-  8) 060105  5.78566E-14  8.73971E-01  4.87367E-02  6.86748E-02
(  9- 12) 060109  9.08664E-13  2.36824E-01  1.30354E-02  1.51801E-02
( 13- 16) 060113  4.30622E-03  5.66186E-14  8.68288E-01  7.53092E-02
( 17- 20) 060117  6.99272E-02  9.19408E-13  1.12514E-01  1.24034E-03
( 21- 24) 060121  1.96439E-02  5.99922E-04  8.32702E-15  8.53641E-01
( 25- 28) 060125  1.85151E-02  1.83138E-02  2.48450E-13  1.12514E-01
( 29- 32) 060129  1.24034E-03  1.96439E-02  5.99922E-04  8.32702E-15
( 33- 36) 060133  8.53641E-01  1.85151E-02  1.83138E-02  2.48450E-13
( 37- 40) 060137  3.52986E-03 -4.75972E-04  6.39194E-04 -2.68501E-04
( 41- 44) 060141 -3.79664E-15  3.46966E-01  2.11087E-02  2.76542E-02
( 45- 48) 060145  3.62756E-13  3.52986E-03 -4.75972E-04  6.39194E-04
( 49- 52) 060149 -2.68501E-04 -3.79664E-15  3.46966E-01  2.11087E-02
( 53- 56) 060153  2.76542E-02  3.62756E-13   .00000E+00   .00000E+00
( 57- 60) 060157   .00000E+00   .00000E+00   .00000E+00   .00000E+00
( 61- 64) 060161   .00000E+00   .00000E+00   .00000E+00 -5.65285E-05
( 65- 68) 060165  2.38661E-05 -1.40929E-05 -1.99619E-06 -2.67962E-17
( 69- 72) 060169  5.92052E+02  1.24995E+03  4.38646E+01  6.19503E-01
```

Figure B-2. ARROTTA Input Listing

```
( 73- 76) 060173  7.68707E+01  1.95628E+03  8.15305E+01  6.19503E-01
( 77- 80) 060177  1.00000E+00   .00000E+00   .00000E+00  2.44667E+00
( 81- 84) 060181  2.44667E+00   .00000E+00  1.55922E+06   .00000E+00
( 85- 88) 060185   .00000E+00   .00000E+00   .00000E+00   .00000E+00
( 89- 92) 060189   .00000E+00  2.09000E-05   .00000E+00   .00000E+00
( 93- 96) 060193  3.63000E-06  2.20000E-03  6.43000E-02   .00000E+00
( 97-100) 060197  1.12000E-02  5.86000E-08  2.42000E-06  2.46358E-04
(101-104) 060100  1.27535E-02  1.45914E-03  3.17843E-02  1.33969E-03
(105-108) 060100  1.19458E-01  2.94599E-03  3.18858E-01  1.05456E-03
(109-111) 060100  1.40265E+00  2.50605E-04  3.92952E+00
(  1-  4) 060201  2.31132E-01  8.86226E-03  1.65086E-02  5.38884E-03
(  5-  8) 060205  7.12520E-14  8.56898E-01  7.50066E-02  9.81175E-02
(  9- 12) 060209  1.29732E-12  2.31132E-01  8.86226E-03  1.65086E-02
( 13- 16) 060213  5.38884E-03  7.12520E-14  8.56898E-01  7.50066E-02
( 17- 20) 060217  9.81175E-02  1.29732E-12  1.06894E-01  1.30244E-03
( 21- 24) 060221  1.85643E-02  6.69172E-04  9.40733E-15  8.02693E-01
( 25- 28) 060225  2.23210E-02  2.74854E-02  3.73593E-13  1.06894E-01
( 29- 32) 060229  1.30244E-03  1.85643E-02  6.69172E-04  9.40733E-15
( 33- 36) 060233  8.02693E-01  2.23210E-02  2.74854E-02  3.73593E-13
( 37- 40) 060237  3.58709E-03 -6.48451E-04  4.03922E-04 -3.57250E-04
( 41- 44) 060241 -5.04631E-15  2.95213E-01  2.18614E-02  3.15468E-02
( 45- 48) 060245  4.12842E-13  3.58709E-03 -5.48451E-04  4.03922E-04
( 49- 52) 060249 -3.57250E-04 -5.04631E-15  2.95213E-01  2.18614E-02
( 53- 56) 060253  3.15468E-02  4.12842E-13   .00000E+00   .00000E+00
( 57- 60) 060257   .00000E+00   .00000E+00   .00000E+00   .00000E+00
( 61- 64) 060261   .00000E+00   .00000E+00   .00000E+00 -5.63395E-05
( 65- 68) 060265  2.33022E-05 -1.35019E-05 -2.36366E-06 -3.18172E-17
( 69- 72) 060269  5.92052E+02  1.24995E+03  4.38646E+01  5.94052E-01
( 73- 76) 060273  6.92607E+01  1.86644E+03  3.89555E+01  5.94052E-01
( 77- 80) 060277  1.00000E+00   .00000E+00   .00000E+00  2.44831E+00
( 81- 84) 060281  2.44832E+00   .00000E+00  1.44387E+06   .00000E+00
( 85- 88) 060285   .00000E+00   .00000E+00   .00000E+00   .00000E+00
( 89- 92) 060289   .00000E+00  2.09000E-05   .00000E+00   .00000E+00
( 93- 96) 060293  3.63000E-06  2.30000E-03  6.43000E-02   .00000E+00
( 97-100) 060297  1.11000E-02  5.86000E-08  2.42000E-06  2.46358E-04
(101-104) 060200  1.27535E-02  1.45914E-03  3.17843E-02  1.33969E-03
(105-108) 060200  1.19458E-01  2.94599E-03  3.18858E-01  1.05456E-03
(109-111) 060200  1.40265E+00  2.50605E-04  3.92952E+00
(  1-  4) 060301  2.30728E-01  8.68072E-03  1.66596E-02  5.38836E-03
(  5-  8) 060305  7.12747E-14  8.61057E-01  7.16198E-02  9.80550E-02
(  9- 12) 060309  1.29703E-12  2.30728E-01  8.68072E-03  1.66596E-02
( 13- 16) 060313  5.38836E-03  7.12747E-14  8.61057E-01  7.16198E-02
( 17- 20) 060317  9.80550E-02  1.29703E-12  1.08263E-01  1.29031E-03
( 21- 24) 060321  1.86970E-02  6.61442E-04  9.28904E-15  8.13425E-01
( 25- 28) 060325  2.20689E-02  2.70222E-02  3.67276E-13  1.08263E-01
( 29- 32) 060329  1.29031E-03  1.86970E-02  6.61442E-04  9.28904E-15
( 33- 36) 060333  8.13425E-01  2.20689E-02  2.70222E-02  3.67276E-13
( 37- 40) 060337  3.92980E-03 -6.28189E-04  4.58229E-04 -3.50382E-04
( 41- 44) 060341 -4.95145E-15  3.03342E-01  2.12240E-02  3.16330E-02
( 45- 48) 060345  4.13950E-13  3.92980E-03 -6.28189E-04  4.58229E-04
( 49- 52) 060349 -3.50382E-04 -4.95145E-15  3.03342E-01  2.12240E-02
( 53- 56) 060353  3.16330E-02  4.13950E-13   .00000E+00   .00000E+00
```

Figure B-2. ARROTTA Input Listing (Continued)

```
( 57- 60) 060357   .00000E+00   .00000E+00   .00000E+00   .00000E+00
( 61- 64) 060361   .00000E+00   .00000E+00   .00000E+00 -5.61257E-05
( 65- 68) 060365  2.32928E-05 -1.34387E-05 -2.35533E-06 -3.16922E-17
( 69- 72) 060369  5.92052E+02  1.24995E+03  4.38646E+01  6.00415E-01
( 73- 76) 060373  6.99841E+01  1.87695E+03  4.39008E+01  6.00415E-01
( 77- 80) 060377  1.00000E+00   .00000E+00   .00000E+00  2.44738E+00
( 81- 84) 060381  2.44737E+00   .00000E+00  1.44791E+06   .00000E+00
( 85- 88) 060385   .00000E+00   .00000E+00   .00000E+00   .00000E+00
( 89- 92) 060389   .00000E+00  2.09000E-05   .00000E+00   .00000E+00
( 93- 96) 060393  3.63000E-06  2.30000E-03  6.43000E-02   .00000E+00
( 97-100) 060397  1.11000E-02  5.86000E-08  2.42000E-06  2.46358E-04
(101-104) 060300  1.27535E-02  1.45914E-03  3.17843E-02  1.33969E-03
(105-108) 060300  1.19458E-01  2.94599E-03  3.18858E-01  1.05456E-03
(109-111) 060300  1.40265E+00  2.50605E-04  3.92952E+00
(  1-  4) 060401  2.29205E-01  8.80488E-03  1.63110E-02  6.24526E-03
(  5-  8) 060405  8.26946E-14  8.67789E-01  7.77139E-02  1.21515E-01
(  9- 12) 060409  1.60900E-12  2.29205E-01  8.80488E-03  1.63110E-02
( 13- 16) 060413  6.24526E-03  8.26946E-14  8.67789E-01  7.77139E-02
( 17- 20) 060417  1.21515E-01  1.60900E-12  1.10299E-01  1.32189E-03
( 21- 24) 060421  1.86197E-02  7.13495E-04  1.00394E-14  8.21630E-01
( 25- 28) 060425  2.44548E-02  3.20648E-02  4.36066E-13  1.10299E-01
( 29- 32) 060429  1.32189E-03  1.86197E-02  7.13495E-04  1.00394E-14
( 33- 36) 060433  8.21630E-01  2.44548E-02  3.20648E-02  4.36066E-13
( 37- 40) 060437  3.87365E-03 -5.70446E-04  5.90810E-04 -3.87558E-04
( 41- 44) 060441 -5.56182E-15  3.00537E-01  1.98783E-02  3.25952E-02
( 45- 48) 060445  4.24570E-13  3.87365E-03 -5.70446E-04  5.90810E-04
( 49- 52) 060449 -3.87558E-04 -5.56182E-15  3.00537E-01  1.98783E-02
( 53- 56) 060453  3.25952E-02  4.24570E-13   .00000E+00   .00000E+00
( 57- 60) 060457   .00000E+00   .00000E+00   .00000E+00   .00000E+00
( 61- 64) 060461   .00000E+00   .00000E+00   .00000E+00 -5.49694E-05
( 65- 68) 060465  2.28228E-05 -1.29062E-05 -2.59853E-06 -3.48548E-17
( 69- 72) 060469  5.92052E+02  1.24995E+03  4.38646E+01  6.09959E-01
( 73- 76) 060473  6.79433E+01  1.85850E+03  4.01900E+01  6.09959E-01
( 77- 80) 060477  1.00000E+00   .00000E+00   .00000E+00  2.44506E+00
( 81- 84) 060481  2.44506E+00   .00000E+00  1.37970E+06   .00000E+00
( 85- 88) 060485   .00000E+00   .00000E+00   .00000E+00   .00000E+00
( 89- 92) 060489   .00000E+00  2.09000E-05   .00000E+00   .00000E+00
( 93- 96) 060493  3.63000E-06  2.30000E-03  6.43000E-02   .00000E+00
( 97-100) 060497  1.11000E-02  5.86000E-08  2.42000E-06  2.46358E-04
(101-104) 060400  1.27535E-02  1.45914E-03  3.17843E-02  1.33969E-03
(105-108) 060400  1.19458E-01  2.94599E-03  3.18858E-01  1.05456E-03
(109-111) 060400  1.40265E+00  2.50605E-04  3.92952E+00
(  1-  4) 060501  2.30486E-01  9.42218E-03  1.57303E-02  6.25176E-03
(  5-  8) 060505  8.26790E-14  8.53257E-01  8.98709E-02  1.22047E-01
(  9- 12) 060509  1.61406E-12  2.30486E-01  9.42218E-03  1.57303E-02
( 13- 16) 060513  6.25176E-03  8.26790E-14  8.53257E-01  8.98709E-02
( 17- 20) 060517  1.22047E-01  1.61406E-12  1.05630E-01  1.39062E-03
( 21- 24) 060521  1.81029E-02  7.41566E-04  1.04644E-14  7.82959E-01
( 25- 28) 060525  2.57032E-02  3.42033E-02  4.65220E-13  1.05630E-01
( 29- 32) 060529  1.39062E-03  1.81029E-02  7.41566E-04  1.04644E-14
( 33- 36) 060533  7.82959E-01  2.57032E-02  3.42033E-02  4.65220E-13
( 37- 40) 060537  4.02163E-03 -7.10698E-04  4.43800E-04 -4.28445E-04
```

Figure B-2. ARROTTA Input Listing (Continued)

```
( 41- 44) 060541 -6.06422E-15  2.73246E-01  1.97482E-02  3.21008E-02
( 45- 48) 060545  4.18523E-13  4.02163E-03 -7.10698E-04  4.43800E-04
( 49- 52) 060549 -4.28445E-04 -6.06422E-15  2.73246E-01  1.97482E-02
( 53- 56) 060553  3.21008E-02  4.18523E-13   .00000E+00   .00000E+00
( 57- 60) 060557   .00000E+00   .00000E+00   .00000E+00   .00000E+00
( 61- 64) 060561   .00000E+00   .00000E+00   .00000E+00 -5.58216E-05
( 65- 68) 060565  2.28303E-05 -1.30755E-05 -2.64127E-06 -3.55219E-17
( 69- 72) 060569  5.92052E+02  1.24995E+03  4.38646E+01  5.87690E-01
( 73- 76) 060573  6.52955E+01  1.80209E+03  2.63488E+01  5.87690E-01
( 77- 80) 060577  1.00000E+00   .00000E+00   .00000E+00  2.44787E+00
( 81- 84) 060581  2.44787E+00   .00000E+00  1.36696E+06   .00000E+00
( 85- 88) 060585   .00000E+00   .00000E+00   .00000E+00   .00000E+00
( 89- 92) 060589   .00000E+00  2.09000E-05   .00000E+00   .00000E+00
( 93- 96) 060593  3.63000E-06  2.30000E-03  6.43000E-02   .00000E+00
( 97-100) 060597  1.10000E-02  5.86000E-08  2.42000E-06  2.46358E-04
(101-104) 060500  1.27535E-02  1.45914E-03  3.17843E-02  1.33969E-03
(105-108) 060500  1.19458E-01  2.94599E-03  3.18858E-01  1.05456E-03
(109-111) 060500  1.40265E+00  2.50605E-04  3.92952E+00
(  1-  4) 060601  2.28724E-01  8.56543E-03  1.65373E-02  6.24368E-03
(  5-  8) 060605  8.27091E-14  8.72742E-01  7.36409E-02  1.21359E-01
(  9- 12) 060609  1.60762E-12  2.34343E-01  1.35402E-02  1.38410E-02
( 13- 16) 060613  6.11932E-03  8.07136E-14  8.70468E-01  1.01492E-01
( 17- 20) 060617  1.24049E-01  1.63620E-12  1.12173E-01  1.31259E-03
( 21- 24) 060621  1.88142E-02  7.04904E-04  9.90261E-15  8.34474E-01
( 25- 28) 060625  2.43555E-02  3.13560E-02  4.26330E-13  1.12173E-01
( 29- 32) 060629  1.31259E-03  1.88142E-02  7.04904E-04  9.90261E-15
( 33- 36) 060633  8.34474E-01  2.43555E-02  3.13560E-02  4.26330E-13
( 37- 40) 060637  3.64155E-03 -5.76616E-04  7.16741E-04 -3.70293E-04
( 41- 44) 060641 -5.30412E-15  3.09186E-01  1.91499E-02  3.29814E-02
( 45- 48) 060645  4.31055E-13  3.64155E-03 -5.76616E-04  7.16741E-04
( 49- 52) 060649 -3.70293E-04 -5.30412E-15  3.09186E-01  1.91499E-02
( 53- 56) 060653  3.29814E-02  4.31055E-13   .00000E+00   .00000E+00
( 57- 60) 060657   .00000E+00   .00000E+00   .00000E+00   .00000E+00
( 61- 64) 060661   .00000E+00   .00000E+00   .00000E+00 -5.44405E-05
( 65- 68) 060665  2.28510E-05 -1.28950E-05 -2.58394E-06 -3.46463E-17
( 69- 72) 060669  5.92052E+02  1.24995E+03  4.38646E+01  6.19503E-01
( 73- 76) 060673  6.81913E+01  1.84712E+03  4.60102E+01  6.19503E-01
( 77- 80) 060677  1.00000E+00   .00000E+00   .00000E+00  2.44408E+00
( 81- 84) 060681  2.44408E+00   .00000E+00  1.38216E+06   .00000E+00
( 85- 88) 060685   .00000E+00   .00000E+00   .00000E+00   .00000E+00
( 89- 92) 060689   .00000E+00  2.09000E-05   .00000E+00   .00000E+00
( 93- 96) 060693  3.63000E-06  2.30000E-03  6.43000E-02   .00000E+00
( 97-100) 060697  1.10000E-02  5.86000E-08  2.42000E-06  2.46358E-04
(101-104) 060600  1.27535E-02  1.45914E-03  3.17843E-02  1.33969E-03
(105-108) 060600  1.19458E-01  2.94599E-03  3.18858E-01  1.05456E-03
(109-111) 060600  1.40265E+00  2.50305E-04  3.92952E+00
(  1-  4) 060701  2.30120E-01  9.24707E-03  1.59016E-02  6.24984E-03
(  5-  8) 060705  8.26831E-14  8.57615E-01  8.62629E-02  1.21828E-01
(  9- 12) 060709  1.61174E-12  2.30120E-01  9.24707E-03  1.59016E-02
( 13- 16) 060713  6.24984E-03  8.26831E-14  8.57615E-01  8.62629E-02
( 17- 20) 060717  1.21828E-01  1.61174E-12  1.06945E-01  1.36884E-03
( 21- 24) 060721  1.82467E-02  7.31615E-04  1.03171E-14  7.94650E-01
```

Figure B-2. ARROTTA Input Listing (Continued)

```
( 25- 28) 060725  2.51750E-02  3.35504E-02  4.56343E-13  1.06945E-01
( 29- 32) 060729  1.36884E-03  1.82467E-02  7.31615E-04  1.03171E-14
( 33- 36) 060733  7.94650E-01  2.51750E-02  3.35504E-02  4.56343E-13
( 37- 40) 060737  3.90052E-03 -6.89465E-04  5.26963E-04 -4.18828E-04
( 41- 44) 060741 -5.90554E-15  2.81980E-01  1.89671E-02  3.20988E-02
( 45- 48) 060745  4.18871E-13  3.90052E-03 -6.89465E-04  5.26963E-04
( 49- 52) 060749 -4.18828E-04 -5.90554E-15  2.81980E-01  1.89671E-02
( 53- 56) 060753  3.20988E-02  4.18871E-13   .00000E+00   .00000E+00
( 57- 60) 060757   .00000E+00   .00000E+00   .00000E+00   .00000E+00
( 61- 64) 060761   .00000E+00   .00000E+00   .00000E+00 -5.57125E-05
( 65- 68) 060765  2.28386E-05 -1.30331E-05 -2.62773E-06 -3.53448E-17
( 69- 72) 060769  5.92052E+02  1.24995E+03  4.38646E+01  5.94052E-01
( 73- 76) 060773  6.60404E+01  1.81849E+03  3.01824E+01  5.94052E-01
( 77- 80) 060777  1.00000E+00   .00000E+00   .00000E+00  2.44705E+00
( 81- 84) 060781  2.44704E+00   .00000E+00  1.36968E+06   .00000E+00
( 85- 88) 060785   .00000E+00   .00000E+00   .00000E+00   .00000E+00
( 89- 92) 060789   .00000E+00  2.09000E-05   .00000E+00   .00000E+00
( 93- 96) 060793  3.63000E-06  2.30000E-03  6.43000E-02   .00000E+00
( 97-100) 060797  1.10000E-02  5.86000E-08  2.42000E-06  2.46358E-04
(101-104) 060700  1.27535E-02  1.45914E-03  3.17843E-02  1.33969E-03
(105-108) 060700  1.19458E-01  2.94599E-03  3.18858E-01  1.05456E-03
(109-111) 060700  1.40265E+00  2.50605E-04  3.92952E+00
(  1-  4) 060801  2.29573E-01  8.14989E-03  1.70858E-02  5.38707E-03
(  5-  8) 060805  7.13370E-14  8.72468E-01  6.25005E-02  9.78341E-02
(  9- 12) 060809  1.29554E-12  2.85348E-01  1.32802E-02  1.43857E-02
( 13- 16) 060813  5.28997E-03  6.97056E-14  8.68745E-01  8.97602E-02
( 17- 20) 060817  9.98313E-02  1.31547E-12  1.12292E 01  1.26831E-03
( 21- 24) 060821  1.91168E-02  6.44816E-04  9.02413E-15  8.42302E-01
( 25- 28) 060825  2.18299E-02  2.56885E-02  3.49044E-13  1.12292E-01
( 29- 32) 060829  1.26831E-03  1.91168E-02  6.44816E-04  9.02413E-15
( 33- 36) 060833  8.42302E-01  2.18299E-02  2.56885E-02  3.49044E-13
( 37- 40) 060837  3.59181E-03 -5.51194E-04  6.85128E-04 -3.19735E-04
( 41- 44) 060841 -4.56132E-15  3.24061E-01  2.11957E-02  3.22854E-02
( 45- 48) 060845  4.23666E-13  3.59181E-03 -5.51194E-04  6.85128E-04
( 49- 52) 060849 -3.19735E-04 -4.56132E-15  3.24061E-01  2.11957E-02
( 53- 56) 060853  3.22854E-02  4.23666E-13   .00000E+00   .00000E+00
( 57- 60) 060857   .00000E+00   .00000E+00   .00000E+00   .00000E+00
( 61- 64) 060861   .00000E+00   .00000E+00   .00000E+00 -5.50669E-05
( 65- 68) 060865  2.32509E-05 -1.33011E-05 -2.33344E-06 -3.12857E-17
( 69- 72) 060869  5.92052E+02  1.24995E+03  4.38646E+01  6.19503E-01
( 73- 76) 060873  7.16049E+01  1.89265E+03  5.93390E+01  6.19503E-01
( 77- 80) 060877  1.00000E+00   .00000E+00   .00000E+00  2.44484E+00
( 81- 84) 060881  2.44485E+00   .00000E+00  1.45795E+06   .00000E+00
( 85- 88) 060885   .00000E+00   .00000E+00   .00000E+00   .00000E+00
( 89- 92) 060889   .00000E+00  2.09000E-05   .00000E+00   .00000E+00
( 93- 96) 060893  3.63000E-06  2.30000E-03  6.43000E-02   .00000E+00
( 97-100) 060897  1.11000E-02  5.86000E-08  2.42000E-06  2.46358E-04
(101-104) 060800  1.27535E-02  1.45914E-03  3.17843E-02  1.33969E-03
(105-108) 060800  1.19458E-01  2.94599E-03  3.18858E-01  1.05456E-03
(109-111) 060800  1.40265E+00  2.50605E-04  3.92952E+00
(  1-  4) 060901  2.29998E-01  9.18663E-03  1.59491E-02  6.25061E-03
(  5-  8) 060905  8.27045E-14  8.59056E-01  8.48884E-02  1.21905E-01
```

Figure B-2. ARROTTA Input Listing (Continued)

```
(  9- 12) 060909  1.61297E-12  2.29998E-01  9.18663E-03  1.59491E-02
( 13- 16) 060913  6.25061E-03  8.27045E-14  8.59056E-01  8.48884E-02
( 17- 20) 060917  1.21905E-01  1.61297E-12  1.07384E-01  1.34724E-03
( 21- 24) 060921  1.83179E-02  7.33275E-04  1.03320E-14  7.98715E-01
( 25- 28) 060925  2.49271E-02  3.33241E-02  4.53183E-13  1.07384E-01
( 29- 32) 060929  1.34724E-03  1.83179E-02  7.33275E-04  1.03320E-14
( 33- 36) 060933  7.98715E-01  2.49271E-02  3.33241E-02  4.53183E-13
( 37- 40) 060937  3.83927E-03 -7.40410E-04  6.09895E-04 -4.13434E-04
( 41- 44) 060941 -5.89046E-15  2.85338E-01  1.83736E-02  3.22233E-02
( 45- 48) 060945  4.20490E-13  3.83927E-03 -7.40410E-04  6.09895E-04
( 49- 52) 060949 -4.13434E-04 -5.89046E-15  2.85338E-01  1.83736E-02
( 53- 56) 060953  3.22233E-02  4.20490E-13   .00000E+00   .00000E+00
( 57- 60) 060957   .00000E+00   .00000E+00   .00000E+00   .00000E+00
( 61- 64) 060961   .00000E+00   .00000E+00   .00000E+00 -5.53976E-05
( 65- 68) 060965  2.28594E-05 -1.30433E-05 -2.62458E-06 -3.52508E-17
( 69- 72) 060969  5.92052E+02  1.24995E+03  4.38646E+01  5.95643E-01
( 73- 76) 060973  6.66776E+01  1.83585E+03  3.15782E+01  5.95643E-01
( 77- 80) 060977  1.00000E+00   .00000E+00   .00000E+00  2.44674E+00
( 81- 84) 060981  2.44675E+00   .00000E+00  1.37450E+06   .00000E+00
( 85- 88) 060985   .00000E+00   .00000E+00   .00000E+00   .00000E+00
( 89- 92) 060989   .00000E+00  2.09000E-05   .00000E+00   .00000E+00
( 93- 96) 060993  3.63000E-06  2.30000E-03  6.43000E-02   .00000E+00
( 97-100) 060997  1.10000E-02  5.86000E-08  2.42000E-06  2.46358E-04
(101-104) 060900  1.27535E-02  1.45914E-03  3.17843E-02  1.33969E-03
(105-108) 060900  1.19458E-01  2.94599E-03  3.18858E-01  1.05456E-03
(109-111) 060900  1.40265E+00  2.50605E-04  3.92952E+00
CASMO     061001  2.73940E-01  2.25826E-03  3.13602E-02
BOTTOM    061006  1.22432E+00  4.15451E-02
REFLECTOR 061010  2.73940E-01  2.25826E-03  3.13602E-02
          061015  1.22432E+00  4.15451E-02
          061019  1.23669E-01 -1.95228E-04  3.42303E-02
          061024  1.19548E+00  1.54364E-02
          061028  1.23669E-01 -1.95228E-04  3.42303E-02
          061033  1.19548E+00  1.54364E-02
          061069  5.49950E+02   .00000E+00  4.70249E+01  1.00000E+00
          061073  1.85923E+01  6.86497E+02   .00000E+00  1.00000E+00
          061098  5.86000E-08  2.42000E-06  2.46358E-04
          061000  1.27535E-02  1.45914E-03  3.17843E-02  1.33969E-03
          061000  1.19458E-01  2.94599E-03  3.18858E-01  1.05456E-03
          061000  1.40265E+00  2.50605E-04  3.92952E+00
CASMO     061101  2.67710E-01  1.93990E-03  2.89336E-02
BAFFLE    061106  1.27873E+00  1.88902E-02
          061110  2.67710E-01  1.93990E-03  2.89336E-02
          061115  1.27873E+00  1.88902E-02
          061169  5.57000E+02   .00000E+00  4.63836E+01  1.00000E+00
          061173  4.64806E+01  2.17710E+03   .00000E+00  1.00000E+00
          061198  5.86000E-08  2.42000E-06  2.46358E-04
          061100  1.27535E-02  1.45914E-03  3.17843E-02  1.33969E-03
          061100  1.19458E-01  2.94599E-03  3.18858E-01  1.05456E-03
          061100  1.40265E+00  2.50605E-04  3.92952E+00
CASMO     061201  2.24013E-01  3.93110E-04  4.45079E-02
RADIAL    061206  1.29687E+00  1.01244E-02
REFLECTOR 061210  2.24013E-01  3.93110E-04  4.45079E-02
```

Figure B-2. ARROTTA Input Listing (Continued)

```
                061215  1.29687E+00  1.01244E-02
                061269  5.92000E+02   .00000E+00  4.63836E+01  1.00000E+00
                061273  7.24347E+01  2.33738E+03   .00000E+00  1.00000E+00
                061298  5.86000E-08  2.42000E-06  2.46358E-04
                061200  1.27535E-02  1.45914E-03  3.17843E-02  1.33969E-03
                061200  1.19458E-01  2.94599E-03  3.18858E-01  1.05456E-03
                061200  1.40265E+00  2.50605E-04  3.92952E+00
CASMO           061301  1.54949E-01  3.57151E-04  2.99239E-02
TOP             061306  9.34036E-01  8.36477E-03
REFLECTOR       061310  1.54949E-01  3.57151E-04  2.99239E-02
                061315  9.34036E-01  8.36477E-03
                061319  1.36735E-01  4.07490E-04  2.85707E-02
                061324  1.00942E+00  8.36477E-03
                061328  1.36735E-01  4.07490E-04  2.85707E-02
                061333  1.00942E+00  8.36477E-03
                061369  5.49950E+02   .00000E+00  4.70249E+01  1.00000E+00
                061373  4.59733E+01  1.62739E+03   .00000E+00  1.00000E+00
                061398  5.86000E-08  2.42000E-06  2.46358E-04
                061300  1.27535E-02  1.45914E-03  3.17843E-02  1.33969E-03
                061300  1.19458E-01  2.94599E-03  3.18858E-01  1.05456E-03
                061300  1.40265E+00  2.50605E-04  3.92952E+00
(  1-  4)       061401  2.30928E-01  7.68564E-03  1.79005E-02  4.37267E-03
(  5-  8)       061405  5.78566E-14  8.73971E-01  4.87367E-02  6.86748E-02
(  9- 12)       061409  9.08664E-13  2.36824E-01  1.30354E-02  1.51801E-02
( 13- 16)       061413  4.30622E-03  5.66186E-14  8.68288E-01  2.00000E-01
( 17- 20)       061417  6.99272E-02  9.19408E-13  1.12514E-01  1.24034E-03
( 21- 24)       061421  1.96439E-02  5.99922E-04  8.32702E-15  8.53641E-01
( 25- 28)       061425  1.85151E-02  1.83138E-02  2.48450E-13  1.12514E-01
( 29- 32)       061429  1.24034E-03  1.96439E-02  5.99922E-04  8.32702E-15
( 33- 36)       061433  8.53641E-01  1.85151E-02  1.83138E-02  2.48450E-13
( 37- 40)       061437  3.52986E-03 -4.75972E-04  6.39194E-04 -2.68501E-04
( 41- 44)       061441 -3.79664E-15  3.46966E-01  2.11087E-02  2.76542E-02
( 45- 48)       061445  3.62756E-13  3.52986E-03 -4.75972E-04  6.39194E-04
( 49- 52)       061449 -2.68501E-04 -3.79664E-15  3.46966E-01  2.11087E-02
( 53- 56)       061453  2.76542E-02  3.62756E-13   .00000E+00   .00000E+00
( 57- 60)       061457   .00000E+00   .00000E+00   .00000E+00   .00000E+00
( 61- 64)       061461   .00000E+00   .00000E+00   .00000E+00 -5.65285E-05
( 65- 68)       061465  2.38661E-05 -1.40929E-05 -1.99619E-06 -2.67962E-17
( 69- 72)       061469  5.92052E+02  1.24995E+03  4.38646E+01  6.19503E-01
( 73- 76)       061473  7.68707E+01  1.95628E+03  8.15305E+01  6.19503E-01
( 77- 80)       061477  1.00000E+00   .00000E+00   .00000E+00  2.44667E+00
( 81- 84)       061481  2.44667E+00   .00000E+00  1.55922E+06   .00000E+00
( 85- 88)       061485   .00000E+00   .00000E+00   .00000E+00   .00000E+00
( 89- 92)       061489   .00000E+00  2.09000E-05   .00000E+00   .00000E+00
( 93- 96)       061493  3.63000E-06  2.20000E-03  6.43000E-02   .00000E+00
( 97-100)       061497  1.12000E-02  5.86000E-08  2.42000E-06  2.46358E-04
(101-104)       061400  1.27535E-02  1.45914E-03  3.17843E-02  1.33969E-03
(105-108)       061400  1.19458E-01  2.94599E-03  3.18858E-01  1.05456E-03
(109-111)       061400  1.40265E+00  2.50605E-04  3.92952E+00
                090100  10 1
                090200   4 1    6 5   14 5   10 7
                090300   8 3   12 3
```

Figure B-2. ARROTTA Input Listing (Continued)

```
090400   4 3    8 7   12 7   16 3
090500  16 1
100000 49.47  49.47  163.77  346.33  49.47
110100  0.0    0.0   3600.0 0.0
110200  0.0    0.0   3600.0 0.0
110300  0.0    0.0   3600.0 0.0
110400  0.0    0.0   3600.0 0.0
110500  0.0 3546.52     0.5 0.0
200001 2250.0   839.81   557.0   12.0   0.041333  0.04015  0.0
200008 0.012867   0.0   0.013125   1.0   2.87E-4   9.375E-4
200014 641.75   0.0   0.0   0.0   0.0   0.0   1000.0
210000  1  1  1
990000
```

Figure B-2. ARROTTA Input Listing (Continued)

```
* HERMITE FOR HZP, EJECTED ROD, HALF CORE STARTING AT 0.0
*
* MASTER CONTROL DATA
*
000100,TIMER,UNUSED,BANNERS
010003,1-3,1-9,1+1,1+1,5-1,1-1,1-3,1+1
010004,1+1,0+0
010010,2,3,1,6                          $ TRANSIENT CASE
*
* BOUNDARY CONDITIONS
*
010002,0,0,1,0,0,0,0,1
091011,/19/0.0
091022,/19/0.0
092011,/19/0.0
092022,/19/0.0
093011,/38/1.0
093022,/38/1.0
094011,/38/0.0
094022,/38/0.0
*
* SUBCASE INPUT
*
600000,1,1                      $ NUMBER OF SUBCASES, FIRST SUBCASE
600201,.1+4                     $ POWER (WATTS)
600301,975.                     $ PPM
600601,111001101                $ EDITS
010501,10,20,30,40,50,89,98 $ NUCLIDES TO BE EDITED
601001,97.4109                  $ ROD POSITIONS  - IN
601002,97.4109                  $ ROD POSITIONS  - IN
601003,66.1609                  $ ROD POSITIONS  - IN
601004,16.2484                  $ ROD POSITIONS  - IN
601005,97.4109                  $ ROD POSITIONS  - IN
*
* TRANSIENT DATA
*
020001,1.70648+7,4.13223+5              $ GROUP VELOCITIES
020002,1.27535-2,3.17843-2,1.19458-1,3.18858-1,1.40265+0,3.92952+0
020003,2.46358-4,1.45914-3,1.33969-3,2.94599-3,1.05456-3,2.50605-4
020004,.510                             $ TIME ZONE WIDTH
020005,.010                             $ TIME STEP SIZE
021002,01                               $ TH EDIT FREQUENCY
021004,01                               $ NEUTRONICS EDIT FREQUENCY
021007,01                               $ TRANSIENT FILE CONTROL
*
* TRANSIENT ROD POSITION DATA
*
702050,0.0,.010,.110462,.51
702051,0.0,0.0,-97.4109,-97.4109 $ ROD MOTION
*
```

Figure B-3. HERMITE Input Listing

```
* GEOMETRY DATA
*
010001,38,19,16,105,12,14,2,0,1,1
*
* RADIAL MESH
*
050101,10.804,1
050201,10.804,2
050301,10.804,38
050401,10.804,19
*
* AXIAL MESH
*
070001,20.00,2,30.48,14,20.00,16
*
* BASIC AND AUXILIARY FIGURES
*
801000,38,19,3,0,4              $ REFLECTOR AND SHROUD
801001,1,00,38.00,19
801002,36,02,36,00,09
801003,5,04,34,09,13
801004,5,06,32,13,15
801005,5,10,28,15,17
*
802000,2,2,2,0,2                $ FULL ASSEMBLY
802001,1,0,2,0,2                $  TYPE 1
802101,2,0,2,0,2                $  TYPE 2
802201,3,0,2,0,2                $  TYPE 3
802301,4,0,2,0,2                $  TYPE 4
802401,7,0,2,0,2                $  TYPE 7
802501,8,0,2,0,2                $  TYPE 8
802601,9,0,2,0,2                $  TYPE 9
802701,10,0,2,0,2               $  TYPE 10
802801,11,0,2,0,2               $  TYPE 11
802901,12,0,2,0,2               $  TYPE 12
*
* FINAL FIGURE OVERLAY
*
170001,105,010,00,00,0,0
170002,001,023,04,-1,0,0, 002,029,06,-1,0,0, 003,021,08,-1,0,0
170003,004,020,10,-1,0,0, 005,022,12,-1,0,0, 006,020,14,-1,0,0
170004,007,021,16,-1,0,0, 008,020,18,-1,0,0, 009,021,20,-1,0,0
170005,010,020,22,-1,0,0, 011,022,24,-1,0,0, 012,020,26,-1,0,0
170006,013,021,28,-1,0,0, 014,029,30,-1,0,0, 015,023,32,-1,0,0
*
170007,016,025,04,01,0,0, 017,024,06,01,0,0, 018,020,08,01,0,0
170008,019,022,10,01,0,0, 020,020,12,01,0,0, 021,022,14,01,0,0
170009,022,020,16,01,0,0, 023,021,18,01,0,0, 024,020,20,01,0,0
170010,025,022,22,01,0,0, 026,020,24,01,0,0, 027,022,26,01,0,0
170011,028,020,28,01,0,0, 029,024,30,01,0,0, 030,025,32,01,0,0
*
```

Figure B-3. HERMITE Input Listing (Continued)

```
170012,031,023,04,03,0,0, 032,020,06,03,0,0, 033,021,08,03,0,0
170013,034,020,10,03,0,0, 035,022,12,03,0,0, 036,020,14,03,0,0
170014,037,022,16,03,0,0, 038,020,18,03,0,0, 039,022,20,03,0,0
170015,040,020,22,03,0,0, 041,022,24,03,0,0, 042,020,26,03,0,0
170016,043,021,28,03,0,0, 044,020,30,03,0,0, 045,023,32,03,0,0
*
170017,046,025,04,05,0,0, 047,026,06,05,0,0, 048,020,08,05,0,0
170018,049,021,10,05,0,0, 050,020,12,05,0,0, 051,022,14,05,0,0
170019,052,020,16,05,0,0, 053,022,18,05,0,0, 054,020,20,05,0,0
170020,055,022,22,05,0,0, 056,020,24,05,0,0, 057,021,26,05,0,0
170021,058,020,28,05,0,0, 059,026,30,05,0,0, 060,025,32,05,0,0
*
170022,                   061,025,06,07,0,0, 062,021,08,07,0,0
170023,063,027,10,07,0,0, 064,021,12,07,0,0, 065,020,14,07,0,0
170024,066,022,16,07,0,0, 067,020,18,07,0,0, 068,022,20,07,0,0
170025,069,020,22,07,0,0, 070,021,24,07,0,0, 071,027,26,07,0,0
170026,072,021,28,07,0,0, 073,025,30,07,0,0
*
170027,                   074,025,06,09,0,0, 075,028,08,09,0,0
170028,076,021,10,09,0,0, 077,020,12,09,0,0, 078,021,14,09,0,0
170029,079,020,16,09,0,0, 080,021,18,09,0,0, 081,020,20,09,0,0
170030,082,021,22,09,0,0, 083,020,24,09,0,0, 084,021,26,09,0,0
170031,085,028,28,09,0,0, 086,025,30,09,0,0
*
170032,                                       087,025,08,11,0,0
170033,088,025,10,11,0,0, 089,026,12,11,0,0, 090,020,14,11,0,0
170034,091,024,16,11,0,0, 092,029,18,11,0,0, 093,024,20,11,0,0
170035,094,020,22,11,0,0, 095,026,24,11,0,0, 096,025,26,11,0,0
170036,097,025,28,11,0,0
*
170037,                   098,025,12,13,0,0, 099,023,14,13,0,0
170038,100,025,16,13,0,0, 101,023,18,13,0,0, 102,025,20,13,0,0
170039,103,023,22,13,0,0, 104,025,24,13,0,0
*
* COMPOSITION-PLANAR REGION CORRESPONDENCE  (PR-COMP-PR)
*
030001,1,10,5, 6,12,6, 7,10,12                          $ BOT REFL
030021,1,1,1, 2,2,2, 3,3,3, 4,4,4, 5,11,5, 6,12,6, 7,5,7, 8,6,8, 9,7,9
030022,10,8,10, 11,9,11, 12,14,12                       $ CORE
030141,1,13,5, 6,12,6, 7,13,12                          $ TOP REFL
*
* COARSE MESH REBALANCE MESH
*
041101,0,2,4,6,8,10,12,14,16,18,20,22,24,26,28,30,32,34,36,38
041201,0,2,4,6,8,10,12,14,16,19
041301,0,2,4,6,8,10,12,14,16
*
* EDIT SETS
*
011001,01,-105,0,01,-12      $ ENTIRE PROBLEM
011011,01,-104,0,01,-12      $ CORE
012001,01,-105,0,01,-12      $ EACH FIGURE
```

Figure B-3. HERMITE Input Listing (Continued)

```
013001,01,-105,0,01,-12       $ EACH REGION
015001,2,-14                  $ CORE
*
* BOX PICTURE EDITS
*
200000,3,15
200001,215,215,215,215,213,213,211,207
200701,4,12 ,2, 1, 3, 1, 2, 1, 2, 1, 3, 1, 2,12, 4
200702,8, 7, 1, 3, 1, 3, 1, 2, 1, 3, 1, 3, 1, 7, 8
200703,4, 1, 2, 1, 3, 1, 3, 1, 3, 1, 3, 1, 2, 1, 4
200704,8, 9, 1, 2, 1, 3, 1, 3, 1, 3, 1, 2, 1, 9, 8
200705,   8, 2,10, 2, 1, 3, 1, 3, 1, 2,10, 2, 8
200706,   8,11, 2, 1, 2, 1, 2, 1, 2, 1, 2,11, 8
200707,   8, 8, 9, 1, 7, 1, 7, 1, 9, 8, 8
200708,        8, 4, 8, 4, 8, 4, 8
201001,3,-106                      $ EDIT SET TO ASSEMBLY ASSIGNMENT
202001,193.,15,96.5,104
*
* CONTROL RODS
*
700000,5,12,5,2,1,1
700002,2,14,40.00,405.76
700010,1
700020,2
700030,3
700040,4
700050,5
*
* CONTROL ROD ZONE STRUCTURE
*
701010,20,405.76
701020,20,405.76
701030,20,405.76
701040,20,405.76
701050,20,405.76
*
* CONTROL ROD BASIC FIGURES
*
0901000,2,2
0901001,1,0,2,0,2
0901101,2,0,2,0,2
0901201,3,0,2,0,2
0901301,4,0,2,0,2
0901401,5,0,2,0,2
*
* CONTROL ROD FINAL FIGURE OVERLAY
*
180001,01,011,06,-1,0,0,  02,010,18,-1,0,0
180002,03,014,30,-1,0,0,  04,013,06,03,0,0
180003,05,012,14,03,0,0,  06,012,22,03,0,0
180004,07,013,30,03,0,0,  08,011,10,07,0,0
180005,09,011,26,07,0,0,  10,013,14,11,0,0
180006,11,011,18,11,0,0,  12,013,22,11,0,0
```

Figure B-3. HERMITE Input Listing (Continued)

```
*
*
*        ARROTTA/
*        HERMITE              HERMITE          ARROTTA ASSEMBLY
*      COMPOSITION/TS       PLANAR REGION          TYPES
*         NUMBERS              NUMBERS
*
*            1                    1          1  FUEL TYPE 1
*            2                    2          2            2
*            3                    3          3            3
*            4                    4          4            4
*            5                    7          7            7
*            6                    8          8            8
*            7                    9          9            9
*            8                   10         10           10
*            9                   11         11           11
*           10                   --         --  BOTTOM REFL
*           11                    5          5  SHROUD/BAFFLE
*           12                    6          6  RADIAL REFL
*           13                   --         --  TOP REFL
*           14                   12         12  FUEL TYPE 12
*
* TABLE SET TO COMPOSITION ASSIGNMENT
*
110001, 1, 1, 2, 2, 3, 3, 4, 4, 5, 5, 6, 6, 7, 7, 8, 8, 9, 9, 10, 10
  +   ,11,11,12,12,13,13,14,14
*
* NUCLIDE ID'S
*
300001, 10,  20, 30, 40, 50      $ BASE
301001,310,   0,  0,  0,  0      $ FUEL TEMP
302001,  0,   0,  0,  0,  0      $ MOD DENS
300501,BASE, (DEL RODS),BORON,CONV,PPM       $
  +   ,(DEL TFUEL), (DEL DENS)
320001,98,89                     $ TFUEL, MOD DENS
320002,88,89,98       $ TH FEEDBACK ID'S FOR TMOD, MOD DENS, TFUEL
320003,30,40,50,606647+7         $ BORON, HYDROGEN, PPM
*
* INITIAL NUMBER DENSITIES
*
100011,10,1.0,98,-7.05272,89,0.0428962 ,40,0.029100
100021,10,1.0,98,-7.05272,89,0.0428962 ,40,0.027905
100031,10,1.0,98,-7.05272,89,0.0428962 ,40,0.028204
100041,10,1.0,98,-7.05272,89,0.0428962 ,40,0.028652
100051,10,1.0,98,-7.05272,89,0.0428962 ,40,0.027606
100061,10,1.0,98,-7.05272,89,0.0428962 ,40,0.029100
100071,10,1.0,98,-7.05272,89,0.0428962 ,40,0.027905
100081,10,1.0,98,-7.05272,89,0.0428962 ,40,0.029100
100091,10,1.0,98,-7.05272,89,0.0428962 ,40,0.027980
100101,10,1.0,98, 0.00000,89,-772548-2 ,40,0.0503581
100111,10,1.0,98, 0.00000,89, 254686-2 ,40,0.0496713
100121,10,1.0,98, 0.00000,89, 254686-2 ,40,0.0496713
```

Figure B-3. HERMITE Input Listing (Continued)

```
100131,10,1.0,98, 0.00000,89,-772548-2 ,40,0.0503581
100141,10,1.0,98,-7.05272,89,0.0428962 ,40,0.029100
*
* MASKS
*
120100,1,5,0
120111,89,0,.097377,.051377,0+0,-0.0126233,-0.022623 $MOD DENS - FUEL TS'S
120200,1,2,0
120211,89,0,0+0,-0.153245                    $ MOD DENS - TOP AND BOT REFL
*
*  TABLE SET 1 - FUEL TYPE 1
*
401001,(FUEL TYPE 1)
401002,88,592.052,89,.702623,98,1249.95
401101, 10,0+0,0+0,0+0,0+0,1.0,0+0
401201, 10,0+0,0+0,0+0,0+0,1.0,0+0
401102, 20, 5.89600E-03 , 5.34976E-03 ,-2.72040E-03 ,-6.64500E-05
   +,       1.00000E+00 , 1.86305E-11
401202, 20,-5.68300E-03 , 2.65725E-02 , 0.00000E+00 , 1.25240E-03
   +,       1.00000E+00 , 8.57873E-12
401103, 30,0+0,7.68707+1,8.15305+1
401203, 30,0+0,1.95628+3,0+0
401104,310,-7.58409E-05 , 3.20197E-05 ,-1.89076E-05 ,-2.67817E-06
   +,       0.00000E+00 , 0.00000E+00
401601,1,1,2,3,4,5,6,7,8,9,10
*
* FUNCTION TABLES - TABLE SET 1
*
130010,4,10,1,1,2,0
130020,4,10,2,1,2,0
130030,4,10,3,1,2,0
130040,4,10,4,1,2,0
130050,4,10,6,1,1,0
130060,4,10,1,2,2,0
130070,4,10,2,2,2,0
130080,4,10,4,2,2,0
130090,4,10,6,2,1,0
130100,4,310,6,1,2,0
130011, 2.46589E-01 , 2.39174E-01 , 2.30928E-01
   +  , 2.28908E-01 , 2.27309E-01
130021, 7.84840E-03 , 7.77379E-03 , 7.68564E-03
   +  , 7.66320E-03 , 7.64521E-03
130031, 2.06352E-02 , 1.93403E-02 , 1.79005E-02
   +  , 1.75478E-02 , 1.72687E-02
130041, 4.45066E-03 , 4.41510E-03 , 4.37267E-03
   +  , 4.36181E-03 , 4.35308E-03
130051, 1.32425E-11 , 1.32376E-11 , 1.32314E-11
   +  , 1.32298E-11 , 1.32285E-11
130061, 9.98942E-01 , 9.38246E-01 , 8.73971E-01
   +  , 8.58747E-01 , 8.46845E-01
130071, 5.17082E-02 , 5.02034E-02 , 4.87367E-02
   +  , 4.84109E-02 , 4.81624E-02
```

Figure B-3. HERMITE Input Listing (Continued)

```
130081, 7.17441E-02 , 7.01618E-02 , 6.86748E-02
   +  , 6.83547E-02 , 6.81138E-02
130091, 1.32424E-11 , 1.32376E-11 , 1.32314E-11
   +  , 1.32298E-11 , 1.32285E-11
130101,-1.09032E-16 ,-1.12893E-16 ,-1.17755E-16
   +  ,-1.19044E-16 ,-1.20092E-16
*
* TABLE SET 2 - FUEL TYPE 2
*
402001,(FUEL TYPE 2)
402002,88,592.052,89,.702623,98,1249.95
402101, 10,0+0,0+0,0+0,0+0,1.0,0+0
402201, 10,0+0,0+0,0+0,0+0,1.0,0+0
402102, 20,0+0,0+0,0+0,0+0,1.0,0+0
402202, 20,0+0,0+0,0+0,0+0,1.0,0+0
402103, 30,0+0,6.92607+1,3.89555+1
402203, 30,0+0,1.86644+3,0+0
402104,310,-7.55874E-05 , 3.12632E-05 ,-1.81147E-05 ,-3.17118E-06
   +,       0.00000E+00 , 0.00000E+00
402601,1,14,15,16,17,18,19,20,21,22,23
*
* FUNCTION TABLES - FUEL TYPE 2
*
130140,4,10,1,1,2,0
130150,4,10,2,1,2,0
130160,4,10,3,1,2,0
130170,4,10,4,1,2,0
130180,4,10,6,1,1,0
130190,4,10,1,2,2,0
130200,4,10,2,2,2,0
130210,4,10,4,2,2,0
130220,4,10,6,2,1,0
130230,4,310,6,1,2,0
130141, 2.46015E-01 , 2.38967E-01 , 2.31132E-01
   +  , 2.29213E-01 , 2.27694E-01
130151, 9.03031E-03 , 8.95403E-03 , 8.86226E-03
   +  , 8.83865E-03 , 8.81965E-03
130161, 1.90892E-02 , 1.78682E-02 , 1.65086E-02
   +  , 1.61752E-02 , 1.59113E-02
130171, 5.47472E-03 , 5.43586E-03 , 5.38884E-03
   +  , 5.37670E-03 , 5.36692E-03
130181, 1.32352E-11 , 1.32293E-11 , 1.32221E-11
   +  , 1.32203E-11 , 1.32187E-11
130191, 9.73814E-01 , 9.17171E-01 , 8.56898E-01
   +  , 8.42572E-01 , 8.31359E-01
130201, 7.85200E-02 , 7.67556E-02 , 7.50066E-02
   +  , 7.46126E-02 , 7.43106E-02
130211, 1.02533E-01 , 1.00296E-01 , 9.81175E-02
   +  , 9.76339E-02 , 9.72652E-02
130221, 1.32351E-11 , 1.32293E-11 , 1.32221E-11
   +  , 1.32202E-11 , 1.32187E-11
130231,-1.30803E-16 ,-1.35134E-16 ,-1.40555E-16
   +  ,-1.41987E-16 ,-1.43149E-16
```

Figure B-3. HERMITE Input Listing (Continued)

```
*
* TABLE SET 3 - FUEL TYPE 3
*
403001,(FUEL TYPE 3)
403002,88,592.052,89,.702623,98,1249.95
403101, 10,0+0,0+0,0+0,0+0,1.0,0+0
403201, 10,0+0,0+0,0+0,0+0,1.0,0+0
403102, 20,0+0,0+0,0+0,0+0,1.0,0+0
403202, 20,0+0,0+0,0+0,0+0,1.0,0+0
403103, 30,0+0,6.99841+1,4.39008+1
403203, 30,0+0,1.87695+3,0+0
403104,310,-7.53005E-05 , 3.12506E-05 ,-1.80299E-05 ,-3.16001E-06
   +,        0.00000E+00 , 0.00000E+00
403601,1,25,26,27,28,29,30,31,32,33,34
*
* FUNCTION TABLES - FUEL TYPE 3
*
130250,4,10,1,1,2,0
130260,4,10,2,1,2,0
130270,4,10,3,1,2,0
130280,4,10,4,1,2,0
130290,4,10,6,1,1,0
130300,4,10,1,2,2,0
130310,4,10,2,2,2,0
130320,4,10,4,2,2,0
130330,4,10,6,2,1,0
130340,4,310,6,1,2,0
130251, 2.45808E-01 , 2.38665E-01 , 2.30728E-01
   +  , 2.28784E-01 , 2.27246E-01
130261, 8.84748E-03 , 8.77171E-03 , 8.68072E-03
   +  , 8.65734E-03 , 8.63852E-03
130271, 1.92596E-02 , 1.80292E-02 , 1.66596E-02
   +  , 1.63238E-02 , 1.60581E-02
130281, 5.47330E-03 , 5.43485E-03 , 5.38836E-03
   +  , 5.37636E-03 , 5.36670E-03
130291, 1.32401E-11 , 1.32345E-11 , 1.32275E-11
   +  , 1.32257E-11 , 1.32242E-11
130301, 9.79616E-01 , 9.22158E-01 , 8.61057E-01
   +  , 8.46541E-01 , 8.35181E-01
130311, 7.50860E-02 , 7.33470E-02 , 7.16198E-02
   +  , 7.12302E-02 , 7.09312E-02
130321, 1.02408E-01 , 1.00200E-01 , 9.80550E-02
   +  , 9.75797E-02 , 9.72177E-02
130331, 1.32401E-11 , 1.32345E-11 , 1.32276E-11
   +  , 1.32258E-11 , 1.32243E-11
130341,-1.24382E-16 ,-1.28521E-16 ,-1.33707E-16
   +  ,-1.35076E-16 ,-1.36189E-16
*
* TABLE SET 4 - FUEL TYPE 4
*
404001,(FUEL TYPE 4)
404002,88,592.052,89,.702623,98,1249.95
```

Figure B-3. HERMITE Input Listing (Continued)

```
404101, 10,0+0,0+0,0+0,0+0,1.0,0+0
404201, 10,0+0,0+0,0+0,0+0,1.0,0+0
404102, 20,0+0,0+0,0+0,0+0,1.0,0+0
404202, 20,0+0,0+0,0+0,0+0,1.0,0+0
404103, 30,0+0,6.79433+1,4.01900+1
404203, 30,0+0,1.85250+3,0+0
404104,310,-7.37492E-05 , 3.06200E-05 ,-1.73155E-05 ,-3.48629E-06
   +,       0.00000E+00 , 0.00000E+00
404601,1,36,37,38,39,40,41,42,43,44,45
*
* FUNCTION TABLES - FUEL TYPE 4
*
130360,4,10,1,1,2,1
130370,4,10,2,1,2,0
130380,4,10,3,1,2,0
130390,4,10,4,1,2,0
130400,4,10,6,1,1,0
130410,4,10,1,2,2,1
130420,4,10,2,2,2,0
130430,4,10,4,2,2,0
130440,4,10,6,2,1,0
130450,4,310,6,1,2,0
130361, 2.44566E-01 , 2.37291E-01 , 2.29205E-01
   +  , 2.27225E-01 , 2.25658E-01
130371, 8.97712E-03 , 8.89849E-03 , 8.80488E-03
   +  , 8.78095E-03 , 8.76173E-03
130381, 1.89029E-02 , 1.76757E-02 , 1.63110E-02
   +  , 1.59767E-02 , 1.57121E-02
130391, 6.33670E-03 , 6.29536E-03 , 6.24526E-03
   +  , 6.23232E-03 , 6.22188E-03
130401, 1.32528E-11 , 1.32477E-11 , 1.32412E-11
   +  , 1.32394E-11 , 1.32380E-11
130411, 9.87432E-01 , 9.29475E-01 , 8.67789E-01
   +  , 8.53125E-01 , 8.41646E-01
130421, 8.14849E-02 , 7.96084E-02 , 7.77139E-02
   +  , 7.72810E-02 , 7.69471E-02
130431, 1.26585E-01 , 1.24034E-01 , 1.21515E-01
   +  , 1.20949E-01 , 1.20516E-01
130441, 1.32527E-11 , 1.32476E-11 , 1.32412E-11
   +  , 1.32394E-11 , 1.32380E-11
130451,-8.82791E-17 ,-9.17008E-17 ,-9.60703E-17
   +  ,-9.72367E-17 ,-9.81876E-17
*
* TABLE SET 5 - FUEL TYPE 7
*
405001,(FUEL TYPE 7)
405002,88,592.052,89,.702623,98,1249.95
405101, 10,0+0,0+0,0+0,0+0,1.0,0+0
405201, 10,0+0,0+0,0+0,0+0,1.0,0+0
405102, 20,0+0,0+0,0+0,0+0,1.0,0+0
405202, 20,0+0,0+0,0+0,0+0,1.0,0+0
405103, 30,0+0,6.52955+1,2.63488+1
```

Figure B-3. HERMITE Input Listing (Continued)

```
405203, 30,0+0,1.80209+3,0+0
405104,310,-7.48925E-05 , 3.06301E-05 ,-1.75426E-05 ,-3.54364E-06
   +,       0.00000E+00 , 0.00000E+00
405601,1,47,48,49,50,51,52,53,54,55,56
*
* FUNCTION TABLES - FUEL TYPE 7
*
130470,4,10,1,1,2,0
130480,4,10,2,1,2,0
130490,4,10,3,1,2,0
130500,4,10,4,1,2,0
130510,4,10,6,1,1,0
130520,4,10,1,2,2,0
130530,4,10,2,2,2,0
130540,4,10,4,2,2,0
130550,4,10,6,2,1,0
130560,4,310,6,1,2,0
130471, 2.45203E-01 , 2.38231E-01 , 2.30486E-01
   +  , 2.28590E-01 , 2.27089E-01
130481, 9.60126E-03 , 9.52006E-03 , 9.42218E-03
   +  , 9.39697E-03 , 9.37667E-03
130491, 1.82477E-02 , 1.70564E-02 , 1.57303E-02
   +  , 1.54052E-02 , 1.51479E-02
130501, 6.34630E-03 , 6.30369E-03 , 6.25176E-03
   +  , 6.23830E-03 , 6.22744E-03
130511, 1.32381E-11 , 1.32322E-11 , 1.32249E-11
   +  , 1.32230E-11 , 1.32215E-11
130521, 9.67016E-01 , 9.11969E-01 , 8.53257E-01
   +  , 8.39279E-01 , 8.28330E-01
130531, 9.38124E-02 , 9.18559E-02 , 8.98709E-02
   +  , 8.94155E-02 , 8.90638E-02
130541, 1.27404E-01 , 1.24720E-01 , 1.22047E-01
   +  , 1.21443E-01 , 1.20979E-01
130551, 1.32380E-11 , 1.32322E-11 , 1.32249E-11
   +  , 1.32230E-11 , 1.32214E-11
130561,-1.17668E-16 ,-1.21758E-16 ,-1.26900E-16
   +  ,-1.28261E-16 ,-1.29367E-16
*
* TABLE SET 6 - FUEL TYPE 8
*
406001,(FUEL TYPE 8)
406002,88,592.052,89,.702623,98,1249.95
406101, 10,0+0,0+0,0+0,0+0,1.0,0+0
406201, 10,0+0,0+0,0+0,0+0,1.0,0+0
406102, 20, 5.61900E-03 , 4.97477E-03 ,-2.69630E-03 ,-1.24360E-04
   +,       1.00000E+00 , 1.60462E-11
406202, 20,-2.27400E-03 , 2.78511E-02 , 0.00000E+00 , 2.69000E-03
   +,       1.00000E+00 , 1.06245E-11
406103, 30,0+0,6.81913+1,4.60102+1
406203, 30,0+0,1.84712+3,0+0
406104,310,-7.30396E-05 , 3.06578E-05 ,-1.73005E-05 ,-3.46672E-06
   +,       0.00000E+00 , 0.00000E+00
```

Figure B-3. HERMITE Input Listing (Continued)

```
406601,1,58,59,60,61,62,63,64,65,66,67
*
* FUNCTION TABLES - FUEL TYPE 8
*
130580,4,10,1,1,2,0
130590,4,10,2,1,2,0
130600,4,10,3,1,2,0
130610,4,10,4,1,2,0
130620,4,10,6,1,1,0
130630,4,10,1,2,2,0
130640,4,10,2,2,2,0
130650,4,10,4,2,2,0
130660,4,10,6,2,1,0
130670,4,310,6,1,2,0
13058i, 2.44340E-01 , 2.36946E-01 , 2.28724E-01
   +  , 2.26710E-01 , 2.25116E-01
130591, 8.73627E-03 , 8.65833E-03 , 8.56543E-03
   +  , 8.54166E-03 , 8.52257E-03
130601, 1.91585E-02 , 1.79169E-02 , 1.65373E-02
   +  , 1.61995E-02 , 1.59323E-02
130611, 6.33426E-03 , 6.29324E-03 , 6.24368E-03
   +  , 6.23090E-03 , 6.22060E-03
130621, 1.32580E-11 , 1.32531E-11 , 1.32469E-11
   +  , 1.32452E-11 , 1.32439E-11
130631, 9.94331E-01 , 9.35413E-01 , 8.72742E-01
   +  , 8.57850E-01 , 8.46194E-01
130641, 7.73842E-02 , 7.55242E-02 , 7.36409E-02
   +  , 7.32095E-02 , 7.28766E-02
130651, 1.26338E-01 , 1.23828E-01 , 1.21359E-01
   +  , 1.20806E-01 , 1.20394E-01
130661, 1.32580E-11 , 1.32530E-11 , 1.32468E-11
   +  , 1.32452E-11 , 1.32438E-11
130671,-8.22707E-17 ,-8.55198E-17 ,-8.96546E-17
   +  ,-9.07562E-17 ,-9.16536E-17
*
* TABLE SET 7 - FUEL TYPE 9
*
407001,(FUEL TYPE 9)
407002,88,592.052,89,.702623,98,1249.95
407101, 10,0+0,0+0,0+0,0+0,1.0,0+0
407201, 10,0+0,0+0,0+0,0+0,1.0,0+0
407102, 20,0+0,0+0,0+0,0+0,1.0,0+0
407202, 20,0+0,0+0,0+0,0+0,1.0,0+0
407103, 30,0+0,6.60404+1,3.01824+1
407203, 30,0+0,1.81849+3,0+0
407104,310,-7.47462E-05 , 3.06412E-05 ,-1.74857E-05 ,-3.52547E-06
   +,       0.00000E+00 , 0.00000E+00
407601,1,71,72,73,74,75,76,77,78,79,80
*
* FUNCTION TABLES - FUEL TYPE 9
*
130710,4,10,1,1,2,0
130720,4,10,2,1,2,0
```

Figure B-3. HERMITE Input Listing (Continued)

```
130730,4,10,3,1,2,0
130740,4,10,4,1,2,0
130750,4,10,6,1,1,0
130760,4,10,1,2,2,0
130770,4,10,2,2,2,0
130780,4,10,4,2,2,0
130790,4,10,6,2,1,0
130800,4,310,6,1,2,0
130711, 2.45016E-01 , 2.37961E-01 , 2.30120E-01
   +  , 2.28200E-01 , 2.26681E-01
130721, 9.42354E-03 , 9.34348E-03 , 9.24707E-03
   +  , 9.22226E-03 , 9.20228E-03
130731, 1.84405E-02 , 1.72386E-02 , 1.59016E-02
   +  , 1.55740E-02 , 1.53146E-02
130741, 6.34319E-03 , 6.30110E-03 , 6.24984E-03
   +  , 6.23656E-03 , 6.22585E-03
130751, 1.32425E-11 , 1.32367E-11 , 1.32296E-11
   +  , 1.32278E-11 , 1.32263E-11
130761, 9.73162E-01 , 9.17229E-01 , 8.57615E-01
   +  , 8.43430E-01 , 8.32321E-01
130771, 9.01162E-02 , 8.82051E-02 , 8.62629E-02
   +  , 8.58167E-02 , 8.54720E-02
130781, 1.27094E-01 , 1.24453E-01 , 1.21828E-01
   +  , 1.21236E-01 , 1.20781E-01
130791, 1.32424E-11 , 1.32367E-11 , 1.32296E-11
   +  , 1.32278E-11 , 1.32263E-11
130801,-1.15729E-16 ,-1.19715E-16 ,-1.24699E-16
   +  ,-1.26014E-16 ,-1.27083E-16
*
* TABLE SET 8 - FUEL TYPE 10
*
408001,(FUEL TYPE 10)
408002,88,592.052,89,.702623,98,1249.95
408101, 10,0+0,0+0,0+0,0+0,0+0,1.0,0+0
408201, 10,0+0,0+0,0+0,0+0,0+0,1.0,0+0
408102, 20, 5.77500E-03 , 5.13031E-03 ,-2.70010E-03 ,-9.71000E-05
   +,       1.00000E+00 , 1.68012E-11
408202, 20,-3.72200E-03 , 2.72597E-02 , 0.00000E+00 , 1.99720E-03
   +,       1.00000E+00 , 9.97897E-12
408103, 30,0+0,7.16049+1,5.93390+1
408203, 30,0+0,1.89265+3,0+0
408104,310,-7.38800E-05 , 3.11944E-05 ,-1.78453E-05 ,-3.13064E-06
   +,       0.00000E+00 , 0.00000E+00
408601,1,82,83,84,85,86,87,88,89,90,91
*
* FUNCTION TABLES - FUEL TYPE 10
*
130820,4,10,1,1,2,0
130830,4,10,2,1,2,0
130840,4,10,3,1,2,0
130850,4,10,4,1,2,0
130860,4,10,6,1,1,0
```

Figure B-3. HERMITE Input Listing (Continued)

```
130870,4,10,1,2,2,0
130880,4,10,2,2,2,0
130890,4,10,4,2,2,0
130900,4,10,6,2,1,0
130910,4,310,6,1,2,0
130821, 2.45205E-01 , 2.37803E-01 , 2.29573E-01
   +  , 2.27557E-01 , 2.25961E-01
130831, 8.31508E-03 , 8.23968E-03 , 8.14989E-03
   +  , 8.12693E-03 , 8.10848E-03
130841, 1.97434E-02 , 1.84873E-02 , 1.70858E-02
   +  , 1.67426E-02 , 1.64710E-02
130851, 5.47029E-03 , 5.43251E-03 , 5.38707E-03
   +  , 5.37538E-03 , 5.36598E-03
130861, 1.32534E-11 , 1.32485E-11 , 1.32423E-11
   +  , 1.32406E-11 , 1.32393E-11
130871, 9.95427E-01 , 9.35791E-01 , 8.72468E-01
   +  , 8.57440E-01 , 8.45683E-01
130881, 6.59330E-02 , 6.42101E-02 , 6.25005E-02
   +  , 6.21152E-02 , 6.18196E-02
130891, 1.02014E-01 , 9.98851E-02 , 9.78341E-02
   +  , 9.73830E-02 , 9.70404E-02
130901, 1.32535E-11 , 1.32485E-11 , 1.32422E-11
   +  , 1.32406E-11 , 1.32392E-11
130911,-8.82110E-17 ,-9.16690E-17 ,-9.60512E-17
   +  ,-9.72161E-17 ,-9.81646E-17
*
* TABLE SET 9 - FUEL TYPE 11
*
409001,(FUEL TYPE 11)
409002,88,592.052,89,.702623,98,1249.95
409101, 10,0+0,0+0,0+0,0+0,0+0,1.0,0+0
409201, 10,0+0,0+0,0+0,0+0,0+0,1.0,0+0
409102, 20,0+0,0+0,0+0,0+0,0+0,1.0,0+0
409202, 20,0+0,0+0,0+0,0+0,0+0,1.0,0+0
409103, 30,0+0,6.66776+1,3.15782+1
409203, 30,0+0,1.83585+3,0+0
409104,310,-7.43237E-05 , 3.06691E-05 ,-1.74994E-05 ,-3.52124E-06
   +,       0.00000E+00 , 0.00000E+00
409601,1,95,96,97,98,99,100,101,102,103,104
*
* FUNCTION TABLES - FUEL TYPE 11
*
130950,4,10,1,1,2,0
130960,4,10,2,1,2,0
130970,4,10,3,1,2,0
130980,4,10,4,1,2,0
130990,4,10,6,1,1,0
131000,4,10,1,2,2,0
131010,4,10,2,2,2,0
131020,4,10,4,2,2,0
131030,4,10,6,2,1,0
131040,4,310,6,1,2,0
```

Figure B-3. HERMITE Input Listing (Continued)

```
130951, 2.44954E-01 , 2.37871E-01 , 2.29998E-01
   +  , 2.28070E-01 , 2.26544E-01
130961, 9.35912E-03 , 9.28118E-03 , 9.18663E-03
   +  , 9.16219E-03 , 9.14248E-03
130971, 1.84995E-02 , 1.72918E-02 , 1.59491E-02
   +  , 1.56202E-02 , 1.53599E-02
130981, 6.34429E-03 , 6.30202E-03 , 6.25061E-03
   +  , 6.23730E-03 , 6.22657E-03
130991, 1.32439E-11 , 1.32384E-11 , 1.32314E-11
   +  , 1.32296E-11 , 1.32281E-11
131001, 9.75231E-01 , 9.18985E-01 , 8.59056E-01
   +  , 8.44799E-01 , 8.33635E-01
131011, 8.86960E-02 , 8.68093E-02 , 8.48884E-02
   +  , 8.44465E-02 , 8.41048E-02
131021, 1.27142E-01 , 1.24514E-01 , 1.21905E-01
   +  , 1.21317E-01 , 1.20865E-01
131031, 1.32438E-11 , 1.32383E-11 , 1.32314E-11
   +  , 1.32295E-11 , 1.32281E-11
131041,-1.03852E-16 ,-1.07641E-16 ,-1.12442E-16
   +  ,-1.13718E-16 ,-1.14757E-16
*
* TABLE SET 10 - BOTTOM REFLECTOR
*
410001,(BOTTOM REFLECTOR)
410002,88,549.95,89,.753245,98,0+0
410101, 30, 0+0, 1.85923+1, 0+0
410201, 30, 0+0, 6.86497+2, 0+0
410601, 2, 106, 107, 108, 109, 110
*
* TABLE SET 10 FUNCTION TABLES
*
131060,4,10,1,1,1,0
131070,4,10,2,1,1,0
131080,4,10,3,1,1,0
131090,4,10,1,2,1,0
131100,4,10,2,2,1,0
*
131061, 2.73940E-01 , 2.48780E-01
131071, 2.25826E-03 , 2.29798E-03
131081, 3.13602E-02 , 2.43962E-02
131091, 1.22432E+00 , 9.81104E-01
131101, 4.15451E-02 , 3.84046E-02
*
* TABLE SET 11 - SHROUD/BAFFLE
*
411001,(SHROUD/BAFFLE)
411002,88,557.00,89,.742973,98,0+0
411101, 10, 2.67710-1, 1.93990-3, 2.89336-2
411201, 10, 1.27873+0, 1.88902-2, 0+0
411102, 30,   00000+0, 4.64806+1, 0+0
411202, 30,   00000+0, 2.17710+3, 0+0
*
```

Figure B-3. HERMITE Input Listing (Continued)

```
* TABLE SET 12 - RADIAL REFLECTOR
*
412001,(RADIAL REFLECTOR)
412002,88,592.00,89,.742973,98,0+0
412101, 10, 2.24013-1, 3.93110-4, 4.45079-2
412201, 10, 1.29687+0, 1.01244-2, 0+0
412102, 30,   00000+0, 7.24347+1, 0+0
412202, 30,   00000+0, 2.33738+3, 0+0
*
* TABLE SET 13 - TOP REFLECTOR
*
413001,(TOP REFLECTOR)
413002,88,549.95,89,.753245,98,0+0
413101, 30, 0+0, 4.59733+1, 0+0
413201, 30, 0+0, 1.62739+3, 0+0
413601, 2, 111, 112, 113, 114, 115
*
* TABLE SET 13 FUNCTION TABLES
*
131110,4,10,1,1,1,0
131120,4,10,2,1,1,0
131130,4,10,3,1,1,0
131140,4,10,1,2,1,0
131150,4,10,2,2,1,0
*
131111, 1.54949E-01 , 1.27131E-01
131121, 3.57151E-04 , 2.74249E-04
131131, 2.99239E-02 , 2.41113E-02
131141, 9.34036E-01 , 7.28673E-01
131151, 8.36477E-03 , 6.66299E-03
*
*  TABLE SET 14 - FUEL TYPE 12
*
*  THIS TABLE SET IS A DUPLICATE OF TABLE SET 1
*  EXCEPT FOR THE ROD THERMAL ABSORPTION
*
*
414001,(FUEL TYPE 12)
414002,88,592.052,89,.702623,98,1249.95
414101, 10,0+0,0+0,0+0,0+0,1.0,0+0
414201, 10,0+0,0+0,0+0,0+0,1.0,0+0
414102, 20, 5.89600E-03 , 5.34976E-03 ,-2.72040E-03 ,-6.64500E-05
   +,       1.00000E+00 , 1.86305E-11
*
* THE THERMAL ABSORPTION ON THE NEXT CARD IS THE ONLY CHANGE FROM
* TABLE SET 1
*
414202, 20,-5.68300E-03 ,   .151263   , 0.00000E+00 , 1.25240E-03
   +,       1.00000E+00 , 8.57873E-12
414103, 30,0+0,7.68707+1,8.15305+1
414203, 30,0+0,1.95628+3,0+0
```

Figure B-3. HERMITE Input Listing (Continued)

```
414104,310,-7.58409E-05 , 3.20197E-05 ,-1.89076E-05 ,-2.67817E-06
   +,       0.00000E+00 , 0.00000E+00
414601,1,1,2,3,4,5,6,7,8,9,10
*
* FUNCTION TABLES SAME AS FOR TABLE SET 1
*
*
* BASIC TH MODEL OPTIONS
*
010017,0,1,2,3,4,5,6,7,8,9,10,11,12,13,14,15,16 $ TH BLOCK BOUNDARIES
500000,0,0,0                          $ TH MODEL SELECTION
500001,20,.01,0,1.0,1.0,0.1,1.0       $ TH PASSES, CONVERGENCE
500002,0,500                          $ NEUT ITERS/TH PASS
500008,1.0                            $ POWER DAMPING FACTOR
500010,2250.                          $ PRESSURE
500011,550.,50,700.,0                 $ TH PROPERTY TABLE
500012,0,0,0,0                        $HOMOGENEOUS MODEL, SLIP = 1.0, NO
*
* FUEL TEMPERATURE MODEL
*
500100,0                              $ FINITE DIFFERENCE
500101,8,2                            $ MESH POINTS IN PELLET AND CLAD
500103,1.0,10.2796,6.55               $ FUEL AND CLAD DENSITY
500104,0.30881,0.003444,0.0225        $ FUEL PELLET DIA, GAP TH, CLAD TH
500105,.000                           $ FRACTION OF HEAT DEP IN COOLANT
503000,0.0,10000.                     $ HGAP TABLE - KW/FT
503001,1000.,1000.                    $              - HGAP
503500,0.0,0.0                        $ TRANSIENT HGAP PARAMETERS
*
* COOLANT CHANNEL DESCRIPTION
*
520001,26.6636,0.28203                $ WP, AC, FULL ASSEMBLY
520002,13.3318,0.141015               $         HALF ASSEMBLY
525000,2,-15,1,-104                   $ CHANNEL TYPE TO CHANNEL ASSIGN
525010,557.,1                         $ INLET TEMPERATURE
525020,3023316.,1                     $ INLET MASS FLOW RATE
*
* FUEL ROD GROUPS
*
540001,282.3636129                    $ FUEL PINS - FULL ASSEMBLY
540002,141.1818065                    $             HALF ASSEMBLY
545000,2,-15,1,-104                   $ FUEL ROD TYPE TO GROUP ASSIGN
545001,3,-106                         $ EDIT SET TO GROUP ASSIGNMENT
*
* TH EDITS
*
590000,1,1,0
591000,0,1,1,0,0
*
*
```

Figure B-3. HERMITE Input Listing (Continued)

```
* FILE SAVING
*
010021,HOT4
010022,0,0,2,0,2,0,2,0          $ TH DATA, TRANS RES., CONC.
010023,1,1,1,1                  $ PSEUDO NUCLIDES ON 221 FILE
600701,000101                   $ STATIC FILE CONTROL
*
.
/EOF
```

Figure B-3. HERMITE Input Listing (Continued)